

PEOPLE'S DEMOCRATIC REPUBLIC OF ALGERIA

MINISTRY OF HIGHER EDUCATION AND SCIENTIFIC RESEARCH



**SAAD DAHLEB Blida 01 University
Institute of Aeronautics and Space Studies
Department of Aeronautical Construction**



Master's Degree Dissertation

**In Fulfilment of The Requirements for the
Degree of Master in Aeronautics
Specialty: Propulsion**

Design and Installation of Measuring Equipment for a Subsonic Wind Tunnel

- By: KERIMI Amir
HIBER Nadir Houssemeddine
- Under the Supervision of: Mr Amri Redha
Mr CHEGRANI Ahmed

Blida, September 2020

Acknowledgement

We first and foremost address our thanks to Allah almighty who gave us the strength and the courage and guided us to this point in our lives who without we wouldn't have been able to accomplish our humble work.

We give our most sincere thanks to our Promotor and Co-Promotor **Prof Chegrani Ahmed** and **Prof Amri Redha** for their unending dedication and support, for guiding us and honouring us with their insights every step of the way. And who believed in us and always helped us overcome every obstacle.

We also would like to sincerely and humbly thank the members of the jury **Dr El hirtsi A** and **Dr Renane R** for taking the time to examine and evaluate our work.

And of course, our gratitude goes to all the teachers and professors that had a hand in enriching and supporting our education from the first cycle to the last semester. And to anyone that helped with even a kind word in our journey.

And finally, to our families and friends for their support, love and understanding that gave us the power to move forward and the candles to light the way.

Dedication

This humble work is dedicated to all the kind souls I encountered along the way.

To my father, my role model and my first hero. For his sacrifices, his unending support, his invaluable advice and his kind attentive heart.

To my mother, my guardian angel and my anchor. For her priceless “force”, her unconditional love and her good innocent spirit.

To my first friend and protector, my brother. For his life-long guidance, companionship and tolerance. And to Epsilon for her delicious culinary support that I wouldn't have held on without, her lending ear and her fun nature.

To the new sister, for her handling of the you know who and her adrenaline shots that kept me going through it all. To Beerus, for nothing useful and for everything cute and to avoid the vengeful bites.

To all the friends I had the honour and pleasure of sharing my years with.

To “mon pote” Elias B, Housseem H my partner, Dulum I the artist, Fares G the wise brother, Youcef K “soge king”, Mahdi I the motivator, Enima D the magician, Abdou D the Tas. KD.

To a very special person with whom I shared the purest and happiest days. Aymen I, forever in my heart.

To everyone who ever helped me. Near or far, where ever you are; a special thanks goes to Prof Chegrani A, Prof Amri Redha, Mr Djalel, Mr Bilal, Hacen H, Ramzy B for their vital help to the making of this work. In addition to the B.S Family for their welcoming warm support along the way. And to our loving classmates and faculty staff for their helpfulness.

I thank you with all my heart and dedicate this piece to you.

Amir K.

Dedication

From this stage, I would like to take this opportunity with great joy to thank my parents and my small family, my aunt Mira and my big Family for supporting me all these years and my companions, B.Elias, K.Amir, I.Mahdi, I.Mouloud, G.Fares, K.Youcef for all the good times and for being with me in my ups and downs,

Mr Djalel and Mr Bilal and Hacem the assassin and my dear teachers Mr Amri and Mr Chegrani for these wonderful opportunities that I learned a lot from and I will not forget. All the teachers who taught me and helped me to become what I am now.

HIBER .NADIR. H. E

Abstract

The purpose of this thesis is the study, design and installation of measuring equipment for a subsonic Wind Tunnel. The measuring equipment is mainly digital and that is to accomplish as much precision as possible in the results obtained in the wind tunnel.

The testing will consist of measuring the aerodynamic properties and the wind speed when it comes to various aerofoils and wings designed and made by our team. In addition to that, the goal is to be able to do the measuring simultaneously.

Key Words

Subsonic Wind Tunnel, Aerodynamic forces, Digital measuring equipment.

تلخيص

يتمحور موضوع التخرج حول تصميم ودراسة وتركيب معدات القياس لقناة تهوية دون سرعة الصوت. معدات القياس رقمية بشكل أساسي وذلك لتحقيق أكبر قدر ممكن من الدقة في النتائج التي تم الحصول عليها في قناة التهوية.

سيكون الاختبار من قياس خصائص الديناميكا الهوائية وسرعة الرياح عندما يتعلق الأمر بأنواع مختلفة من الجنحات و الأجنحة التي صممها وصنعها فريقنا. بالإضافة إلى ذلك، فإن الهدف هو القدرة على القيام بالقياس في نفس الوقت.

الكلمات المفتاحية

قناة تهوية دون سرعة الصوت، قوى الديناميكا الهوائية، معدات قياس رقمية.

Résumé

Le sujet de ce mémoire de fin d'étude est la conception, l'étude et l'installation d'équipements de mesure pour une soufflerie subsonique. L'équipement de mesure est principalement numérique et devait permettre d'avoir le plus de précision possible dans les résultats obtenus en soufflerie.

Les tests consistaient à mesurer les propriétés aérodynamiques et la vitesse du vent en ce qui concerne les différents profils et ailes conçus et fabriqués par notre équipe. En plus de cela, l'objectif est de pouvoir effectuer la mesure simultanément.

Mots Clés

Soufflerie Subsonique, Forces Aérodynamiques, Equipements de mesure numérique.

TABLE OF CONTENTS

ABSTRACT	
TABLE OF CONTENTS	
LIST OF TABLES	
LIST OF FIGURES	
LIST OF SYMBOLS	
LIST OF ABBREVIATIONS	

CHAPTER I: Chronological Classification of Wind Tunnel Evolution

I. INTRODUCTION.....	1
I.1 Wind Tunnel Definition	1
I.2 Description and main components.....	1
a) The Collector	2
b) The Test Chamber	3
c) The Diffuser	4
d) The Fan	4
I.3 Chronological History of Wind Tunnels	5
I.3.1 Before the modern Wind Tunnel.....	5
I.3.2 The First Wind Tunnels powered by a Steam Engine	5
I.3.3 The emergence of the air driven Wind Tunnels	6
I.3.4 Post Wright Brothers and Downstream fans	7
I.3.5 A leap to modern day Wind Tunnels.....	8
I.3.6 Modern age and High-Speed Wind Tunnels	10
I.4 Wind Tunnel Classification and Types	11
I.5 Instrumentation and Sensors used in Wind Tunnels.....	13
I.6 Conclusion.....	15

CHAPTER II: Theoretical Study and Aerodynamic Properties

II. INTRODUCTION	16
II.1 Airfoils and Aerodynamic Shapes	16
II.1.1 Airfoils.....	16
II.1.1.1 Airfoils Description	17
II.1.1.2 Airfoils History	18
a) Early days	18
b) First organized series	18
c) British and USA efforts (1910-1930).....	18
d) NACA Four-Digit Airfoils.....	19
e) NACA Five-Digit Airfoils	19
f) NACA 1/6/7/8-Series Airfoils	20
g) Modern Airfoils.....	21
II.1.1.3 Airfoils Types.....	21

II.1.1.4 NACA Airfoils Classification and Identification.....	22
II.1.2 Finite/Infinite Wings	23
II.2 Aerodynamic Properties	25
II.2.1 Lift/Drag and the Aerodynamic Moment	25
II.2.2 Aerodynamic Coefficients.....	26
II.2.3 The Center of Pressure	27
II.2.4 The Aerodynamic Center	28
II.3 Examples of Aerodynamic curves and schematics	29
II.3.1 Pressure distribution around an Airfoil	29
II.3.2 Drag and Lift coefficients curves	29
II.4 CONCLUSION	31

CHAPTER III: Numerical simulation

III. INTRODUCTION.....	32
III.1 Numerical Simulation on NACA 0012 Airfoil	32
III.1.1 Launching from Ansys Workbench	33
III.1.2 Creating the Geometry on Design modeler	33
III.1.3 Preparing the Mesh on Ansys Mesh Creator	37
III.1.4 Setting Up and Launching the Simulation on the Fluent Solver.....	38
III.1.5 Results and Parameter sets.....	41
III.1.6 Results Discussion and Comparison with Known Data	42
III.2 Numerical Simulation on NACA 0015 Airfoil	48
III.2.1 Geometry and Mesh	49
III.2.2 Simulation on Fluent and Results	49
III.2.3 Results Discussion and Comparison with Known Data	50
III.3 Numerical Simulation on NACA 4412 Airfoil	55
III.3.1 Geometry and Meshing	55
III.3.2 Simulation on Fluent and Results	56
III.3.3 Results Discussion and Comparison with Known Data	56
III.4 CONCLUSION.....	60

CHAPTER IV Wind Tunnel Testing: Set-Up and Instrumentation

IV. INTRODUCTION	61
IV.1 Description of the Electronic Measuring Equipment.....	61
IV.1.1 Electronic circuit for Data Acquisition.....	61
IV.1.1.1 General description.....	61
IV.1.2 Hardware.....	62
IV.1.2.1 PIC 18F4620 Microcontroller.....	62
IV.1.2.2 Degraw Load Cell with an HX711 Electronic module.....	63
IV.1.2.3 GY61-ADXL335 Accelerometer (for AoA measurement)	64

IV.1.2.4 NXP MPXV7002Dp Air Speed sensor.....	64
IV.1.3 Software.....	65
IV.1.4 Description of the data acquisition system.....	65
IV.1.5 Experimental testing.....	67
IV.1.5.1 Experimental measurement setup.....	67
IV.2 The Conception and Design Process on SolidWorks.....	68
IV.3 Conception and methods of Production.....	69
IV.3.1 Core Materials for the Airfoils/Wings.....	69
IV.3.1.1 Composite materials.....	69
IV.3.1.1.1 Definition.....	69
IV.3.1.2 Reinforcements.....	71
IV.3.1.3 Fibers.....	71
IV.3.1.4 The Matrix.....	73
IV.3.1.5 Molding.....	73
IV.3.2 Materials used in the Support Items.....	73
IV.4 Production and Realisation.....	74
IV.4.1 Wing construction.....	74
IV.4.2 Design and Production of the Measuring Equipment Support.....	78
IV.5 CONCLUSION.....	79

GENERAL CONCLUSION

APPENDIXES

REFERENCES

LIST OF TABLES

CHAPTER I

Table I-1 Post Wright brothers Wind Tunnels.....	7
Table I-2 Characteristics of wind tanners designed for the different speed regimes.....	10

CHAPTER II

Table II-1 Evolution of the NACA Airfoil series	21
---	----

CHAPTER III

Table III-1 Importing the Airfoil coordinates into an Excel.txt file	34
Table III-2 The Input and Output Parameters concerned with the results	41
Table III-3 Airfoil Data for the NACA 0012.....	43
Table III-4 Airfoil Data for the NACA 0015.....	51
Table III-5 Airfoil Data for the NACA 4412.....	58

CHAPTER IV

Table IV. 1 Some Glass Fiber Properties	72
---	----

LIST OF FIGURES

CHAPTER I

Figure I. 1. Low-Speed Closed Tunnel (NASA)	2
Figure I. 2. Pitsco AirTech tunnel (NASA)	2
Figure I. 3. Collector of Pitsco AirTech Tunnel (NASA).....	2
Figure I. 4. model of an F-5 fighter in the Test Chamber of a Pitsco AirTech Tunnel	3
Figure I. 5. The Diffuser of a Pitsco AirTech Tunnel (NASA)	4
Figure I. 6. The Fan of a Pitsco AirTech Tunnel located downstream of the Test Chamber	5
Figure I. 7. First Aerodynamic Tunnel (1885) of Horatio Philips (1845-1924).....	6
Figure I. 8. Prandtl's second generation Wind Tunnel (1916).	8
Figure I. 9. Cross section of the VDT showing the annular flow of returning air.....	9
Figure I. 10. View of the large S1Ch wind tunnel in Meudon (© ONERA)	9
Figure I. 11. Sutherland's Formula for Viscosity as a function of Temperature.	10
Figure I. 12. Some Types of Wind Tunnels.	13
Figure I. 13. Full-Scale Wind Tunnel Force Balance for Lift and Drag measurement	13
Figure I. 14.a. General View of Wind Tunnel Test equipment	14
Figure I. 14.b. Air Speed Controller	14
Figure I. 14.c. Air Speed Sensor	14
Figure I. 15. Example of a Strain Gage and the Principle it is based on	14
Figure I. 16. An example of a Pitot-Static Tube and the Principle it is based on.....	15

CHAPTER II

Figure II. 1. Aerodynamic Lift explained by Bernoulli's Law	16
Figure II. 2. Sketch of an Airfoil relative to the wing.....	17
Figure II. 3. Airfoil Nomenclature of a NACA 4415	17
Figure II. 4. Horatio Philips's cambered Airfoils series design.....	18
Figure II. 5. Typical Airfoils in 1917.....	19
Figure II. 6. Evolution of Airfoils from the 1900s to the 1940s	20
Figure II. 7. Shape comparison between the modern LS(1)-0417 and a conventional Airfoil. 21	
Figure II. 8. Data and Shape of a Symmetrical Airfoil (NACA 0006).....	22
Figure II. 9. Data and Shape of a Cambered Airfoil (NACA 4412)	22
Figure II. 10. Front and Top views of the flow pattern on a 3D Finite Wing.....	24
Figure II. 11. Comparison of a 2D Airfoil section (a) and a 3D Wing (b)	24
Figure II. 12. The Resultant aerodynamic force and its components	25
Figure II. 13. Nomenclature of the integration of P/τ distributions over a 2D body surface... 26	
Figure II. 14. Center of Pressure for a 2D body (Airfoil).	27
Figure II. 15. Equivalent ways of specifying the force-and-moment system on an Airfoil	27
Figure II. 16. Forces/Moment Systems of an Airfoil at Zero and Finite Angles of Attack.....	28
Figure II. 17. Typical Pressure distributions around an Airfoil at 0-degree angle of attack....	29
Figure II. 18. Typical pressure distributions around an Airfoil at high (8 and 14) AoA	29
Figure II. 19. Lift and Drag Coefficients Variations with the Angle of Attack.....	30
Figure II. 20. Drag Coefficient Variations with Flight Velocity	30
Figure II. 21. Lift to Drag Ratio Variations with Flight Velocity.....	30
Figure II. 22. Lift to Drag Ratio Variations with the Angle of Attack	31

CHAPTER III

Figure III. 1. NACA 0012 DATA from Airfoiltools.com	32
Figure III. 2. The Application Window of ANSYS 19.0 Workbench	33
Figure III. 3. NACA 0012 Dat file from Airfoiltools.com	33
Figure III. 4. Final look at the Airfoil plot from the XY Plane after importing the Dat file ...	34
Figure III. 5. The Full Sketch containing the Airfoil and the Domain Surrounding it	35
Figure III. 6. Separating the Airfoil from the Domain body	35
Figure III. 7. Domain after the First Face Split with Respect to the ZX Plane.....	36
Figure III. 8. Final look at the Geometry of NACA 0012	36
Figure III. 9. Mesh Refinement around the Airfoil Nose	37
Figure III. 10. Final look at the desired Mesh.....	38
Figure III. 11. The Named Selections of the Airfoil-Wall.....	38
Figure III. 12. The Fluent Launcher Configuration	38
Figure III. 13. Main Panel for Configuring and Launching the Simulation	40
Figure III. 14. Simulation results after convergence for NACA 0012.....	40
Figure III. 15. Lift and Drag Coefficients Versus the Angles of Attack (-12 to 22 degrees) ..	42
Figure III. 16. CL/CD and the Pitching Moment Versus the AoA (-12 to 22 degrees).....	42
Figure III. 17. Lift Coefficient Versus Drag Coefficient	43
Figure III. 18. Comparison NACA 0012 Ansys Simulation Results and XFOIL Data	44
Figure III. 19. XFOIL Results from Airfoiltools.com for NACA 0012.....	44
Figure III. 20. Pressure Coefficient Contours for NACA 0012 at 0 angle of Attack	45
Figure III. 21. Pressure Coefficient Contours for NACA 0012 at -12 Angle of Attack	45
Figure III. 22. Velocity Magnitude Contours for NACA 0012 at 0 AoA and -12 AoA.....	46
Figure III. 23. Y+ values Plots for NACA 0012 at 0 angle of Attack	46
Figure III. 24. Y+ values Plots for NACA 0012 at -12 Angle of Attack.....	47
Figure III. 25. Pressure Coefficient Plots for NACA 0012 at 0 AoA and -12 AoA	47
Figure III. 26. Velocity Streamlines for NACA 0012 at 0 angle of Attack.....	48
Figure III. 27. Velocity Streamlines for NACA 0012 at -12 AoA.	48
Figure III. 28. NACA 0015 DATA from Airfoiltools.com	48
Figure III. 29. Final look at the NACA 0015 Airfoil after importing the DATA File	49
Figure III. 30. Complete Mesh of the NACA 0015 Airfoil	49
Figure III. 31. Solution Convergence and Results from ANSYS Fluent for NACA 0015.....	49
Figure III. 32. Lift and Drag Coefficients Versus the Angles of Attack (-12 to 22 degrees) ..	50
Figure III. 33. CL/CD and the Pitching Moment Versus the AoA (-12 to 22 degrees).....	50
Figure III. 34. Lift Coefficient Versus Drag Coefficient	50
Figure III. 35. Comparison NACA 0015 Ansys Simulation Results and XFOIL Data	51
Figure III. 36. Pressure Coefficient Contours for NACA 0015 at -12 AoA and 18 AoA	52
Figure III. 37. Velocity Magnitude Contours for NACA 0015 at -12 AoA and 18 AoA	53
Figure III. 38. Velocity Streamlines for NACA 0015 at -12 AoA and 18 AoA	54
Figure III. 39. Pressure Coefficient Plots for NACA 0015 at -12 angle of Attack.....	54
Figure III. 40. Y+ values Plots for NACA 0015 at 18 Angle of Attack	54
Figure III. 41. NACA 4412 DATA from Airfoiltools.com	55
Figure III. 42. Final look at the NACA 4412 Airfoil after importing the DATA File	55
Figure III. 43. Meshing of the NACA 4412.....	55
Figure III. 44. Solution Convergence and Results from ANSYS Fluent for NACA 4412.....	56
Figure III. 45. Lift and Drag Coefficients Versus the AoA with comparison to XFOIL Data ..	56
Figure III. 46. CL/CD and the Pitching Moment Versus the AoA (-12 to 22 degrees)	57
Figure III. 47. Lift Coefficient Versus Drag Coefficient for NACA 4412	57
Figure III. 48. Velocity Streamlines for NACA 4412 at 0 AoA and -12 AoA.....	58

Figure III. 49. Pressure Coefficient Contours for NACA 4412 at 0 AoA /-12 AoA/18 AoA 59
 Figure III. 50. Velocity Magnitude Contours for NACA 4412 at 0 AoA /-12 AoA /18 AoA 60

CHAPTER IV

Figure IV. 1.	System architecture.....	62
Figure IV. 2.	Microcontroller architecture	63
Figure IV. 3.	Load cell (left), and electronic module of load cell (right).....	63
Figure IV. 4.	Accelerometer sensor.....	64
Figure IV. 5.	The NXP MPXV7002Dp Airspeed Sensor Kit	65
Figure IV. 6.	Data acquisition electronic circuit	66
Figure IV. 7.	LabVIEW Interface	67
Figure IV. 8.	The Test set-up	67
Figure IV. 9.	The Preliminary Prototype of the Test Chamber Model	68
Figure IV. 10.	The Wing Model	68
Figure IV. 11.	The PlexiGlass Panel Model	68
Figure IV. 12.	The Holder.....	69
Figure IV. 13.	The Stand.....	69
Figure IV. 14.	The Load Cell Model	69
Figure IV. 15.	The Platform Model	69
Figure IV. 16.	The Assembly of all the Pieces into the Wind Tunnel.....	69
Figure IV. 17.	Final look at the Wind Tunnel Design on SolidWorks	70
Figure IV. 18.	A close-up picture of Glass Fiber Bundles.....	71
Figure IV. 19.	Different States of Fibers	71
Figure IV. 20.	Glass Fiber sheets.....	72
Figure IV. 21.	Description of Molding using Glass Fiber and Resin Reinforcement	73
Figure IV. 22.	The Boards made out of Plexiglas.....	74
Figure IV. 23.	Construction of the Airfoil Surface	74
Figure IV. 24.	The Process of Shaping the Wing.....	75
Figure IV. 25.	Preparation of the Glass Fiber and Epoxy Mixture and the Matrix.....	75
Figure IV. 26.	Attaching Glass Fibers to the Wing Surface.....	76
Figure IV. 27.	Impurities Removal and Polishing Process	76
Figure IV. 28.	The Painting of and the Final look at the Wing.....	77
Figure IV. 29.	The Preliminary Steps in the Design of the Support Pieces	78
Figure IV. 30.	Final Look at the Designed Pieces after the Paint job	78

LIST OF SYMBOLS

Symbols	Description
α	Gliding Angle / Angle of Attack
α_i	Induced Angle of Attack
α_{eff}	Effective Angle of Attack
τ	Shear stress distribution
τ_l	Shear stress per unit span on lower surface
τ_u	Shear stress per unit span on upper surface
μ	Dynamic Viscosity
A	Axial Force/Section
c	Sound Velocity
C	Chord Line
C°	Degree Celsius
C_A	Axial Force Coefficient
C_f	Skin Friction Coefficient
C_D	Drag Coefficient
$C_{D_{min}}$	Minimum Drag Coefficient
C_L	Lift Coefficient
CLmax	Maximum Lift Coefficient
C_M	Moment Coefficient
C_N	Normal Force Coefficient
C_P	Pressure Coefficient
d	Diameter
D	Drag Force
D_i	Induced Drag
dA	Section Variation
dV	Velocity Variation
dP	Pressure Variation
dS	Element Area
dp	Density Variation
dMI	Moment per unit span on Lower Surface
dMu	Moment per unit span on Upper Surface
g	Gravity acceleration

I	Reference length
L	Lift
M	Meter
<i>m</i>	Rate of flow
M	Mach number/Moment
M_{LE}	Moment about the leading edge
M_{c/4}	Moment about ¼ chord
M_{TE}	Moment about the Trailing edge
P	Pressure
p	Pressure distribution
p_l	Pressure per unit span on lower surface
p_u	Pressure per unit span on upper surface
q_∞	Dynamic Pressure
ρ_∞	Freestream Density
R	Resultant aerodynamic Force/Ideal gas Cst
Re	Reynolds Number
T	Temperature
U_a	Free Stream Velocity
U_{eff}	Effective freestream Velocity
V, v	Velocity
V_∞	Freestream Velocity
w	downwash
w_i	Induced downwash
X_{cp}	Center of Pressure
Y+	Y Plus Value
Z	Height

LIST OF ABBREVIATIONS

Abbreviation	Description
NASA	The National Aeronautics and Space Administration of the USA
U S A	United States of America
G B	Great Britain
Ft	Feet
Kg	kilogramme
VDT	Variable Density Tunnel
W T	Wind Tunnel
HP	Hours Power
ONERA	National Office for Aerospace Studies and Research (Office National d'Etudes et de Recherches Aérospatiales).
V/STOL	Short or vertical take-off and landing aircraft
PIV	Particle image velocimetry
AoA	Angle of attack
C F D	Computational fluid dynamics
RAF	Royal Aircraft Factory
NPL	National Physical Laboratory
ID	Identification
NACA	National Advisory Committee for Aeronautics
CFX	Compact Form Factor
CD	Drag Coefficient
CL	Lift Coefficient
SW	SolidWorks

Introduction:

Since the dawn of time, human kind has looked to explore the world and conquer its limits. But to do so requires certain risks and calculations to be made beforehand. So instead of going blindly into the abyss of an ocean or into the darkness of space, scientists have always looked for a way to minimize the failed attempts and to experiment in the safest way possible.

And with that came the creation of Wind Tunnels; with the first one built in 1871 by one Frank H Wenham. A trunk as he called it became the first step towards more than a century of technological advancements.

Wind Tunnels were and still are used to test aerodynamical properties of various objects and of various shapes, and then applying those properties on bigger scale modules of the same shape using Dimensional Analysis and Similarity (The Buckingham Pi Theorem).

And so, this has helped us limit the risk of human lives in airplane, automobile and submarine testing.

“They have allowed replacing the flair of the pioneers by the art of the engineers” as stated by the famous scientist “Gustave Eifel”.

Even though nowadays we use Numerical Analysis and Computer power in most of our calculations but we still rely on Wind Tunnels for confirmation and realistic results.

So, Scientists are still improving and thinking of new ways to add to the design and the precision of wind tunnels, whether it be new designs, bigger wind tunnels to test out full scale objects. Or new ways to measure coefficients and give more precise results which we will be working on in this thesis. [1]

This work will consist of:

- An exploration into Wind Tunnel History and Technological Evolution.
- A Theoretical Study of Airfoils and Various Aerodynamic Properties.
- A Numerical Simulation of 3 different NACA Airfoils (NACA 0012,0015,4412)
- A Discussion about the Design, Production and the Instrumentation used in the Experience Conducted in this work.

I- INTRODUCTION:

For more than a century (**Beginning of the 17th Century – 1871**), the aeronauts of the time depended solely on Whirling Arms invented by **Benjamin Robins (1707 - 1751)** to try to measure aerodynamic properties essential to flight.

Although very important breakthroughs were made using them such as the first design of a fixed wing plane model by **Sir George Cayley (1773-1857)** allowing scientists to realise new facts about air resistance and rotary motion; it did not have the desired results because of its many flaws noting primarily the inability to install measuring equipment on it due to the high speed spinning, in addition to the abundance of turbulence caused by the rotary motion.

And thus, a new approach was needed, or rather an improved version of an old thought. The first researchers used the blowing wind in natural caves to replicate the conditions of flight but they still could not control the parameters in use.

Finally facing a dead end, and as the saying goes: “Necessity is the source of Invention”, a breakthrough was made and the first early Wind Tunnel was constructed by the British engineer **Francis Herbert Wenham (1824 – 1908)** and his colleague **John Browning (1831 – 1925)**. A realisation that would lead to many advancements in aerodynamics and with it the first human successful Flight. [2, pp. 1-2] [3]

I.1 Wind Tunnel Definition:

A **Wind Tunnel** is used to replicate real life conditions of flows through full scale models with smaller versions that are easier to handle and run tests on, with the requirement of maintaining the same key parameters stated by **the rules of similarity (geometric, cinematic, dynamic)** in addition to the same **Mach** and **Reynolds** number.

Wind Tunnels can be used in a variety of fields including aerospace engineering, buildings and bridges, submarines and marine vehicles testing, automobile testing...etc

Throughout the years, researchers employed these facilities to comprehend the aerodynamic laws that govern flight in a more detailed manner and are still to this day exploring different avenues even with the arrival of numerical solutions and computational methods. A fine example of that would be **NASA** (The National Aeronautics and Space Administration of the USA) or its predecessor

NACA (National advisory committee for Aeronautics), the **AeroDyn wind Tunnel** in **Mooreville, North Carolina, USA** or the **European Transonic Wind Tunnel** located in **Cologne, Germany**. [3]

I.2 Description and main components:

Although the composition of each wind tunnel varies according to its purpose and its usage; some are designed in a specific way to reach **supersonic** and **hypersonic** speeds, some are modified to be able to withstand very low temperatures (**Cryogenic Wind Tunnels**) in order to **adjust viscosity (μ)** and thus respecting the **Reynolds number** required.

Yet they all essentially utilize the same principal components which are: (**the collector, the test chamber, the diffuser also the walls and the fan with its motor**). [4]

<https://www.grc.nasa.gov/www/k-12/airplane/tunpart.html> [4]

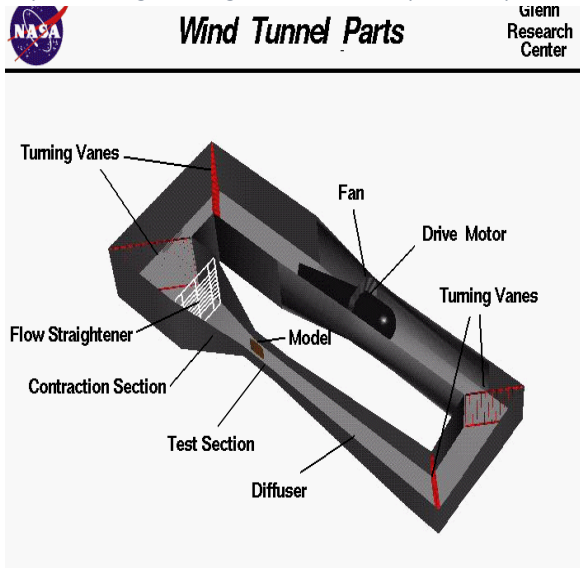


Fig (I-1). Low-Speed Closed Tunnel (NASA)

Fig (I-2). Pitsco AirTech tunnel (NASA)

a) **The Collector:**

As the first component, **the Collector** is of great importance to the functionality of the Wind Tunnel; its main purpose is to **let in** and **slow down** the **Air** coming in through the entry. Specifically, through **flow straighteners** that manage to **stabilize the flow** and **“collect”** the air as the name suggests.

<https://www.grc.nasa.gov/www/k-12/airplane/tunpart.html> [4]



Fig (I-3). Collector of Pitsco AirTech Tunnel (NASA).

The principle here that leads to flow speed reduction is based on **Hugoniot’s relation** concerning the **variation of the velocity (dV)** of the studied fluid along the Wind Tunnel with the **variation of the section of that same Tunnel (dA):**

$$\frac{dA}{A} = (M^2 - 1) \frac{dV}{V} \dots\dots\dots (I.1)$$

- Where “M” is the Mach number defined as: $M = \frac{v}{c} \dots\dots\dots (I.2)$

- And c is the velocity of sound such as: $c = \sqrt{\frac{dP}{d\rho}} \dots\dots\dots (I.3)$

Pierre Henri Hugoniot (1851-1887) implies that the relationship between the **variation of velocity** and the **variation of the section** in question depends on the **Mach number**; meaning **the Flow Regime**.

With: $M < 1 \rightarrow$ Subsonic Flow.

$M = 1 \rightarrow$ Sonic Flow.

$M > 1 \rightarrow$ Supersonic Flow.

And so, if the flow is **subsonic** the section ($M^2 - 1$) becomes **negative** leading to **opposite variations** of the **velocity** and **section** which means that as the section **gets smaller**, the **speed increases** like in the case of **the collector**.

The **opposite** happens in **the diffuser** characterized with an **increasing section** that results in **decreasing speed**.

On a parallel view, it also depends on the mass conservation law:

$$\dot{m} = V.S = Cst \quad \dots\dots\dots (I.4)$$

Which states that the **product of the velocity(V) and section (S)** is always **constant** meaning **the rate of flow (\dot{m})** is always **constant**. Hence, if you **decrease the section**; the **velocity** would **increase** automatically which is precisely what we want [1] [4] [5]

b) **The Test Chamber:**

The most important part of a Wind Tunnel is its **Test Chamber**. It's where the **model** is located and where we install the different instruments to measure **Lift, Drag** and other coefficients. Air Flows through the exit of the collector and into through the studied **model** and into **the diffuser**, the chamber's dimensions are always the smallest part of the Tunnel (**the throat**) to get the biggest Velocity possible as stated by **(I.1)**.

To understand how the flow behaves around the body, many **visualisation techniques** are used; From **dye to threads** attached to the model. And In order to pick up data concerning **the aerodynamic factors**, the walls of the chamber have a window on both sides of it to observe what happens during the process. [4]

<https://www.grc.nasa.gov/www/k-12/airplane/tunpart.html> [4]



Fig (I-4). model of an F-5 fighter in the Test Chamber of a Pitsco AirTech Tunnel (NASA).

c) **The Diffuser:**

A revolutionary development in Wind Tunnel technology, **the Diffuser** allowed researchers to cut down drastically on the electrical power needed to operate **the Fan (a reduction by a factor of 3 from its predecessor)** while also improving the airflow speed **(an increase of almost 78% at the time)**.

It generally comes right after the **Test Chamber** separated by a **small Collector** at the exit of the Chamber with a diameter larger than that of the entrance. **The Diffuser** is a **divergent tube** that is placed there to reduce the air **velocity** coming out of testing and simultaneously recovering **Pressure** in front of the **Fan**.

It was patented on **November 28th 1911** by the **French scientist Gustave Eiffel (1832-1923)**. And it was inspired by **Bernoulli's Law** stating that the **Pressure** and the **Velocity** of a fluid for an **incompressible flow** vary Inversely.

$$\text{It goes as follows: } \frac{v^2}{2} + gz + \frac{\rho}{P} = cte \dots\dots\dots (I.5)$$

$$\text{Which leads to: } \frac{v^2}{2} + gz = cte \times \frac{P}{\rho} \dots\dots\dots (I.6)$$

-By **decreasing** the **Velocity** of the air coming in through **the Diffuser**, the **Pressure** of the **Test section** exit is **reduced**. In result, the **Pressure difference (ΔP)** of either side of the **Fan** is much less than if the **Wind Tunnel** had no **Diffuser** and in consequence, it needs **less electrical power** to operate.

<https://www.grc.nasa.gov/www/k-12/airplane/tunpart.html> [4]



Fig (I-5). The Diffuser of a Pitsco AirTech Tunnel (NASA)

-The **decrease** in **velocity** is achieved following the **Hugoniot relation** discussed before; Thus, in **subsonic flow** if the section **gets larger**, the **speed decreases** like in **the Diffuser**. [1] [4]

d) **The Fan:**

The last component is the **Fan** that draws the Air in through the **Collector**. Powered mainly by an **electrical motor**, it may seem like a trivial part but it actually determines largely the **velocity of the flow** fed into the **Testing section**; recirculating the air through the room in the case of an **open Wind Tunnel** or through its own tubes in the case of a **closed one**.

It comes in many sizes and materials depending on the mission of the Tunnel it's employed in. For the most part it's located **downstream** of the **Test Chamber (Suction)** so that it doesn't interfere with **the model** and also to guarantee **quality flow**, yet it can also be situated **upstream** of the model in some older Tunnels. [4]

<https://www.grc.nasa.gov/www/k-12/airplane/tunpart.html> [4]

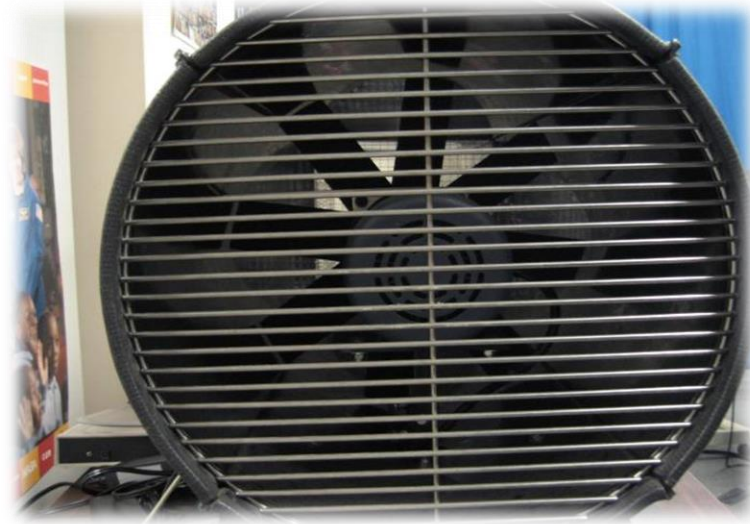


Fig (I-6). The Fan of a Pitsco AirTech Tunnel (NASA) located downstream of the Test Chamber.

With:

- **Upstream:** The direction where the air is **coming** from relative to the **Test Chamber**.
- **Downstream:** The direction where the air is **going** relative to the **Test Chamber**.

I.3 Chronological History of Wind Tunnels:

In order for the **Wind Tunnel Technology** to get where it is right now, it had to go through many steps along the way; steps that helped it become the main research mean for **aerodynamics** and **Fluid Mechanics** throughout the **20th century** and still standing to this day. Steps like:

I.3.1 Before the modern Wind Tunnel:

After the **aerodynamicists** realised that to be able to fly a heavier than air object they needed to be able to replace the natural winds with a controlled stable substitute, they began using natural sources such as cave mouths and ridges where they placed a model above it to let the air flow pass through it. Others adopted the opposite method. Meaning instead of letting air pass through the object they would throw the object into the air but they soon returned to the new found principle of **Wind Tunnels**.

They also employed other **aerodynamic** tools like the **whirling arms** that helped create the first successful **unmanned gliders** by **Sir George Cayley (1773-1857)**. [2, pp. 1-2]

I.3.2 The First Wind Tunnels powered by a Steam Engine:

In time, whirling arms proved to have many flaws such the difficulty to put instruments on it and get results at such high rotating speeds. council member of the **Aeronautical society of Great Britain** **Frank H Wenham (1824-1908)** was the first to act and urge the council to build it with his partner, he is credited designing and testing the first **Wind Tunnel** in **1871**. it "**had a trunk 12 feet long and 18 inches square, to direct the current horizontally, and in parallel course.**" As he put it. It had a **fan blower upstream** of the model powered by a **steam engine** like that of **Horatio Frederick Philips (1845-1924)** in which he studied a wide variety of Airfoil shapes to investigate **Lift**. [2, pp. 2-5]

<https://ntrs.nasa.gov/archive/nasa/casi.ntrs.nasa.gov/19930086410.pdf> [6]

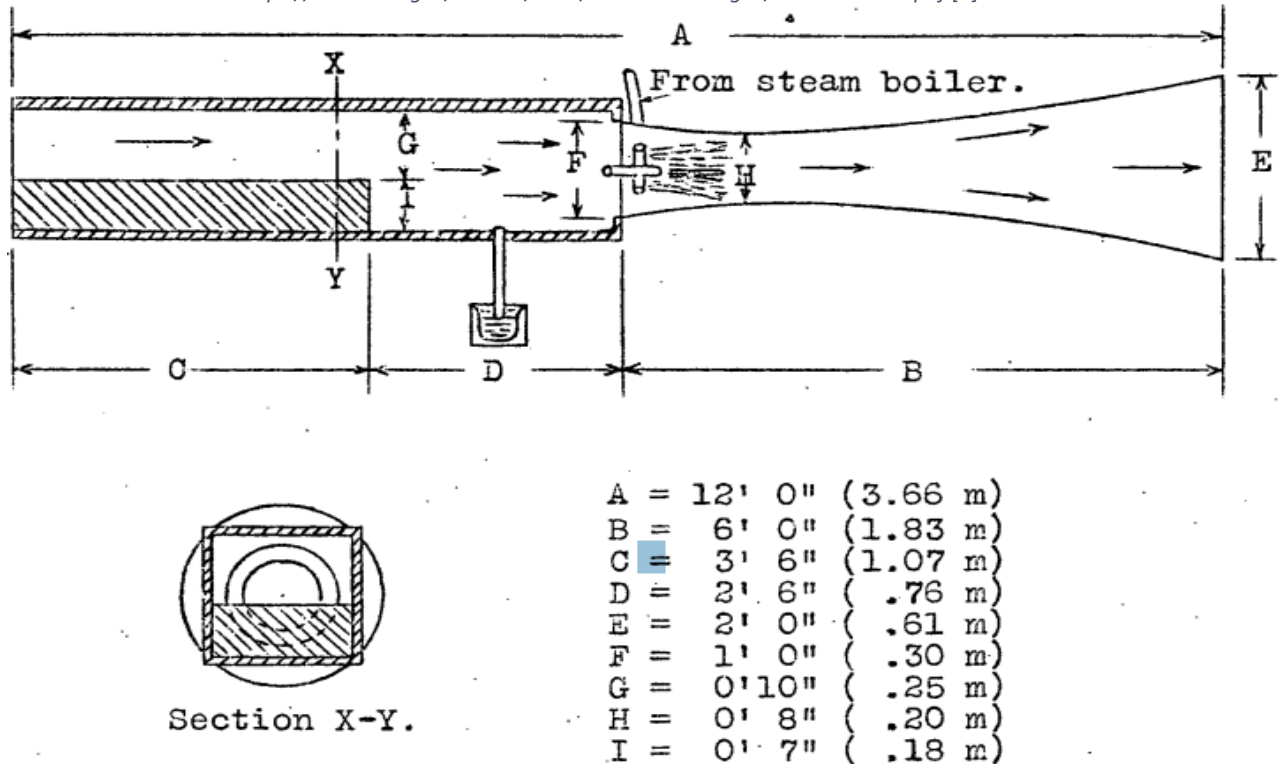


Fig (I-7). First Aerodynamic Tunnel (1885) of Horatio Philips (1845-1924)

I.3.3 The emergence of the air driven Wind Tunnels:

As technology advanced so did the ambition of the coming scientists, this time to develop the means of pushing air through the **Tunnel**; and thus, came the idea of using a **fan** located **upstream** of the **model** to propel airflow into the **Chamber**. Adopted by a lot of renowned and famous researchers like “**Charles Renard (France,1896)**”; “**Hiram Maxim (Great Britain,1896)**”; **Konstantin Tsiolkovsky (Russia,1897)** it gave the push the field of aviation needed, **but then came the wrights:**

Orville (1871-1948) and Wilbur (1867-1912) Wright (USA,1901):

Following **Samuel P. Langley (1834-1906)** and observing his problems with whirling arms, the **Wright brothers** decided to switch their focus on **Wind Tunnels** instead. After building their first flying machine “**glider n°1**” in **1899** and testing it they noticed it was generating so much less **Lift** and much more **Drag** than they calculated so they began studying **aerofoils** and comparing them. Coming to the conclusion that the available **aerodynamic** tables at the time were immensely in error.

The brothers started making modifications to their model and made “**Glider n°2**” that flew but did not perform as they wanted it to, as stated in their own words : “**Having set out with absolute faith in the scientific data, we were driven to doubt one thing after another, till finally after two years of experimentation, we cast it all aside, and decided to rely entirely upon our own investigations.**” They began with a series of Tests on different aerofoils confirming their suspicions to cast aside the existing data. Having to write their own **data book**, they required a **Wind Tunnel**.

Their first **Tunnel** had a square section to channel the air, a fan **upstream** of the **model** and a **balance** mounted in the airstream composed of two elements; a **calibrated** and a **cambered plane surfaces** with the second inclined at the **same angle** but **opposite** in direction. As the air moved the **vane-type balance** turned indicating the relative **Lifting forces**.

The results were so promising that the **Wrights** built a second bigger and more elegant **Tunnel** with **16 square-inch (103cm²)** test section and that’s where they got their very important data to operate their first manned powered aircraft “**Wright Flyer**”. And consequently, they surpassed in just **3 years**

aerodynamicists of the time by leaps and bounds and after the brothers changed the game in the flight field, **European** countries started making their own advancement in an effort to catch up. [2, pp. 5-9]

I.3.4 Post Wright Brothers and Downstream fans:

<https://history.nasa.gov/SP-440/ch2-2.html> [2]

Date	Size	Individual	Location
1901	16 x 16 in.	Wright Bros.	Dayton, Ohio
1901	6 x 6 ft	Zahm	Catholic University, USA
1903	2 ft diameter	Stanton	National Physical Laboratory, England
1903	1 x 1 m	Crocco	Rome, Italy
1904	1.2 m diameter	Riabouchinsky	Koutchino, Moscow, Russia
1908	2 x 2 m	Prandtl	Gottingen, Germany
1909	1.5 m diameter	Eiffel	Champ de Mars, France
1910	4 x 4 ft	n/a	National Physical Laboratory, England
1912	7 x 7 ft	n/a	National Physical Laboratory, England
1912	2 m diameter	Eiffel	Auteuil, France
1912	Junkers	Aachen, Germany	n/a
1913	8 x 8 ft	Zahm	Washington Navy Yard, USA
1914	4 x 4 ft	Hunsaker	MIT, USA
1916	2.2 x 2.2 m	Prandtl	Gottingen, Germany
1917	5.5 ft diameter	Durand	Stanford University, USA
1917	7 ft diameter	Curtiss	Hempstead, New York, USA
1918	7 x 14 ft	n/a	National Physical Laboratory, England
1918	4.5 ft octagon	n/a	Bureau of Standards, USA
1919	4 x 4 ft	Ober	MIT, USA
1919	7.5 ft diameter	Durand	Stanford University, USA

Table (I-1). Post Wright brothers Wind Tunnels.

Another considered configuration was placing **the Fan downstream** of the **model** that meant no interference with the flow inside **the Chamber** and with it came the introduction of **the diffuser** that led to revolutionary steps toward the current **Wind Tunnel**. This method had been developed very quickly and before the first half of the century there were hundreds of it all over the world.

Many scientists at the time favoured this method and worked with it such as **Nikolai Zhukovsky (Russia,1902)**; **Thomas Stanton (Britain,1903)**; **Dimitri Riabouchinsky (Russia,1905)**.

Gustave Eiffel (France,1909)

Alexandre Gustave Eiffel (1832-1923) started the **French** race for the development of flight with his **drop machine** that he used from the **Eiffel tower's second floor**. But that did not satisfy his thirst for a breakthrough so he built his **Wind Tunnel** at the foot of the **Eiffel tower** named after him in **1909** in the "**champ de Mars**". It remained operational **until 1911** and was moved by a **Fan** powered by a **50 Horsepower electric motor**, with a **diameter of 1.5m** and an **air speed of 18m/s**.

he proceeded to compare the results obtained from the **Tunnel** with the ones from the **drop machine** and then validated the **Wind Tunnel Principle** that stated that studying an object at rest with air flowing through it is the same as testing it in movement through resting air.

Eiffel had to relocate in the beginning of **1912** and rebuild a **Tunnel in Auteuil**. He kept the same engine but wanted to get a new larger **Fan of 3.8m in diameter** weighing **8500kg** to get better performance that corresponds with his brilliant idea of adding a Diffuser. The new Design had a test section of **6.56feet (2m) in diameter** and a wind speed of **105 feet/s (32m/s)** which is a huge leap from the previous recorded speed (**almost 78% increase**) making the fastest Tunnel at the time. He made numerous tests in **Auteuil** on Wings, landing gear, fuselages ...etc and his work helped **France** immensely to get ahead in **Aircraft Technology**. [1]

Ludwig Prandtl (Göttingen, 1909):

The German Engineer **Ludwig Prandtl (1875-1953)** in his turn also made a breakthrough in the field of **Wind Tunnels** with the first ever closed-circuit return flow Tunnel, it provided better fuel efficiency and controlled test conditions (**Temperature, Pressure, Humidity...etc**). He placed vanes at the corners to turn the airflow and honeycombs and screens in various places to stabilize it. **The German** tested **aerofoils, streamlined bodies** and many components in addition to the first of measuring **pressure distributions** over rotating propeller blades.

<https://history.nasa.gov/SP-440/ch2-5.html> [2]

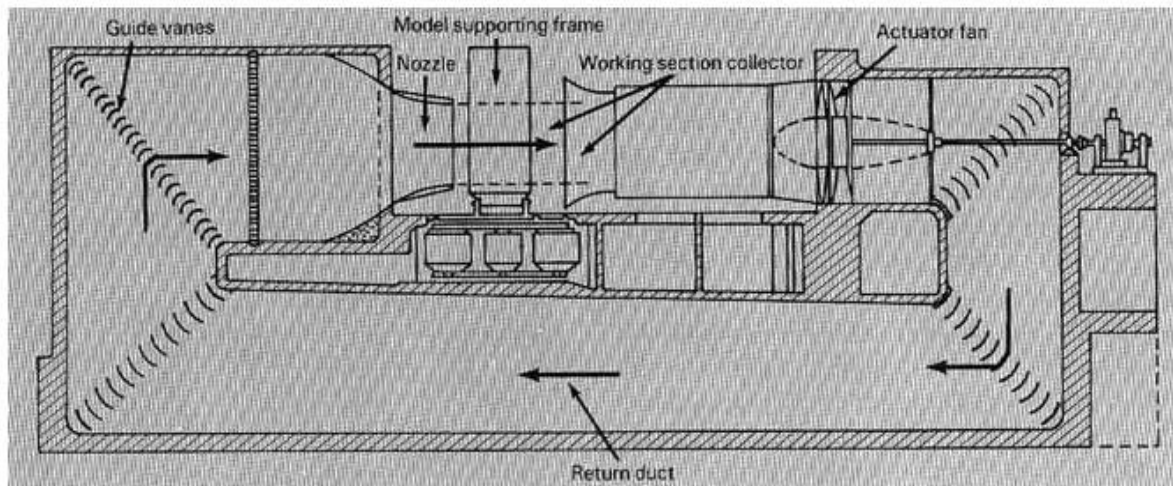


Fig (I-8). Prandtl's second generation Wind Tunnel (1916).

Modern **Wind Tunnels** incorporate both **Eiffel** and **Prandtl's** designs (**Closed Circuit Tunnels and the Diffuser**). **Prandtl's** Tunnel had a clash with **Eiffel's** when **Gustave Eiffel's** measurement for the drag of a sphere got less than half the results that **Prof August Föppl (1854-1924)** got with **Prandtl's** machine. So, after being declared at error, he started doing tests on sphere with different dimensions.

He discovered that there are two separate flow regimes for each sphere depending on the **velocity** and that **transition** happens for the same "**Vxd**" (**V** being the **velocity** and **d** being the **diameter**) considering **viscosity as constant**; which is similar to **Reynolds's number** confirming its importance and the value of knowledge exchange between scientists. [1]

Reynolds number being given by **Osborne Reynolds (1842-1912)** as: $Re = \frac{\rho \cdot V \cdot l}{\mu}$ (I.7)

I.3.5 A leap to modern day Wind Tunnels:

The beginning of NACA (1915-1958):

American scientific societies took it into their own hands and decided to build their first facility during and after the events of **WWI** and resulted in "**NACA Wind Tunnel N°1**" (**1920**) which was not very successful or of any significance in terms of new feats due to the inexperience of the **American** staff but it helped them put roots in and gain some experience. But then came the **VDT (Variable Density Tunnel)** which took the world by surprise, because all previous facilities were unable to fully replicate flight conditions due to the inability to condition the same **Reynolds** number which is a must as stated **by the rules of Similarity**: [2, pp. 14-19]

The Rules of Similarity:

For accurate results when trying to simulate wind and flight conditions in high altitudes in **Wind Tunnels** and similar machines, it is conventional that some rules need to be respected **which are**:

- 1- Same **geometrical Shape** of the **full-scale body** and the **replicated model**.
- 2- Same **Mach** number $M = \frac{v}{c}$. (I.8)
- 3- Same **Reynolds** number '**Re**' (**Same** ρ, μ, v). [1]

To compensate for the low Re , the VDT operated under the pressure of **20 atm** which would in return raise the air density according to the perfect gas law " $P = \rho RT$ ". (I.8) It was an obvious solution but never thought of before NACA, the Re would be then the same as in full scale flight.

The VDT (June 1921) was the first high pressure tunnel of any size, it had a massive pressure tank wall of **34.5 feet (10.56m)** in longitude and **15 feet (4.57m)** in diameter, the thickness of the walls was around **2-1/8 inches (5.08cm)** while the test section was around **5 feet (1.52m)** in diameter and the max speed was only **50mph (80km/h)** because it was the pressure that was relevant.

<https://history.nasa.gov/SP-440/ch2-8.html> [2]

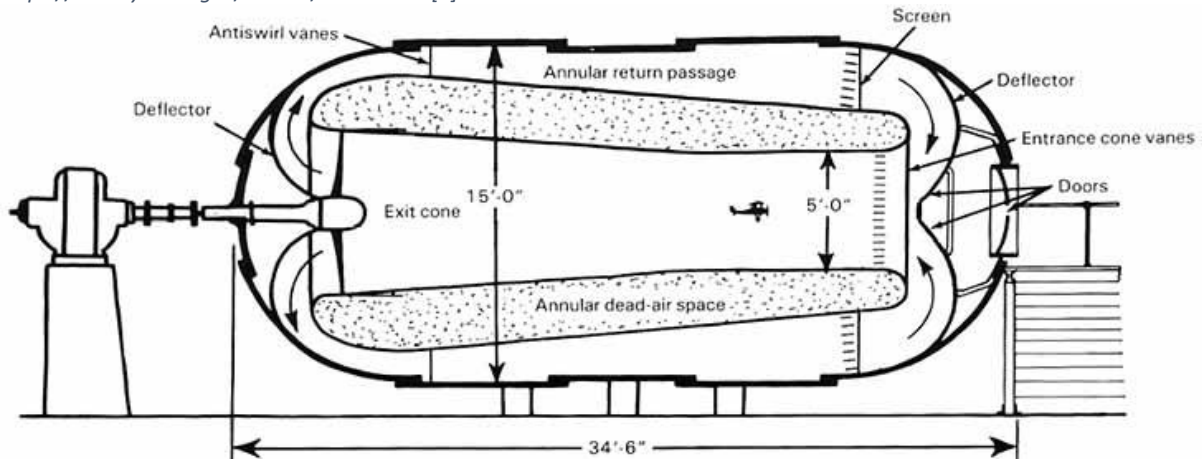


Fig (I-9). Cross section of the variable density tunnel showing the annular flow of returning air.

It became the main source of **aerodynamical data**, a lot of models and shapes were tested but the most important contribution to the scientific society was **around 1933** with the published **NACA Technical Report 460** that contained aerodynamical data for the famous **NACA aerofoils** still used to this day that massively helped develop flight technology. without forgetting the **5-foot tunnel** constructed to replace **Wind Tunnel n°1**. The new thing in it is that it's rotated by **90 degrees** so allowing the study of aircraft spinning which was and still is a problem for pilots when losing control of the airplane. [2, pp. 14-19].

European efforts following NACA:

The **European** community had a different view on how to overcome the **Reynolds number** issue, their approach was to build bigger tunnels allowing to study full scale models. Like the **large Chalais-Meudon S1Ch Wind Tunnel (France)** built between **1932 and 1934**. It had an entrance of **350m²** to reach the velocity of **180km/h** and was equipped with **6 Fans of 1000 HP each**. It was discontinued in **1977** when it became outdated and was replaced by the **F1 Wind Tunnel of Le Fauga-Mauzac (France, 1974)** that was a pressurized Tunnel of a rectangular **Test chamber (4.5m x 3.5m)** with a speed of **430 km/h**. It followed the same principle of NACA's VDT of adjusting air density to raise the **Reynolds number (its pressure reached 3.85bar)**.

[A%20century%20of%20wind%20tunnels%20since%20Eiffel.pdf](#) [1]



Fig (I-10). View of the large S1Ch wind tunnel in Meudon (© ONERA).

But the real accomplishment was made in **Cologne-Germany** being the **ETW (European Transonic Wind Tunnel)** in **1994**. Its principle was to rather than manipulate the **density** only, why not work also on the **dynamic viscosity (μ)** since it's also a part of the **Re number** composition and it depends on **Temperature** as stated by the **Sutherland Formula**. In result, by lowering the **Temp of the Tunnel** we decrease the **viscosity** and cause an increase in **density** due to the **ideal gas law**. Its **Temperature** could reach **100K** and **Mach 1.35** being a **Transonic Tunnel**. [1]

<https://www.grc.nasa.gov/WWW/K-12/airplane/viscosity.html> [4]

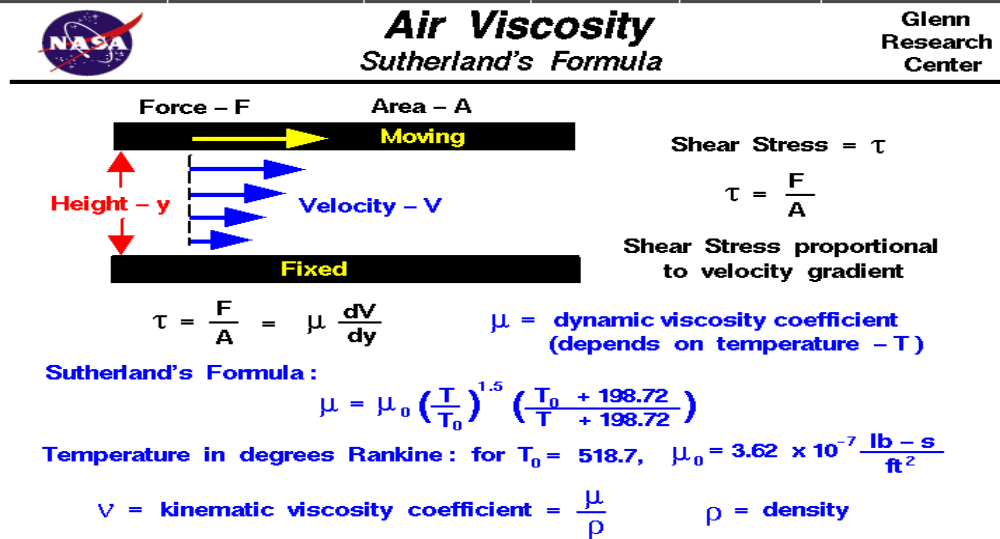


Fig (I-11). Sutherland's Formula for Viscosity as a function of Temperature.

I.3.6 Modern age and High-Speed Wind Tunnels:

The repercussions of WW2 called for immediate considering of the next level of manned or unmanned flight, nations started investing in the new comer **Supersonic Wind Tunnels** to simulate faster than sound aircrafts. And this is where **Hugoniot's** relation comes into play where everything is reversed above **Mach 1**; a **convergent** section would slow air down instead of speeding it and the opposite happens for the **divergent** part so the Tunnels had to adapt to this newfound realisation. [1] **And so, breaking the sound barrier was what every aeronautics scientist and enthusiast would talk or think about at the time and thus it led to this new generation of Tunnels:**

A new Solution appears for supersonic:

<https://history.nasa.gov/SP-440/ch5-2.htm> [2]

Speed Regime	Typical flow (model)	Nozzle/test section	Compression ratio	Drive system
Subsonic (M = 0 to 0.7)			1.0+	
Transonic (M = 0.7 to 1.2)			1.1	
Supersonic (M = 1.2 to 5)			2 (M = 2)	
Hypersonic (M > 5)			20 (M = 5)	

Table (I-2). Characteristics of wind tanners designed for the different speed regimes.

In light of this new development, Test sections were placed **downstream** of the **throat** (**Mach = 1**).
But to get the desired result, A set of 3 major modifications had to be made for this to work:

- 1- **Interchangeable nozzles** or flexible moving walls or changing its shape for each **Mach** number.
- 2- Compensating the huge energy losses during **Supersonic flow** by adding **multistage compressors**.
- 3- The **airflow** must be completely clean and pure and avoiding the condensation of its moisture is of the utmost importance. This can be avoided drying the air to extremely low dew points.

It also requires it to be in the form of a **Convergent-Divergent** duct made possible by the **Swiss Jacob Ackeret (1898-1981)** by building the first **Supersonic Tunnel** in **1935** inspired by the **Swedish** engineer **Carl de Laval (1845-1913)** and his idea. For example: The **Tunnels** designed post **WW2** by **NACA** at **Langley (1948)**, **Ames (1945)** and **Lewis (1948)**. [2, pp. 49-75]

Without forgetting to their European counterparts being the **S5Ch wind tunnel in Meudon (1954)** taking their part in uncovering the mystery of **Supersonic** flight. [1]

Hypersonic speeds and the space age Wind Tunnels:

Hypersonic regime is basically where aerodynamic heating becomes important in the design and that is generally considered to be from **Mach 5** and above. **Hypersonic Tunnels** are essentially the same as their **Supersonic** counterparts in design with the modification of nozzle size and shape and the fact that they consume much more energy and so need to be **intermittent**, it goes without saying that in these high speed regimes **Fans** are replaced with **fuel powered alternatives** to get the power needed for such a feat.

But the major difference is the emergence of a new factor, which is the extreme **Temperatures drops** due to the transformation of **latent heat** to **kinetic energy**. In **Supersonic** facilities we solve this problem by merely keeping the air moisture from **condensing**, but in this case the air itself is in risk of complete liquification (**Air in the nozzle at around 93C° would drop to -212C° in the Test Chamber**) and so an obvious solution would be to heat the air before entering the nozzle (**up to 1648C° and a pressure of 100atm**).

The first **Hypersonic Wind Tunnels** were designed by the **Germans in WW2** to test their hyper speed ballistic missiles, they could attain **Mach 5 to 10** on an intermittent basis. Decades later and during the cold war with the successful orbiting of **Sputnik**, began the race of the space age and that refreshed the investment into **Hypersonic Tunnels** with the **USA's** new **NASA** organization- following **NACA** and so in **1957 Ames** engineers designed a large **Wind Tunnel** that could subject larger models than previously possible to airspeeds between **Mach 5** and **Mach 10** with interchangeable nozzles of **Mach 5,7,10 and 14**. [2, pp. 49-100] [1]

1.4 Wind Tunnel Classification and Types:

There are many criteria that goes into classifying a Wind Tunnel depending on the regime, the mission and other things. Mentioning:

- Speed Regime:

The main thing that is used to differentiate between Tunnels is the Speed with which the airflow passes through the facility.

The Mach number is what separates them and makes these different classifications:

- 1- **Subsonic Wind Tunnels:** ($M < 0.8$) The effects of compressibility are often ignored and that makes it relatively simpler to use.
- 2- **Transonic Wind Tunnels:** ($0.8 < M < 1.2$) The effects of compressibility are considered.
- 3- **Supersonic Wind Tunnels:** ($1.2 < M < 5$) The effects of compressibility are considered and we must make preparations to avoid air moisture condensation.
- 4- **Hypersonic Wind Tunnels:** ($M > 5$) The effects of compressibility are important and strict preparations are made to avoid the complete air liquification. [7]

- **Tunnel Geometry:**

For this, they can be put into 3 distinctive categories:

- 1- **Open Return Wind Tunnels:** It's open on both ends of it and lets air circulate through the room and back into it.
- 2- **Closed Return Wind Tunnels:** It is closed down and uses its own structure to recirculate the airflow, it comes in many shapes and designs.
- 3- **Blow Down Wind Tunnels:** They possess highly pressurized containers upstream of the Testing Chamber and low-pressure ones on the other end of it and are used for Supersonic and Hypersonic operations. Shock Tubes are a kind of Blow Down Tunnels. [7]

- **Fluid running through it:**

It also depends on the working fluid it contains; different fluids are tested for different purposes for example:

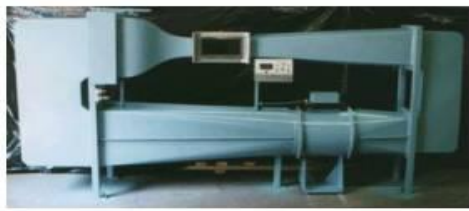
- 1- **Air:** most Low speed Tunnels use air because it is obviously what we want to be testing in aerodynamics.
- 2- **Water:** To visualise Shockwaves of highspeed operations since air is invisible, water is used in Tunnels sometimes in addition to submarine testing and other sea vehicles.
- 3- **Gases:** such as Nitrogen or Helium were used in Hypersonic Tunnels for their special characteristics, for ex: Helium has a very low liquifying temperature of around 0K, or cryogenic Nitrogen for high Reynolds numbers in Transonic flows. [7]

- **Mission:**

Requirements for Wind Tunnels also differ depending on what they are designed and used for, take as an example:

- 1- **Aeronautical Wind Tunnels:** This means all the Tunnels used in aircraft development such as High Reynolds number Tunnels, Pressurised Tunnels, Cryogenic Tunnels, High-Altitude Tunnels, V/STOL and Spin Tunnels...etc
- 2- **Automotive Wind Tunnels:** Used for the testing of automobiles they primarily focus on studying the flow through the chassis like External Flow Tunnels or to study braking systems and other systems under the influence of different climatic situations named Climatic Tunnels.
- 3- **Aeroacoustics Wind Tunnels:** As their name suggest, they are used in the study of noise reduction and all Aeroacoustics phenomena.
- 4- **High Enthalpy Wind Tunnels:** Used primarily to simulate Hypersonic conditions.
- 5- **Propulsion and engine Testing Wind Tunnels:** This type of Tunnels require a precise study of their material resistance to extreme thermal and chemical conditions from exhaust gases of turbines and Rockets. [3] [7]

<https://www.grc.nasa.gov/WWW/K-12/airplane/tuntype.html> [7]



Subsonic, Closed Return



Water Tunnel



**Subsonic
Open Return
Full Scale**



**Supersonic
Closed Return
Propulsion**



**Subsonic
Open Return
Smoke Tunnel**

Fig (I-12). Some Types of Wind Tunnels.

1.5 Instrumentation and Sensors used in Wind Tunnels:

Designing a Wind Tunnel is really complicated and requires a thorough study before realising it

Since any aerodynamical theory cannot be validated unless it is proven experimentally in **Wind Tunnels** then in flight, and with the rise of electronics, Instrumentation now is wildly appreciated and with it **Wind Tunnels** now can do a massive amount of work in just a few hours due to the automation of the tasks and with **Hybrid Tunnels** being under development.

With digital and computer assisted calculations and laser based instruments, cryogenic and magnetic operations, Technology is certainly agreeing with the **Wind Tunnel** pace so we can safely say that as they did in the past century, we can assume that these facilities will always play an real role in the advancement of science, aerodynamics, flight both economic, military and of course Space discovery.

In addition, Wind Tunnels are equipped with:

- Balances to measure Lift and Drag coefficient.
- Gauges and equipment to test the moments.
- Instrumentations like Pitot's tube to note and calculate the airspeed.

www.gavinkananda.com/design-build-and-assembly-of-a-3component-wind-tunnel-force-balance-for-low-re-wings [8]



Fig (I-13). Full-Scale Wind Tunnel Force Balance for Lift and Drag measurement.

Figures (I-14), (I-15), (I-16), illustrate examples of Wind Tunnel test equipment such as Force Balances, Air speed sensors, Strain gages and Pitot Tubes.

https://www.researchgate.net/publication/324623926_Experimental_validation_of_a_novel_piezoelectric_energy_harvesting_system_employing_wake_galloping_phenomenon_for_a_broad_wind_spectrum/figures?lo=1 [9]

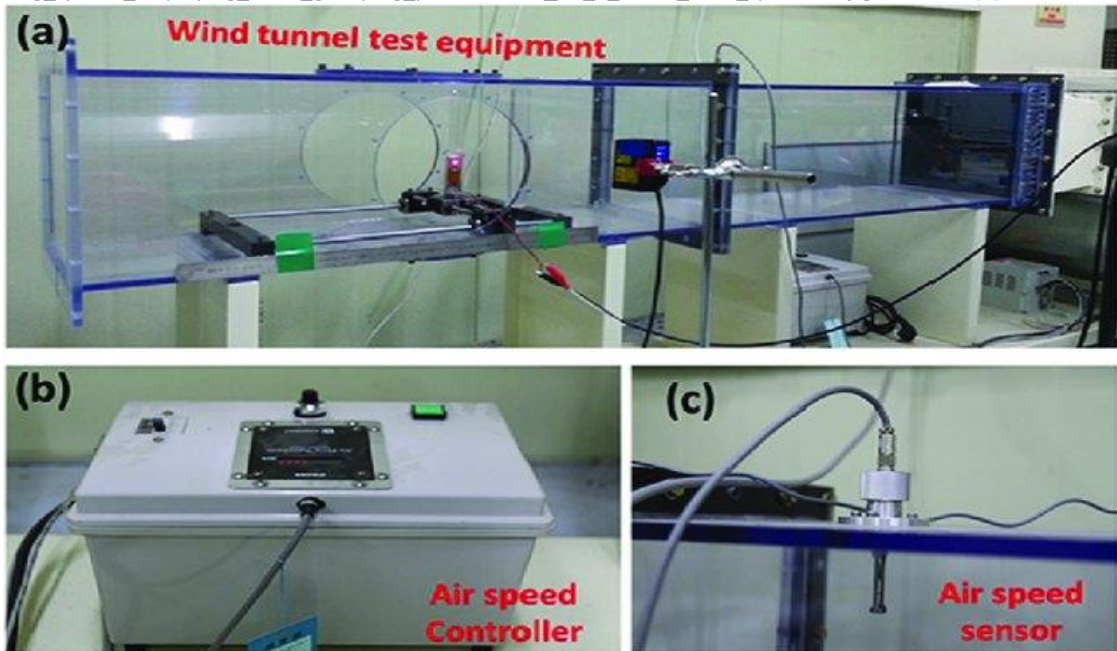


Fig (I-14). (a) General View of Wind Tunnel Test equipment – (b) Air Speed Controller – (c) Air Speed Sensor.

<https://www.grc.nasa.gov/www/k-12/airplane/shortt.html> [4]

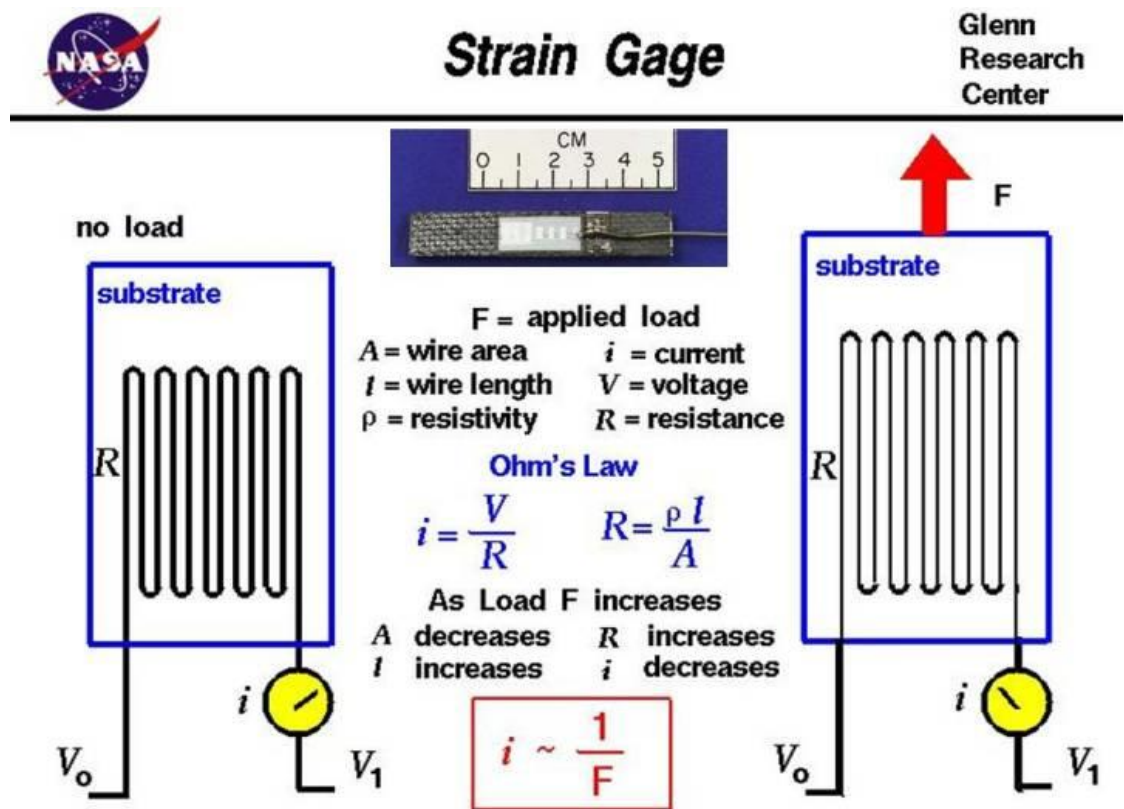


Fig (I-15). Example of a Strain Gage and the Principle it is based on.

<https://www.grc.nasa.gov/www/k-12/airplane/shortt.html> [4]

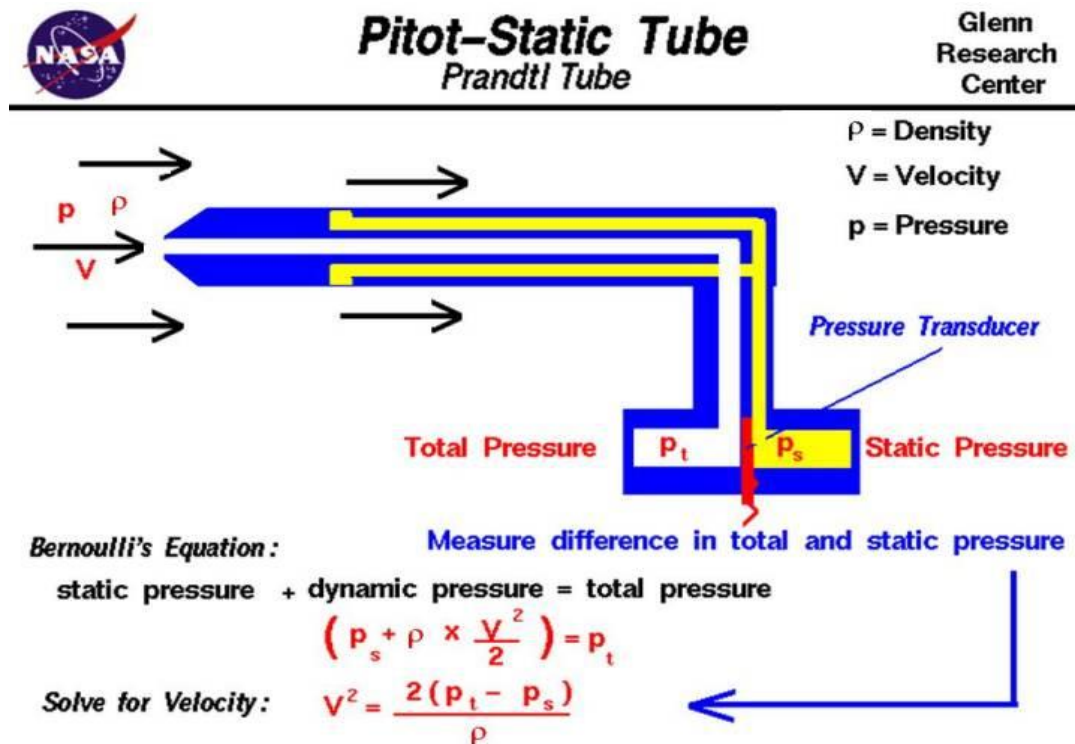


Fig (I-16). An example of a Pitot-Static Tube and the Principle it is based on.

I.6. Conclusion:

With the advancement of technology and the birth of new ideas and since we live in the electronic age, CFD methods and computer-based research schemes are what dominates scientific studies. Numerical solutions play a massive role for the study, the analysis and the simulation of the aerodynamic problems.

All of this required always and still requires validation using Wind Tunnels as the source of real-life experimental data and so Huge facilities are still exploited to this day by space agencies, automobile manufactures, aeroacoustics researchers, even by racing specialists to determine the most efficient aerodynamical shape for their respective field.

And so, we still expect breakthroughs and new methods, new schemes and techniques to better integrate modern technology into our Wind Tunnels. Scientists still are ambitious about new and more advanced Tunnels that have once helped man fly, reach space and make it all possible.

II- INTRODUCTION:

In Aerodynamics, the shape of the object is essentially all that matters. The goal is to get as much Lift as possible with as little Drag as possible, to achieve that; a thorough study is made through various stages. This kind of study is made in Wind Tunnels, researchers were always interested in the perfect shape that allows efficient flight with as minimal setbacks as possible and experimented with plane rectangular objects, spheres, blunt shapes.... Etc

As a result, they discovered numerous properties and revelations such as the center of pressure and that the most efficient form was the shape of wings. More precisely, airfoils which are a cross section of wings were studied and categorized giving us the famous NACA airfoils series and with it a new chapter in Aeronautics.

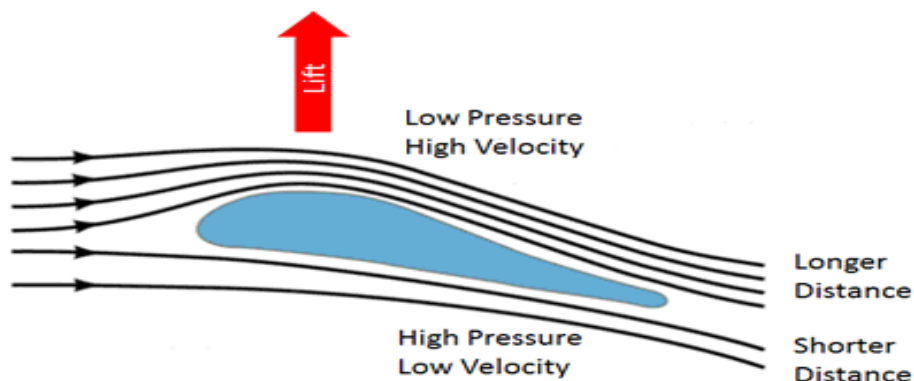
II.1. Airfoils and Aerodynamic Shapes:

The Wright Brothers opened the world's eyes for the importance of Aerodynamics, Scientists began thinking of better ways to produce Lift to fly fixed plane surfaces and later rotors for helicopters, they even experimented on other shapes to see their aerodynamic capacity such as calculating drag coefficients for Spheres and Cylinders.

With the later realisation that the optimal shape was fixed surfaces containing some kind of curvature to create the difference in pressure distribution that results in Lift according to the momentum conservation Law stated by Daniel Bernoulli (1700-1782). [10, p. 277]

https://www.mpoweruk.com/flight_theory.html [11]

Aerodynamic Lift – Explained by Bernoulli's Conservation of Energy Law



Also known as the "Longer Path" or "Equal Transit" Theory

Fig (II-1). Aerodynamic Lift explained by Bernoulli's Law.

II.1.1. Airfoils:

The work on Airfoils was the gateway to the realisation of last century's most incredible aerial designs. Dating back to the 1700s, they were what gave wings their current form. Things further developed around 1912-1918 in the Gottingen Wind Tunnel in Germany, when Ludwig Prandtl and his fellow researchers explained that the study of wings could be split in two:

- 1- The study of the Airfoil.
- 2- The changes in those Airfoils to account for the complete finite wing. [10, p. 277]

II.1.1.1. Airfoils Description:

An Airfoil is simply the cross-sectional shape obtained by the intersection of an airplane wing and a perpendicular plane as shown in the Fig (II-2).

Anderson-Introduction to Flight [12, p. 197]

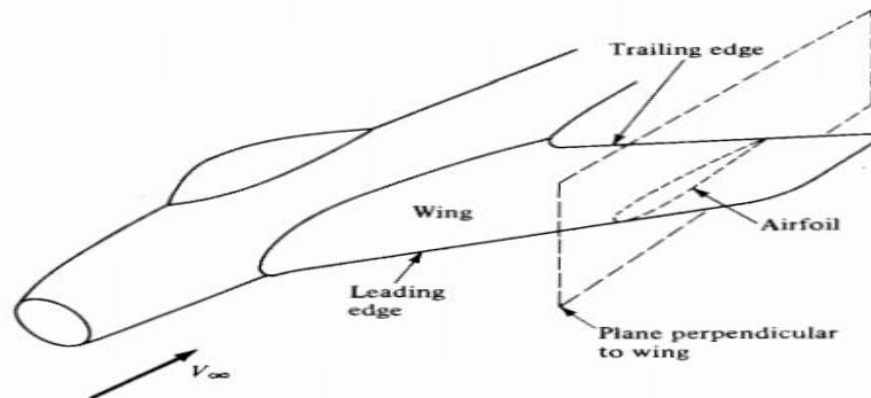


Fig (II-2). Sketch of an Airfoil relative to the wing.

To describe Airfoils, we need to go through the following defining characteristics such as:

-The mean camber line: The most important of them and it's defined as the group of points halfway between the upper and lower surfaces as measured perpendicular to the mean camber line itself.

-The Leading and the Trailing edges: We call the leading edge the most forward point of the mean camber line and the point in the absolute rear the trailing edge.

-The Chord line: It's the straight line connecting the leading and trailing edges, the distance of that line is the Chord of the Airfoil known by the symbol 'c'.

-The Camber: The maximum distance possible between the mean camber line and the chord line.

-The Suction/ Pressure surfaces: The upper surface is also called the suction surface because it is the low static pressure region while the bottom or the Pressure surface has higher static pressure. This difference in pressure is what causes the pressure gradient that generates Lift.

-Airfoil Thickness: It varies along the chord and is measured either perpendicular to the camber line (USA) or to the chord line (GB) depending on the convention.

Anderson-Introduction to Flight [12, p. 180]

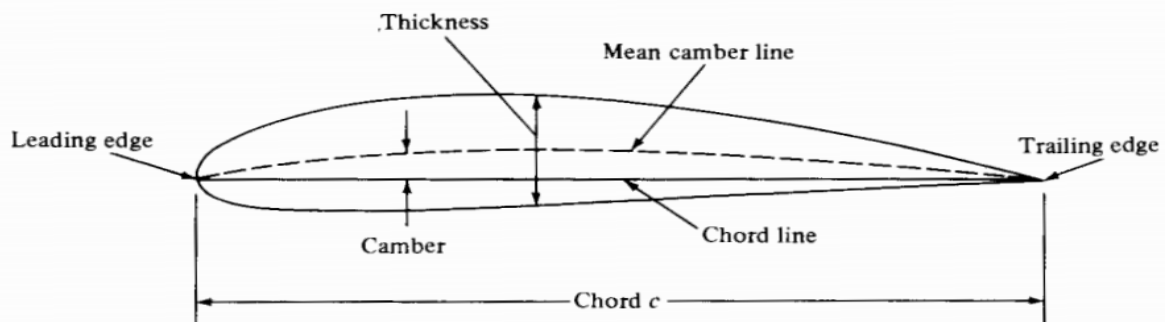


Fig (II-3). Airfoil Nomenclature of a NACA 4415.

-Pitch Angle: Or the setting angle is the angle between the chord and the plane of rotation.

-Angle of Inclination: The angle between the relative Velocity vector and the plane of rotation.

-Angle of Incidence (of attack): AoA is the one between the relative V vector and the chord line.

But the ones that control the Lift and the moment properties of the Airfoil are essentially the camber, the shape of that mean camber line and in a smaller role the thickness distribution of the Airfoil; which is why changing the geometry of an Airfoil section gives us different aerodynamic properties. [13, p. 45] [12, pp. 179-180]

II.1.1.2. Airfoils History:

a) Early days:

Around 1799, Sir George Cayley had the brilliant idea that a curved surface creates more Lift than a flat one. His idea was that Lift is produced by an area of low pressure on the top of the wing and high pressure on its bottom. And so, his work revolutionized aeronautics; Before, enthusiasts would simply imitate mechanically the motion of birds. He gave the world the notion of separating Lift with his fixed wing inclined to the airstream and Propulsion that is gained from another component. [12, p. 178]

A century later, The Wrights following in his footsteps took their own shot at manned flight and to the aviation world's surprise as they corrected the available data deeming it at error, they succeeded and made history confirming his Proposal to be true and superior to all other methods at the time. [2, p. 5]

b) First organized series:

The development of the first Airfoil series is patented in 1884 to Horatio Philips (as shown in figure II-4) for his work on double-surface cambered Airfoils as a result of many Wind Tunnel experiments on every shape he could. After him, aerodynamicists proceeded to search for the most efficient shapes. [12, p. 238]

Anderson-Introduction to Flight [12, p. 238]

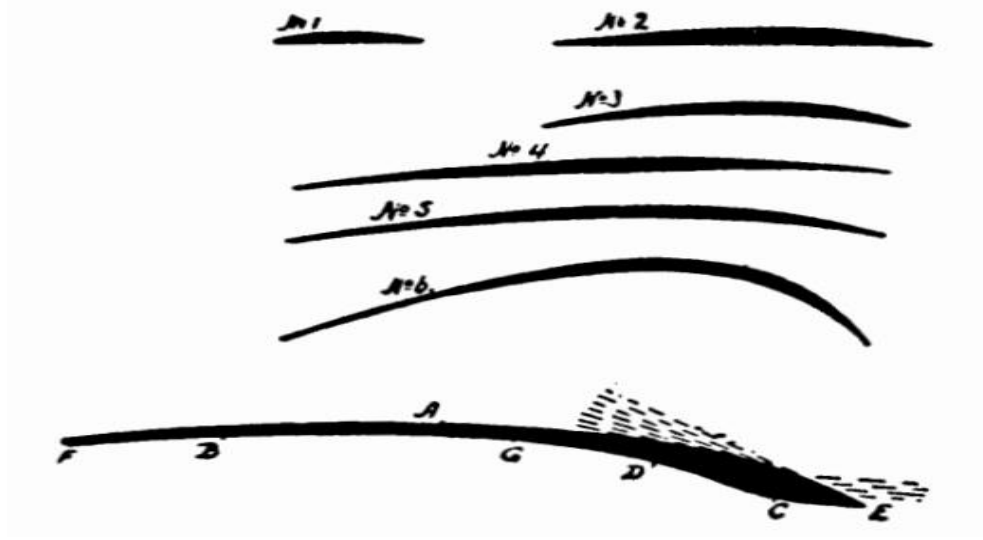


Fig (II-4). Horatio Philips's cambered Airfoils series design.

c) British and USA efforts (1910-1930):

The research on Airfoils was always dependant on the work and mission at hand, and so no one thought of making a standardized series until it was realised by the National Physical Laboratory (NPL), when they first introduced the Royal Aircraft Factory (RAF) Airfoil series.

This created the need for “the evolution of more efficient wing sections of practical form, representing suitable dimensions for an economical structure, with moderate travel of the center of

pressure and still affording a large angle of attack combined with efficient action” as stated in NACA’s first annual report in 1915. NASA to this day is still working on this.

And so first made public in 1917 by a Lt. Col. Edgar S. Gorrell and a Major H. S. Martin, a series of tests on a large group of Airfoils resulted in the U.S.A. Airfoil series and gave Wind Tunnel data from the U.S.A. 1 to 6. Having used that data in making wings and testing them in the MIT Wind Tunnel, The USA Airfoils represented the first systematic series produced by NACA. [12, p. 240] (as shown in figure II-5 below).

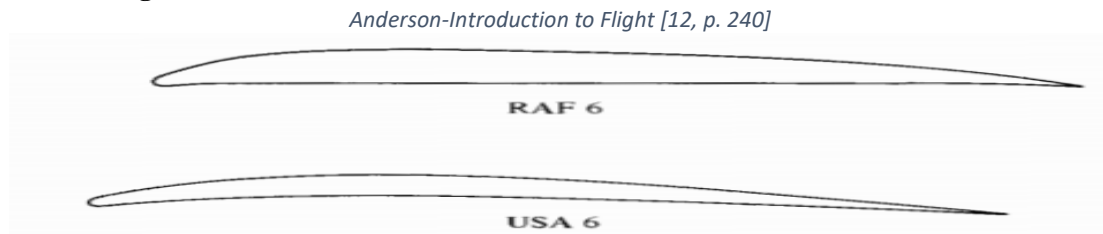


Fig (II-5). Typical Airfoils in 1917.

Gorrell and Martin also noticed that slight change in Airfoil design has a large impact on aerodynamic performances which presents the problem in Airfoil research. That led to a collection of Airfoil shapes in the 1920s resulting from Wind Tunnel data based on that notion.

A variation of wing sections were the most used in the USA at the time :

Mentioning the Clark Y, Clark Y-15, Gottingen G-387, G-398, G-436, NACA M-12, Navy N-9, N-10, N-22, RAF-15, Sloane, USA-27, USA-35A, USA-35B as stated in the “NACA report no. 331” .

d) NACA Four-Digit Airfoils:

The Variable Density Tunnel was a major factor in the famous work of 1933, when NACA report no. 460 brought to the world for the first time the NACA Four-Digit Airfoil Series, it finally gave order and standards to Airfoil designs in the USA. They tested those Airfoils in the VDT and gave curves of C_L , C_D and L/D for the 5in x 30in finite wing they tested them on, and would later correct their obtained data to go with the infinite wing case. The NACA 4-Digit Airfoils had so much success worldwide and are still used today such as the NACA 2412 on some light Aircrafts. [12, p. 241]

e) NACA Five-Digit Airfoils:

It was the 1930s, NACA kept advancing their Airfoil research with a new camber line family in an effort to increase max Lift. Combining it with the standard NACA thickness distribution, they developed the NACA Five-Digit Airfoil series, the likes of NACA 23012. Followed by entire families of high speed Airfoils and laminar flow Airfoils in the 1940s. New precise means of testing is always required, and so, NACA constructed a new Low-Turbulence 2D Tunnel with a rectangular test section (3ft wide x 71ft high) and a pressure up to 10atm at Langley in 1939, its sole mission was Airfoil testing. It had the ability to allow Airfoil models to span the test section completely providing infinite wing data directly without the need for a correction. [12, p. 241] (as shown in figure II-6).

<https://www.century-of-flight.net/history-of-the-airfoil/>

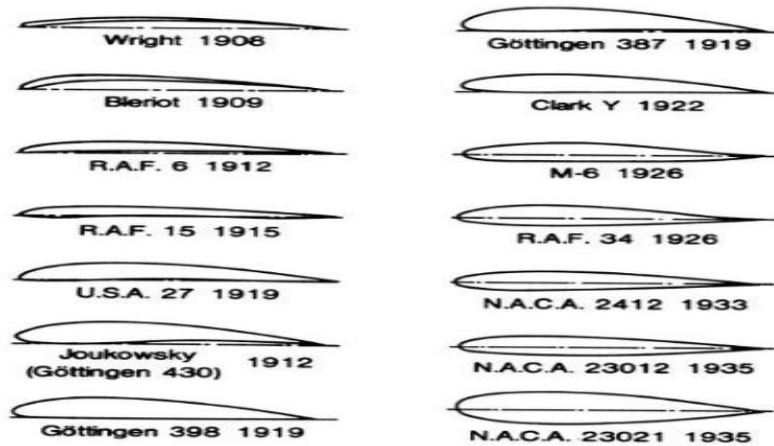


Fig (II-6). Evolution of Airfoils from the 1900s to the 1940s.

f) NACA 1/6/7/8-Series Airfoils:

After the 4-digit and the 5-digit series, some alternatives were actually developed by the NACA team as a potential other method to get better performance. The most valued examples were:

1- The 1-series (16-series):

Unlike the previous series, the 16-series as based on Airfoil theory and not on geometrical difference. They were designed in the late 1930s after many advances had been made in inverse Airfoil design methods. The principle here is to work on the desired pressure distribution over the Airfoil because of its effect on the Lift of the shape, and then derive the geometrical properties of the corresponding shape.

An example would be the NACA 16-212 Airfoil and since the 16-XXX Airfoils are the only ones that were of use, the 1-series is referred to as the 16-series. [14]

2- The 6-digit series:

In their pursuit of improving Airfoil behaviour, NACA developed this series with a similar pressure-based method of that of the 1-series. Their goal was to come up with Airfoils that maximized the region where the airflow remains laminar and thus reducing the drag over a small range of Lift coefficients.

Its nomenclature is rather confusing and one of the most common examples of this series would be the NACA 64₁-212, $a=0.6$. [14]

3- The 7-digit series:

NACA continued pursuing their idea of differentiating the minimum pressure distribution on the upper and lower surfaces. That result was the 7- digit series.

Having a relatively simple Nomenclature in comparison with the 6-digit series, an example would be the NACA 747A315. [14]

4. The 8-digit series:

Following its predecessors, the 8-digit series adopted the same methodology but the difference was in its mission which was for flight at supercritical speeds. Its goal was practically the same as the 6 and 7-digit series; to maximize the extent of laminar flow on the upper/lower surfaces independently. A famous example of one its Airfoils would be the NACA 835A216. [14]. (as shown in Table (II-1).

<https://slideplayer.com/slide/5280118/>

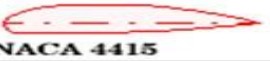
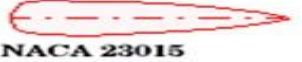
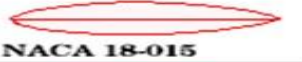
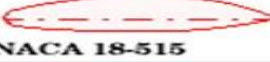
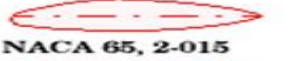
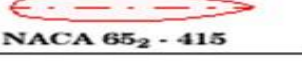
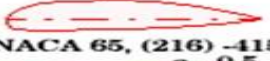
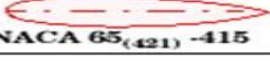
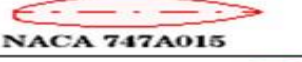
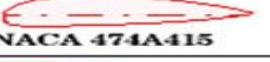
FOUR-DIGIT SERIES AIRFOILS	 NACA 0015	 NACA 4415
FIVE-DIGIT SERIES AIRFOILS	 NACA 23015	 NACA 23115
1-SERIES AIRFOILS	 NACA 18-015	 NACA 18-515
6-SERIES AIRFOILS	 NACA 65, 2-015  NACA 65 ₂ - 415	 NACA 65, (216) -415 a - 0.5  NACA 65 ₍₄₂₁₎ -415
7-SERIES AIRFOILS	 NACA 747A015	 NACA 474A-415
SUPERSONIC AIRFOILS	 NACA 1S - (70)(03) - (70)(03)  NACA 2S - (30)(03) - (30)(03)	

Table (II-1). Evolution of the NACA Airfoil series.

g) Modern Airfoils:

Around the 1950s, Airfoil research was halted due to the race for supersonic and hypersonic flight. It wasn't until 1965 when Richard T. Whitcomb would make a breakthrough with the NASA supercritical Airfoil that had allowed the production of wings with high critical Mach numbers and consequently would help the interest in Airfoils return to NASA. It remained to this day with the addition of the high-speed digital computer that carried a lot of the weight concerning routine work carried by Wind Tunnels.

This development would later result in the advanced modern low-speed Airfoil series or the LS(1) that carried superior Lift properties that allowed for the use of smaller wing areas which means less Drag. [12, p. 242] (as shown in figure II-7).

Anderson-Introduction to Flight [12, p. 243]

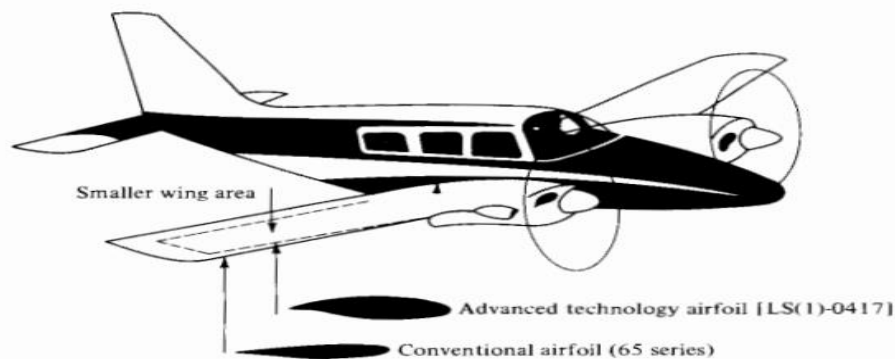


Fig (II-7). Shape comparison between the modern LS(1)-0417 and a conventional Airfoil.

II.1.1.3. Airfoils Types:

The many evolutionary changes in the Airfoil history created many types and classifications:

1- Symmetrical Airfoils:

The likes of the famous NACA 0012, a symmetrical Airfoil has identical upper and lower surfaces which makes the mean camber line and the chord line also the same resulting in no Lift at zero Angle of Attack. They are mostly used in light helicopters specifically in their main rotor blades. [15]

Examples of Symmetrical Airfoils:

Drela HT05/HT08/HT12–Gottingen 443/444–NACA 0006/16-006–NACA/Munk M-1. [16]
(as shown in figure II-8).

<http://airfoiltools.com/airfoil/details?airfoil=naca0006-il> [16]

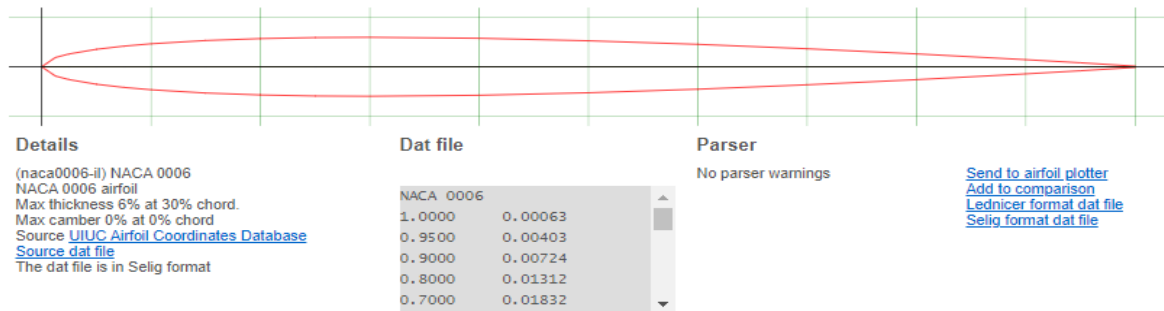


Fig (II-8). Data and Shape of a Symmetrical Airfoil (NACA 0006).

2- Non-Symmetrical Airfoils (cambered):

Basically, unlike their symmetrical counterparts, the upper and lower surfaces differ resulting in separate chord lines and camber lines and a greater curvature of the Airfoil above the chord line than below it and it is worth mentioning that it is able to produce useful Lift at zero Angle of Attack. It can also produce more Lift, better Lift to Drag ratio and stall characteristics but in return it creates undesirable torque and it costs more to make. [15] [17]

Examples of Non-Symmetrical Airfoils: Basically, all other Airfoils other than the symmetrical ones like: NACA 2414/1408/63₁-212. [16] (as shown in figure II-9).

<http://airfoiltools.com/airfoil/details?airfoil=naca0006-il> [16]

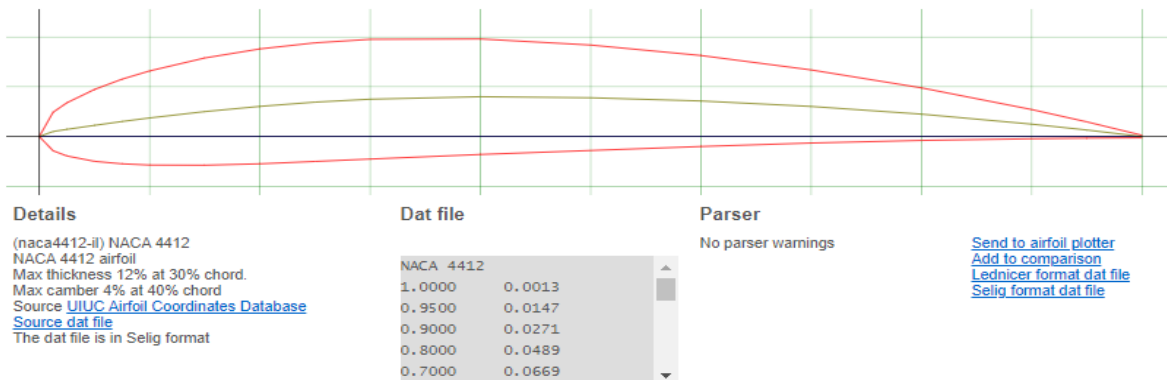


Fig (II-9). Data and Shape of a Cambered Airfoil (NACA 4412).

II.1.1.4. NACA Airfoils Classification and Identification:

The classification (NACA Airfoils) essentially serves as an ID for an Airfoil, each series has its own code for recognizing its properties:

1- The 4-Digit Series:

It's better to work with an example: NACA 2415

- 2: the maximum camber (m) in percentage of the chord (a camber of 2%).
- 4: the position of the max camber (p) in tenths of chord; (40% back from the Airfoil leading edge (or 0.4c)).
- 15: the maximum thickness (t) of the Airfoil in percentage of chord. (15%). [14]

2- The 5-Digit Series:

For ex: NACA 23012.

- 2: when multiplied by 3/2, yields the design lift coefficient (cl) in tenths (0.3).
- 30: when divided by 2, give the position of the maximum camber (p) in tenths of chord (maximum camber located 15% back from the leading edge).
- 12: the maximum thickness (t) in percentage of chord (maximum thickness of 12%). [14]

3- **The 1-Series:**

For ex: NACA 16-212.

- 1: indicates the series.
- 6: the location of minimum pressure (60% back from the leading edge).
- 2: the design lift coefficient in tenths (0.2).
- 12: the maximum thickness in tenths of chord (12%). [14]

4- **The 6-Digit Series:**

One of the more common examples: NACA 64₁-212, a=0.6.

- 6: denotes the series.
- 4: the location of the minimum pressure in tenths of chord (0.4c).
- 1: indicates that low drag is maintained at lift coefficients 0.1.
- 2: the design lift coefficient (0.2).
- 12: the thickness in percentage of chord, (12%).
- For a=0.6: the percentage of the Airfoil chord over which the pressure distribution on the Airfoil is uniform, (60% chord). [14]

5- **The 7-Digit Series:**

For ex: NACA 747A315.

- 7: denotes the series
- 4: provides the location of the minimum pressure on the upper surface (40%).
- 7: the location of the minimum pressure on the lower surface in tenths of chord (70%).
- A: the thickness distribution and mean line forms used from a standardized form.
- 3: the design lift coefficient in tenths (0.3).
- 15: the Airfoil thickness in percentage of chord (15%). [14]

6- **The 8-Digit Series:**

For ex: NACA 835A216.

- 8: designates the series.
- 3: the location of minimum pressure on the upper surface in tenths of chord (0.3c).
- 5: the location of minimum pressure on the lower surface in tenths of chord (50%).
- A: distinguishes airfoils having different camber or thickness forms.
- 2: denotes the design lift coefficient in tenths (0.2).
- 16: the Airfoil thickness in percentage of chord (16%). [14]

II.1.2. Finite/Infinite Wings:

Theoretically, an infinite wing has no end to it and no limit and we can only study it in real life with the help of Wind Tunnels and attach it to its walls, it also has the same aerodynamic properties as an Airfoil which makes one think that is enough evaluate the behaviour of aircrafts. Unfortunately, that is not the case; Unlike a 2D Airfoil, 3D Finite wings that are employed in real life Aircrafts have an additional component in its additional dimension. The pressure difference that causes the Lift also results in the flow curling near the tips and being forced from the bottom to the upper surface which in return causes the streamlines on the top surface to bend toward the wing root. (as shown in figure II-10).

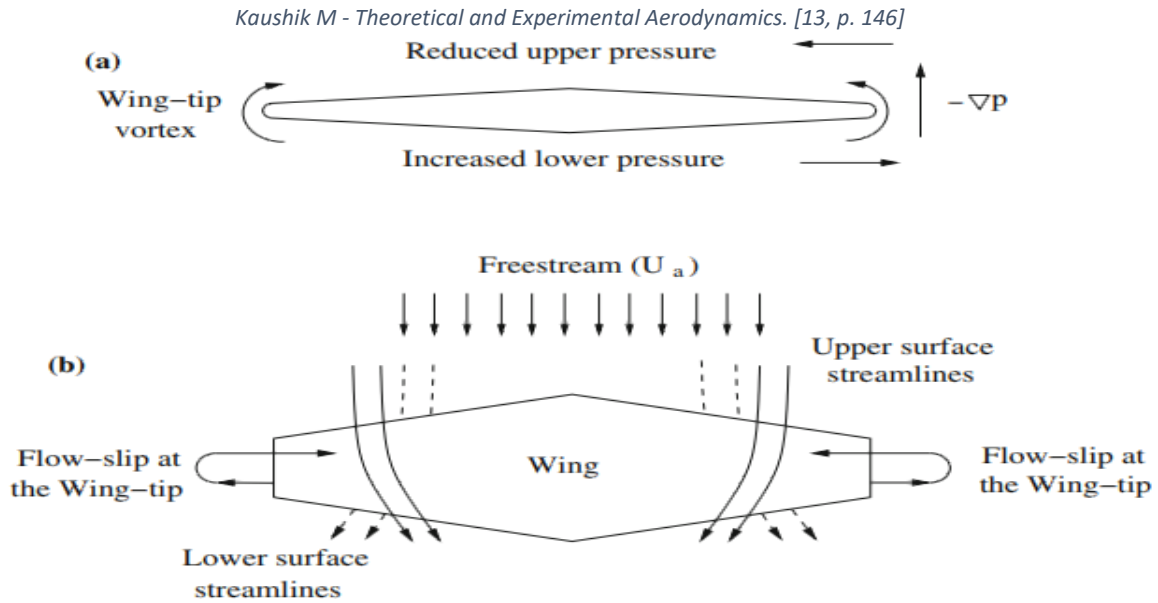


Fig (II-10). Front and Top views of the flow pattern on a 3D Finite Wing.

This phenomenon starts circular motions downstream of each of the wing tips, we call them trailing vortices. They induce a small downward component of air velocity opposite to Lift near the wing known as downwash denoted by “w”. adding it with the freestream velocity “ U_a ”, creates a local relative wind that goes downward near each Airfoil section **as shown in Fig (II-11)**.

Kaushik M - Theoretical and Experimental Aerodynamics [13, p. 147]

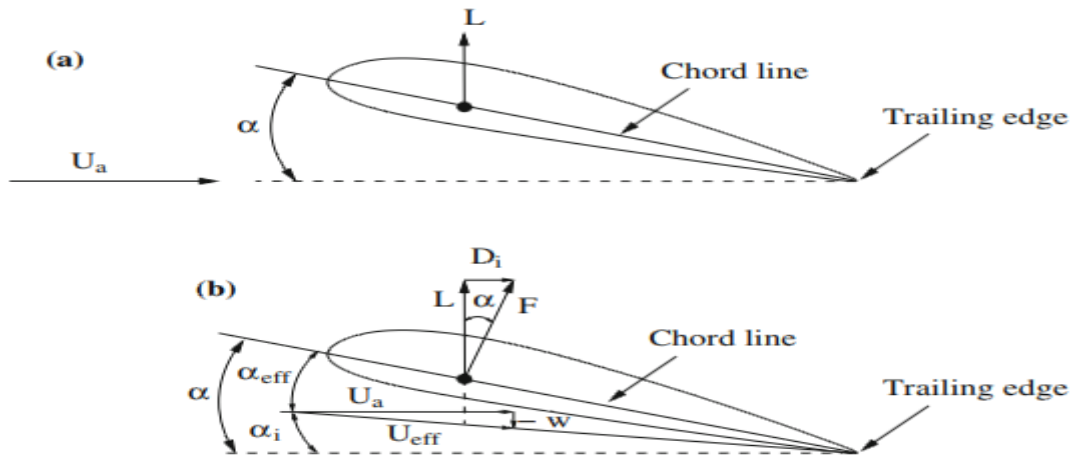


Fig (II-11). Comparison of a 2D Airfoil section (a) and a 3D Wing (b).

By examining it, we notice that the local air speed is inclined below U_a with an induced angle of attack **given by:** “ $\alpha = \tan^{-1}\left(\frac{-w_i}{U_a}\right)$ ”... (II.1), or “ $\alpha = \frac{-w_i}{U_a}$ ”... (II.2).

we deduce that the downwash has three major effects on the local Airfoil section:

1- Lowering the actual AoA below the geometric AoA (α) and is referred to as the effective AoA (α_{eff}) **given by:** “ $\alpha_{eff} = \alpha - \alpha_i$ ”... (II.3).

2- The effective freestream velocity (U_{eff}) becomes “ $U_{eff} = (U_a^2 + w^2)^{1/2}$ ” ... (II.4).

3- Creating additional drag called induced Drag (D_i) **as:** “ $D_i = \rho U_a \int_{-b}^b \left(\frac{w_i}{U_a}\right) \cdot \Gamma(y) \cdot dy$... (II.5).

And so, the Lift generated by a 3D wing is less than an Airfoil if the downwash is missing. Meaning that a finite wing needs greater geometric AoA to get the same Lift per unit span as an Airfoil. many solutions are set to counter it including adding winglets or using circular ring wings. [13, p. 145]

II.2. Aerodynamic Properties:

To be able to conquer and fly through air, we need an understanding of the aerodynamic properties to consider:

Essentially, all aerodynamic forces and moments on a body result from two basic things:

1- Pressure distribution “p”.

2-Shear stress distribution “τ”.

While P acts normal to the surface, τ is tangential to it. What we get from the effect of their distributions integrated over a body surface is the resultant aerodynamic force R [10, p. 16] [13, p. 42]

II.2.1. Lift/Drag and the Aerodynamic Moment:

The resultant force R has two components, representing the one perpendicular to the freestream velocity is the Lift L while we name Drag D the horizontal component in the direction of the freestream velocity separated by the gliding angle α . (as shown in figure II-12).

Geometrically, R can be split into another set of components relative to the chord; the normal Force N perpendicular to C and the axial force A parallel to C. Linking the two sets is the angle of attack α :

$$L = N \cdot \cos(\alpha) - A \cdot \sin(\alpha) \dots \text{(II.6)} \dots \dots \dots D = N \cdot \sin(\alpha) + A \cdot \cos(\alpha) \dots \text{(II.7)}$$

ANDERSON – Fundamentals of aerodynamics [10, p. 16]

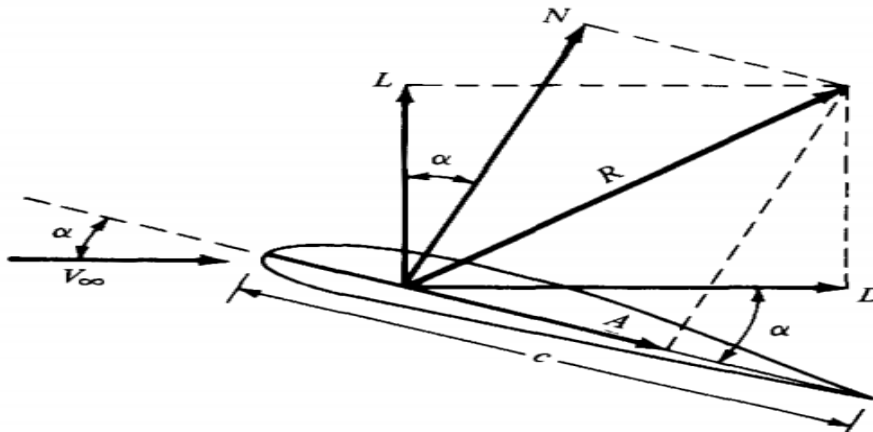


Fig (II-12). The Resultant aerodynamic force and its components.

Aerodynamic moment: where there is a force, there is a moment. And the one exerted on a body aerodynamically depends on where it is taken for ex: The Leading/Trailing edge. Conventionally, moments that tend to increase are considered positive and vice versa for those that decrease. **Following Fig (II-13):**

the moment per unit span about the leading edge due to P and τ , on the elemental area dS on the upper surface is: $dM_u = (P_u \cos \theta + \tau_u \sin \theta)x \, dS_u + (-P_u \sin \theta + \tau_u \cos \theta)y \, dS_u \dots \text{(II.8)}$

ANDERSON – Fundamentals of aerodynamics [10, p. 17]

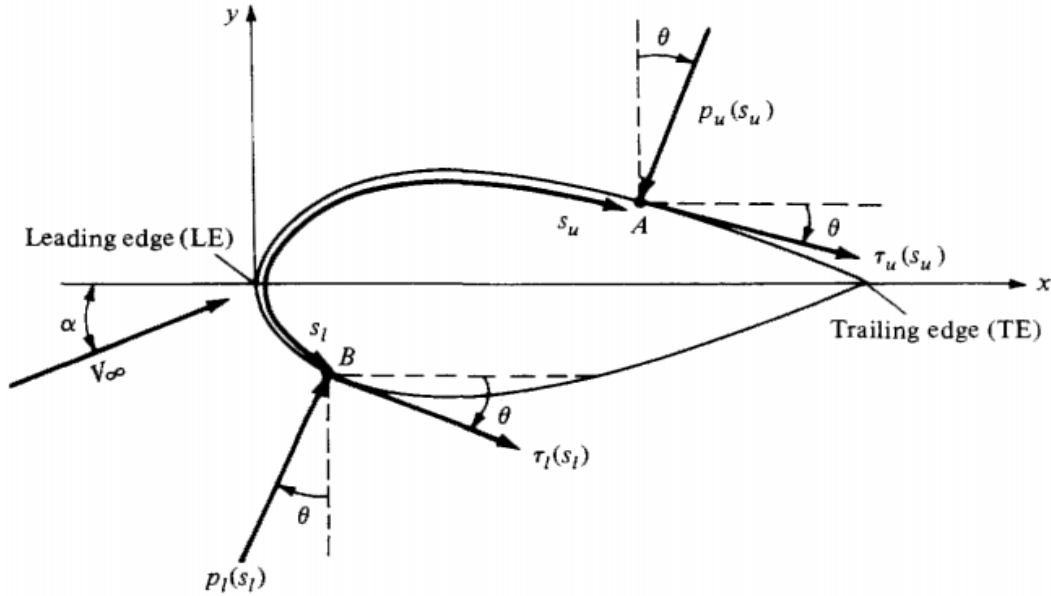


Fig (II-13). Nomenclature for the integration of P and τ distributions over a 2D body surface.

While on the bottom surface: $dM_I = (-P_l \cos \theta + \tau_l \sin \theta)x \, dS_l + (P_l \sin \theta + \tau_l \cos \theta)y \, dS_l \dots$ (II.9)

And since the aerodynamic moment depends on the point from which it is taken, we obtain the moment about the leading edge per unit span by integrating the last two equations as follows:

$$M_{LE} = \int_{LE}^{TE} [(P_u \cos \theta + \tau_u \sin \theta)x - (P_u \sin \theta - \tau_u \cos \theta)y] ds_u + \int_{LE}^{TE} [(-P_l \cos \theta + \tau_l \sin \theta)x + (P_l \sin \theta + \tau_l \cos \theta)y] ds_l \dots \text{ (II.10). [10, p. 16]}$$

II.2.2. Aerodynamic Coefficients:

Even more fundamentally than aerodynamic forces and moments lie their dimensionless coefficients with V_∞ and ρ_∞ the freestream velocity and density respectively. By defining a dimensional quantity called the dynamic pressure q_∞ as: $q_\infty = \frac{1}{2} \rho_\infty V_\infty^2 \dots$ (II.11).

We obtain the following dimensionless coefficients with "l" and "S" a reference length and area:

- Lift Coefficient : $C_L = L / (q_\infty \cdot S)$. (II.12) giving us the Lift as: $L = q_\infty \cdot S \cdot C_L$. (II.13).
- Drag Coefficient : $C_D = D / (q_\infty \cdot S)$. (II.14) giving us the Drag as: $D = q_\infty \cdot S \cdot C_D$. (II.15)
- Normal Force Coefficient : $C_N = N / (q_\infty \cdot S)$. (II.16) with the Normal F as: $N = q_\infty \cdot S \cdot C_N$. (II.17).
- Axial Force Coefficient: $C_A = A / (q_\infty \cdot S)$. (II.18) giving us the Axial F as: $A = q_\infty \cdot S \cdot C_A$. (II.19).
- Moment Coefficient : $C_M = M / (q_\infty \cdot S \cdot l)$. (II.20) giving us the Moment as: $M = q_\infty \cdot S \cdot l \cdot C_M$. (II.21).

The reference area and length S and l are different depending on the studied body shape. For ex: for an airplane wing, S is the Planform area and l is the mean chord length.

Two more dimensionless quantities are used in aerodynamic studies and are defined as follows:

- Pressure Coefficient : $C_p = (P - P_\infty) / q_\infty$. (II.22) where: P_∞ is the freestream pressure.

- Skin friction Coefficient : $C_f = \tau / q_\infty$. (II.23) [10, p. 20]

II.2.3 The Center of Pressure:

The question of where to place the resultant aerodynamic force still remains, seeing as how aerodynamically it's very important to be able to simplify things to the point where we only consider the Lift and Drag forces. And that's to be able to design the proper Thrust systems and evaluate the ideal weight for our body for actual Lift. The answer would be that we should place it where it produces the same effect as the pressure and shear stress distributed loads.

ANDERSON – Fundamentals of aerodynamics [10, p. 28]

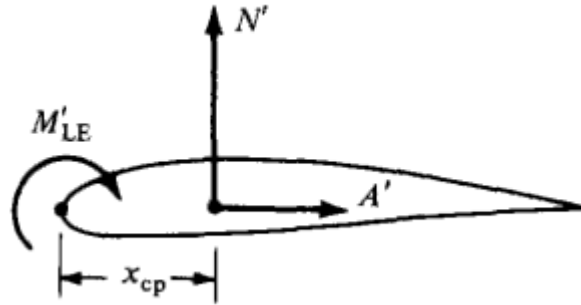


Fig (II-14). Center of Pressure for a 2D body (Airfoil).

For example: For a two-dimensional body like an Airfoil, the local distributions produce a moment about the leading edge as in **Equation** (M_{LE}), and so we need to place the normal and axial force in a way to generate the same effect and moment about the considered point. **As shown above in Fig (II-14)**. A is placed on the chord line and N has to be located downstream of the leading edge by a certain distance to satisfy our conditions **such as:** $M_{LE} = - (X_{CP}) \cdot N$. **(II.24)**

We call the point where we end up placing it the center of pressure defined as:
 $X_{CP} = - (M_{LE} / N)$. **(II.25).**

If we take the moments about the center of pressure, and so it can also be defined as the point where the aerodynamic moment is zero. In the cases where the Angle of attack is very small, we can say that $N \approx L$ ($\sin \alpha \approx 0$; $\cos \alpha \approx 1$). **(II.26)** Making: $X_{CP} = - (M_{LE} / L)$. **(II.27).**

We notice that as L and N decrease toward zero, the angle of attack increase towards infinity; because of this, we cannot always rely on the center of pressure but it doesn't matter that much, we can place the resultant force R at any point in the body as long as we know the moment about it.

ANDERSON – Fundamentals of aerodynamics [10, p. 29]

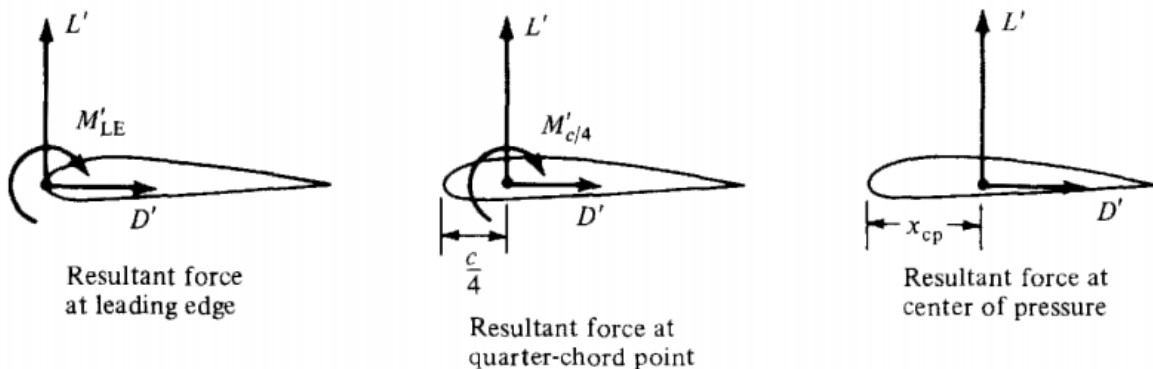


Fig (II-15). Equivalent ways of specifying the force-and-moment system on an Airfoil.

For example: Fig (II-15) Shows different ways of getting the force and moment of an Airfoil. With the left one being placed at the leading edge we get the previously obtained moment M_{LE} . In the case of the middle figure, the resultant is located at $X = c/4$ (a quarter of the chord) giving us a

finite value of $M_{C/4}$. However, in the final one, it's placed at the center of pressure where the moment is zero. **We can get a relation between these different cases: $M_{LE} = -\frac{c}{4}L + M_{C/4} = -X_{CP}L$. (II.28).**

So: $X_{CP} = \frac{c}{4} - (M_{C/4} / L)$. (II.29) For a thin symmetrical Airfoil CP is at the quarter of the chord, for a non-symmetrical Airfoil such as NACA4412 it located behind that point.

The center of pressure could lie outside the Airfoil section and it changes with the variation of the Lift coefficient and with it the angle of attack. Furthermore, the contribution of Drag is not considered when $\alpha=0$ since the line of action for Drag passes through the leading edge. For it to be important, we need to work with different **angles of attack ($\alpha \neq 0$)** where we would need to employ the **Aerodynamic Center 'AC'**. [10, pp. 28-30]

II.2.4 The Aerodynamic Center:

The aerodynamic center is defined as the point where the pitching moment coefficient (C_M) for an Airfoil is independent from the **angle of attack α** . In regular conditions, it's located at $C/4$ behind the leading edge with C the chord length, while at Supersonic Mach numbers it's placed at $C/2$. What effects its position is the viscosity (moving it toward the leading edge) and the compressibility (toward the trailing edge). Unlike the center of pressure, the aerodynamic center is fixed point that lies within the profile of the Airfoil.

If we consider in our study the effect due to Drag, the angle of attack needs to be unequal to zero, and so the aforementioned equation of the location of the center of pressure needs to be changed to:

$$\frac{X_{cp}}{c} = \frac{X_{AC}}{c} - \frac{C_{MAC}}{C_L}. \quad (\text{II.30})$$

$$\text{From: } M_{LE} = M_{AC} - (L \cos\alpha - D \sin\alpha)X_{AC} = -(L \cos\alpha + D \sin\alpha)X_{CP} \quad (\text{II.31}).$$

(Considering that for small values of angles of attack ($\alpha \approx 0$), $\sin\alpha \approx 0$; $\cos\alpha \approx 1$) [13, p. 40] (as shown in figure II-16).

Kaushik M - Theoretical and Experimental Aerodynamics [13, p. 41]

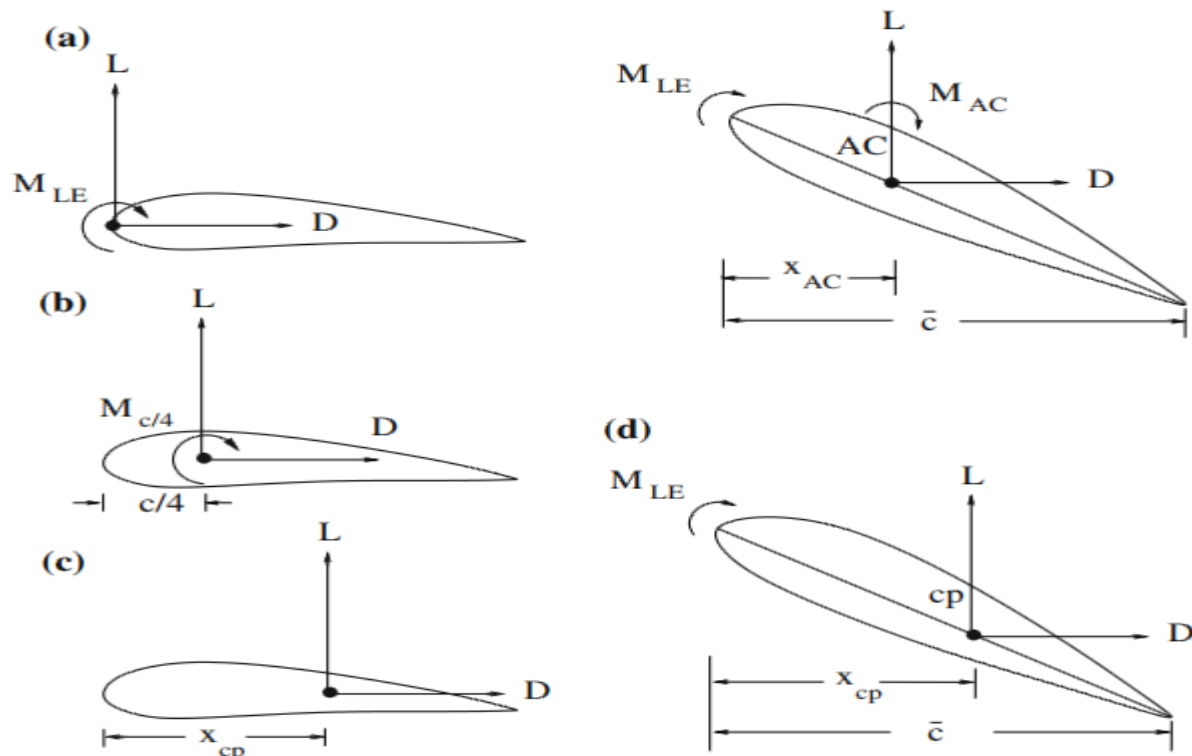


Fig (II-16). Forces and Moment Systems of an Airfoil at Zero and Finite Angles of Attack.

II.3 Examples of Aerodynamic curves and schematics:

II.3.1 Pressure distribution around an Airfoil:

Due to the geometry of the Airfoil, it is obvious that the pressure distribution is not uniform but rather it varies with the angle of attack, the following figures demonstrate the difference in pressure distribution that creates Lift necessary for flight and highlights the effect of surpassing C_{Lmax} , the max value at which the airplane can maintain steady flight and not stall (depends on α). [13, p. 35]

Kaushik M - Theoretical and Experimental Aerodynamics

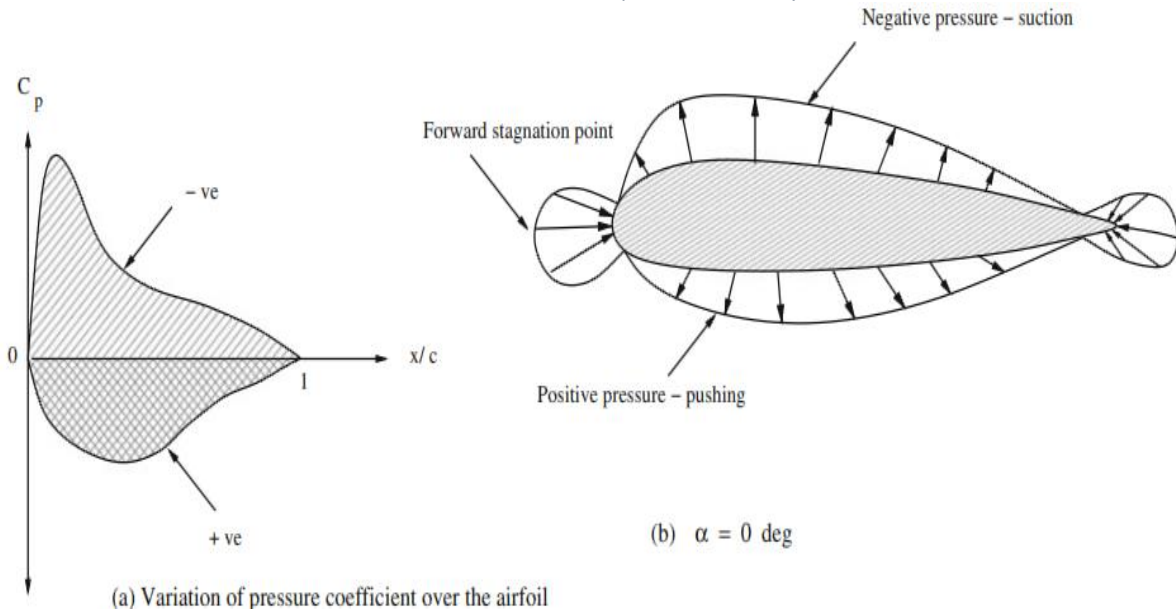


Fig (II-17). Typical Pressure distributions around an Airfoil at 0-degree angle of attack.

Kaushik M - Theoretical and Experimental Aerodynamics

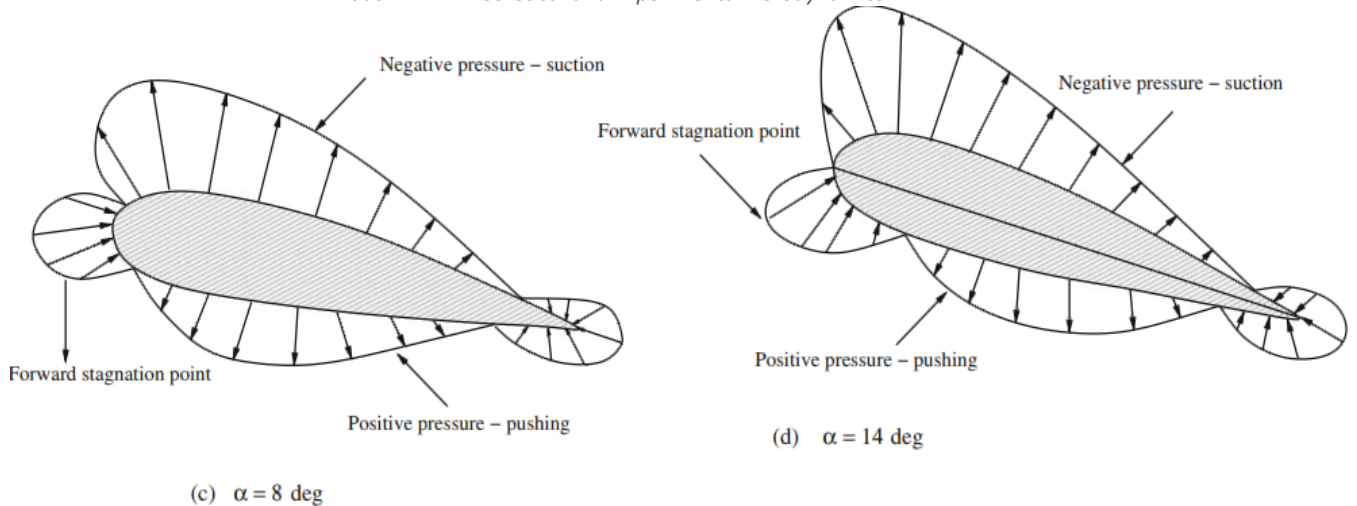


Fig (II-18). Typical pressure distributions around an Airfoil at high (8 and 14) angles of attack.

II.3.2 Drag and Lift coefficients curves:

C_L and C_D are fundamental quantities for any aerodynamic study. In order to keep a body in flight, typically an aircraft, Thrust and Lift must counter Drag and Weight (mostly, L and W are much larger than D and T). but it is essential to remember that C_L and C_D Are functions of α meaning the orientation of the body during flight.

The following figures show exactly how C_L increases linearly with α until a specific angle of attack correspondent with $C_{L,max}$ where the wing stalls and C_L drops rapidly as we keep increasing the AoA. On the other hand, they also portray the changes of C_D with velocity and α where the maximum thrust is determined by the value of the minimum drag coefficient $C_{D,min}$. Without forgetting the effect of Lift to Drag ratio variations with velocity and α on Airfoil and Aircraft performance. [10, p. 41]

ANDERSON – Fundamentals of aerodynamics [10, p. 41]

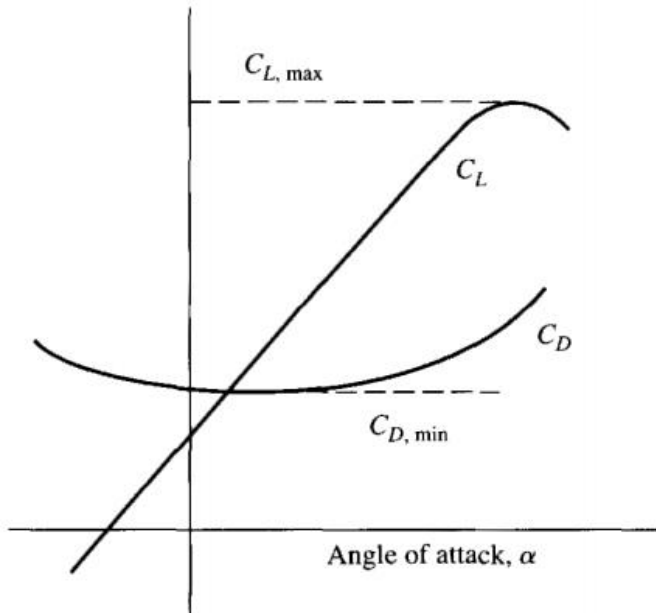


Fig (II-19). Lift and Drag Coefficients Variations with the Angle of Attack.

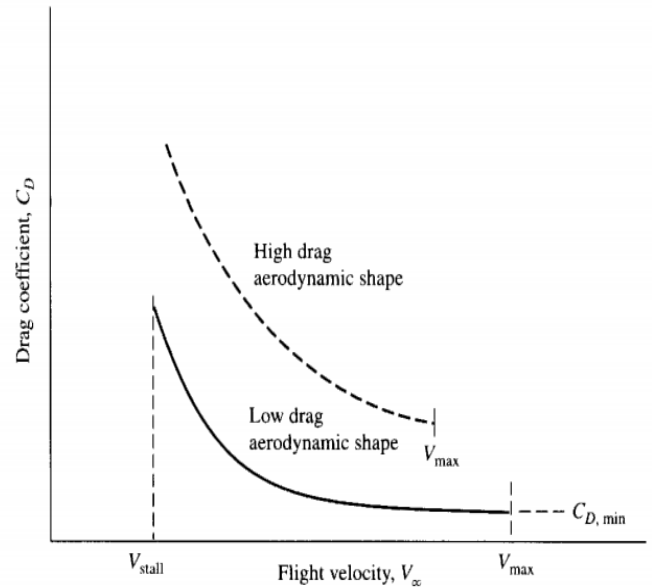


Fig (II-20). Drag Coefficient Variations with Flight Velocity.

ANDERSON – Fundamentals of aerodynamics [10]

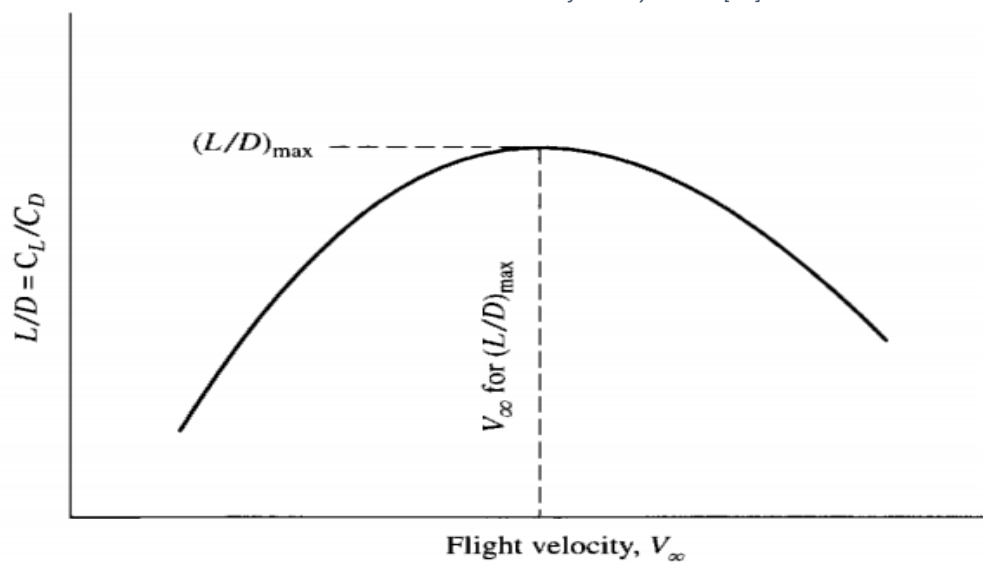


Fig (II-21). Lift to Drag Ratio Variations with Flight Velocity.

ANDERSON – Fundamentals of aerodynamics [10]

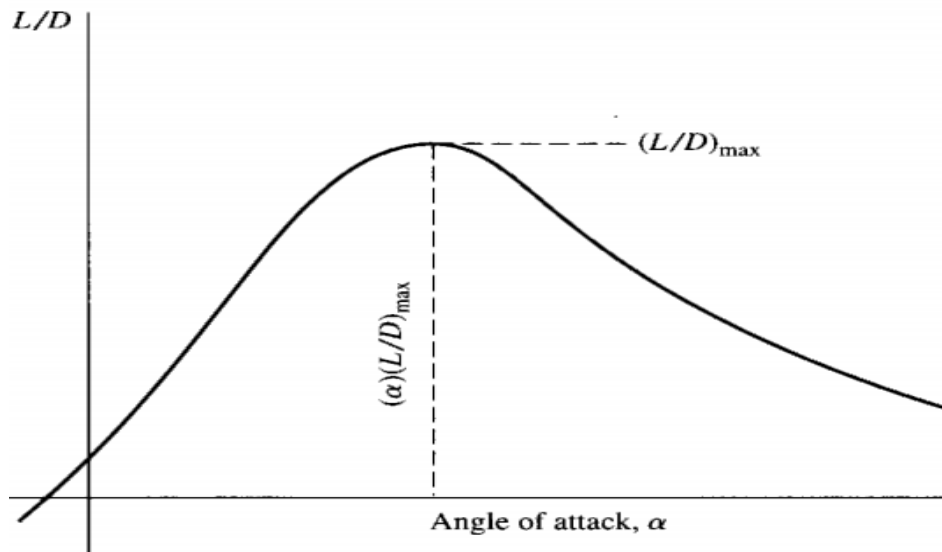


Fig (II-22). Lift to Drag Ratio Variations with the Angle of Attack.

II.4. Conclusion:

It is evident that a theoretical and aerodynamical study of any kind of body before attempting to deploy it in a real-life mission is of the utmost importance, even before testing it in a Wind Tunnel. It continues to go hand in hand with the practical study after as the Tunnel study goes on, calculating Lift and Drag coefficients and therefore the Lift and Drag produced by a body is what determines whether it is viable for actual flight.

In that way, research and Technology have determined that the ideal body for flight pairing its economical and performance value is the modern Airfoil. And so, with the advancements of science and the new tools that provided for more room for aerodynamics to grow:

- The next step is Numerical and computer assisted Studies.

III- INTRODUCTION:

During this chapter, we will proceed into computer assisted studies and show how we performed our numerical simulations on ANSYS Workbench. In this part, Three Airfoils were analysed (NACA 0012, NACA 0015, NACA 4412). We obtained all the aerodynamic results from the data we got in our simulations made with the Ansys Software, those results were compared late with previous validated scientific research and experiments as well as our own wind tunnel tests. **The operation will consist of 4 major steps:**

- 1-** Making the geometry of the model.
- 2-** Meshing the model with great care and accuracy.
- 3-** Configuring the simulation to copy real life situations accurately and launching it.
- 4-** Obtaining and discussing the results.

Simulations Allow us to get numerical results imitating real-life conditions and situations provided we insert the proper boundary conditions for the physical problem. Numerical Simulations also let us study how air behaves around our Airfoils and to see how the Lift and Drag properties generated from the operation among other aerodynamic factors vary versus different angles of attack.

- Ansys Software was selected for our simulations because it’s enriched with many technical and scientific options and has various solutions for different physical phenomena including aerodynamic studies of all kinds of Airfoils and bodies.

This chapter will display:

- The Importance and utility of using Advanced Software for Aerodynamic Simulations on Airfoil such as Ansys Inc.
- The steps taken to perform the simulations and obtain the results for different angles of attack simultaneously.

Finally, we will go into the results obtained by the software and compare it with the already obtained data concerning the aerodynamic properties of Airfoils and bodies and prepare it for a comparison with our Real-life Wind Tunnel test results.

Our Reynolds number will be around 1,000,000 more or less (28m/s like our Tunnel and respecting Air Sea level conditions for viscosity and density and a chord of 1m).

III.1. Numerical Simulation on NACA 0012 Airfoil:

NACA 0012 is a symmetrical Airfoil of the NACA 4-digit series, meaning it has 0 maximum camber. With a maximum thickness (t) of 12% at 30% of the chord. **As shown in Fig (III-1)** where we got the Airfoil data to implement in our model from.

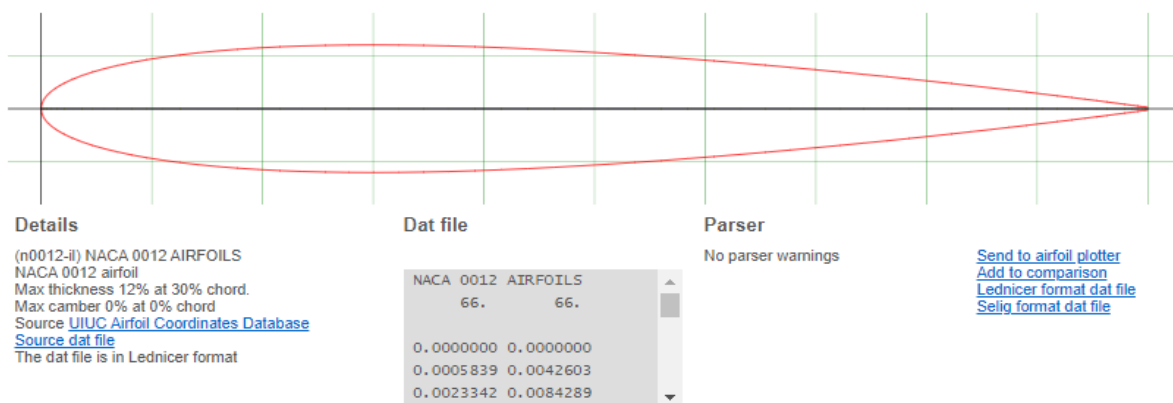


Fig (III-1). NACA 0012 DATA from Airfoiltools.com.

III.1.1. Launching from Ansys Workbench:

As shown in Fig (III-2), during this simulation we made the decision to use the Fluent solver instead of the CFX solver for our fluid flow problem based on the following reasons:

- Fluent has more developed meshing approaches (Cell-centered approach) while CFX uses a vertex-centered approach that sticks to traditional mesh topologies.
- Fluent has its own post-processing capabilities while CFX needs a dedicated post-processor.
- Mesh adaption capabilities are stronger in Fluent compared to CFX.

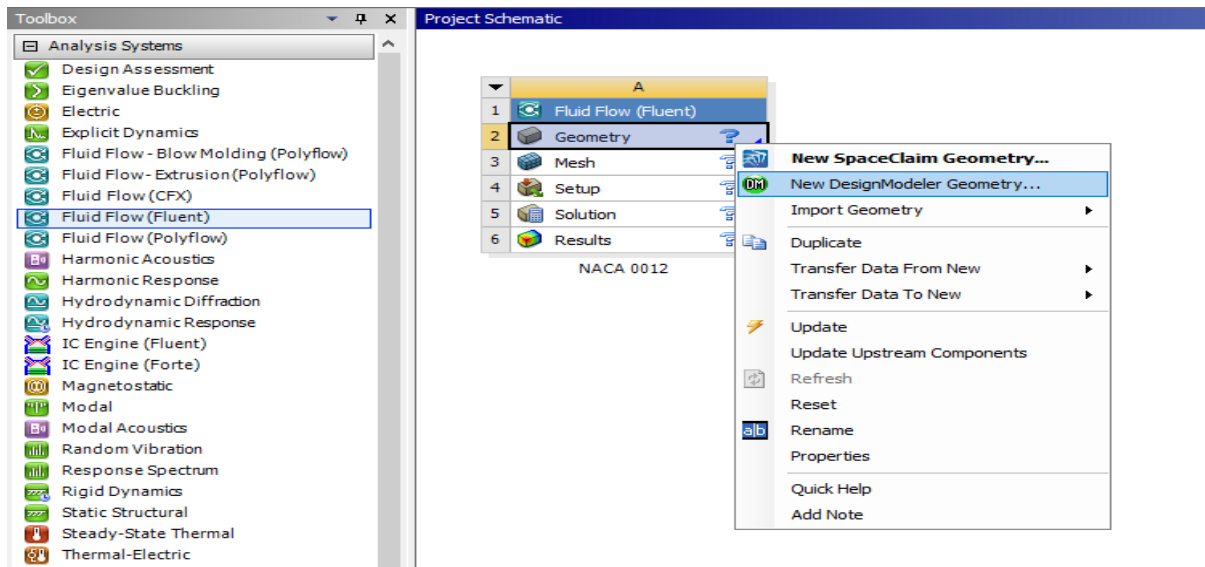


Fig (III-2). The Application Window of ANSYS 19.0 Workbench.

And so, the next steps were followed in order to realise our work:

III.1.2. Creating the Geometry on Design modeler:

Designing the geometry is relatively simple, but one needs an understanding of what needs to be done in the meshing part of the simulation which heavily impacts the way the model is made as portrayed in the following steps:

1. The first task is importing the geometry data and modify it in a way that helps us in our work. We imported our data from the airfoiltools.com website as shown in figure (III-3).

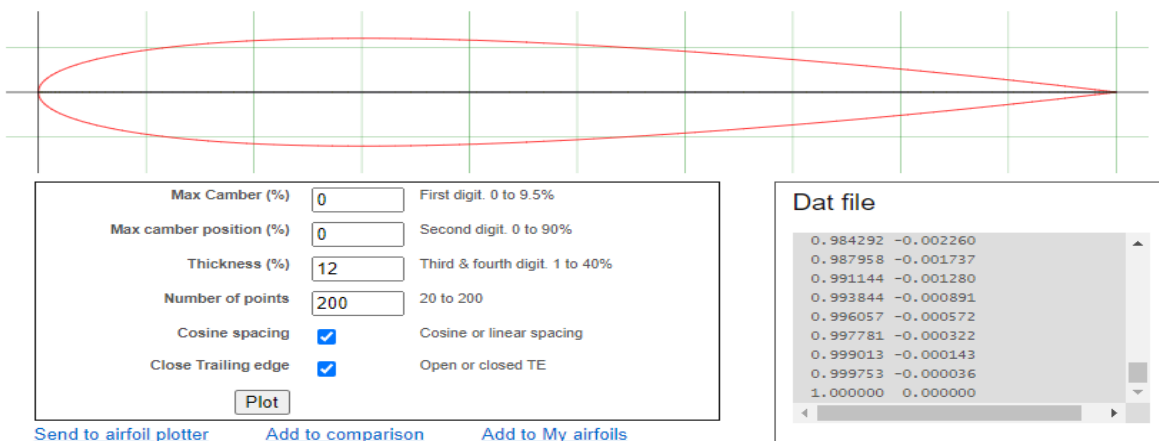


Fig (III-3). NACA 0012 Dat file from Airfoiltools.com.

Before copying the **Data** file content on the right, we produced this Airfoil using the NACA 4-digit generator from the website and implemented what we required which is a **max camber value of “0”** and **200 points** for maximum accuracy in our plot, in addition to **check the “Cosine spacing” box** for better resolution around the leading edge and the **“close trailing edge”** so that it’s a closed plot.

And to successfully import our data to ANSYS, we first needed to modify it so that the software can read it properly **as shown in Table (III-1), that means:**

- Copying the data in an excel file to adjust it and saving it as a text in the end (IMPORTANT).
- Adding a few cells in the top of the columns to turn it into the ANSYS format.
- The “group” column indicates that the points are all part of the same plot numbered “1” here.
- The “point” column indicates the points of our plot and it needs to end with “0” so that ANSYS understands that it’s a closed curve.
- We also add the “Z-cord” column and fill all its values with zeros just because ANSYS needs to have z coordinates even though we aren’t going to use them in the case of 2D Airfoils.

#Group	Point	X-cord	Y-cord	Z-cord
1	1	1	0	0
1	2	0.999753	0.000036	0
1	3	0.999013	0.000143	0
1	4	0.997781	0.000322	0
1	5	0.996057	0.000572	0
1	6	0.993844	0.000891	0
1	7	0.991144	0.00128	0
1	8	0.987958	0.001737	0
1	9	0.984292	0.00226	0
1	10	0.980147	0.002849	0

Table (III-1). Importing the Airfoil coordinates into an Excel.txt file.

Now that the data is ready for use in DesignModeler, we simply go to **Concept > 3D Curve**. Then we pick the plane on which we’d like to draw our curve (we picked the **XYPlane**) and the way in which we desire to plot our Airfoil (in our case **From Coordinates File**).

The result is portrayed in Fig (III-4):

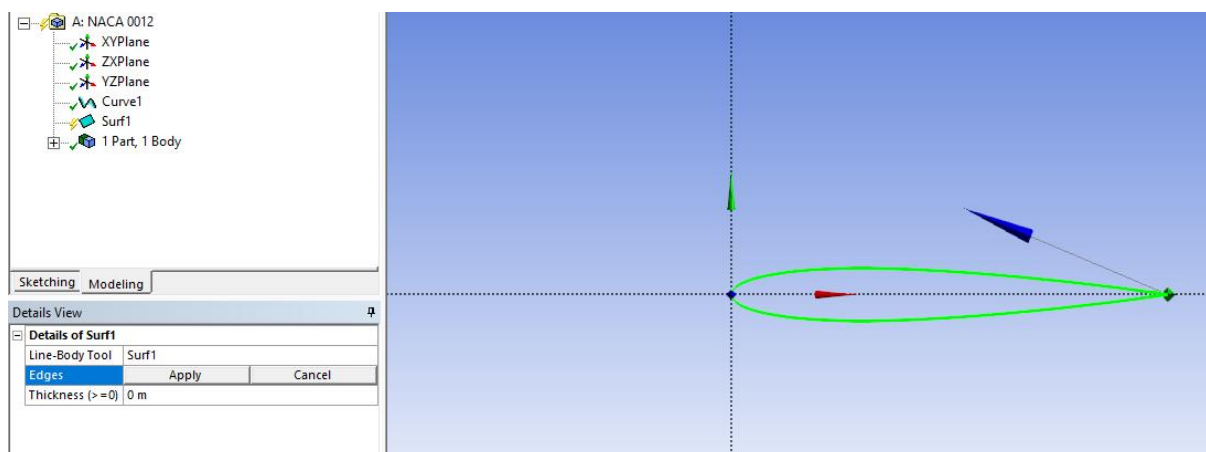


Fig (III-4). Final look at the Airfoil plot from the XY Plane after importing the Dat file.

2. **The second step** is to create a surface body from our plot so that it makes a 2D Airfoil surface, we do that by going to **Concept > Surfaces From Edges** this time, which will allows us to choose our Airfoil plot as the edge and then clicking **Generate**  **Generate** which will create and save the action.

3. **Thirdly**, we started the sketching process, we used a **C type** domain with the rectangle part mostly downstream of the Airfoil as shown in Fig (III-5), and the circle having its center around the trailing edge to be able to have better meshing and consequently better results.

The process is initiated by simply pressing the **New Sketch**  > **Draw** > **Rectangle** and drawing around our Airfoil. For the Circle, the same steps but instead from **Arc by Center** (the center is in the Airfoil Chord and the rest of the two points linking the Arc are the 2 edges of the rectangle).

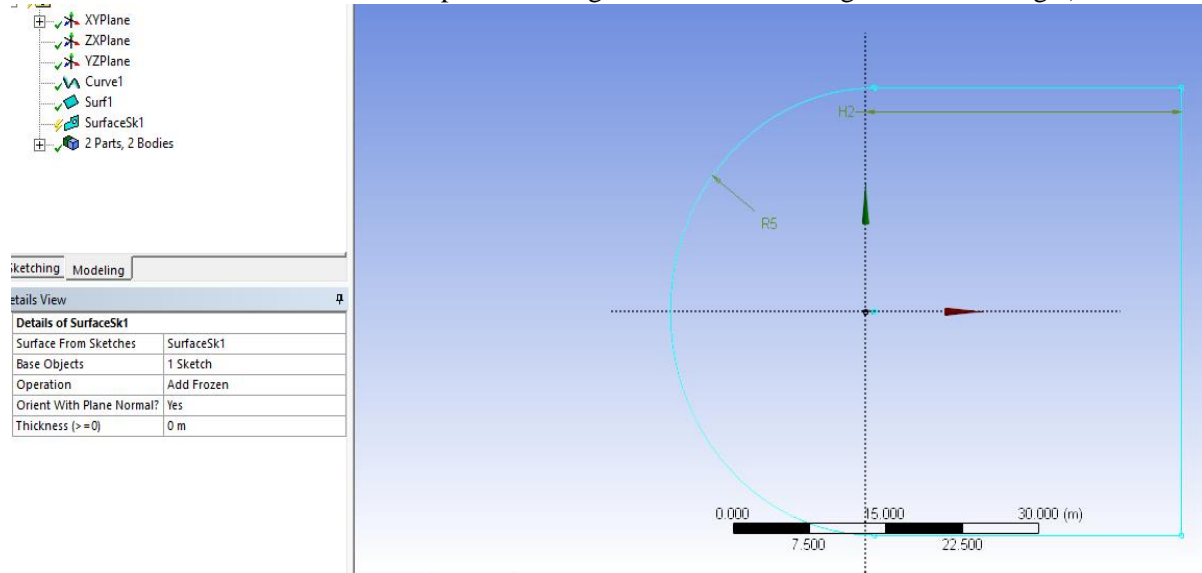


Fig (III-5). The Full Sketch containing the Airfoil and the Domain Surrounding it.

4. **Next**, Giving the domain dimensions **as follows**:

- Assigning the value of **0.1m** to the horizontal distance between the **Y-Axis** and the line of the rectangle closest to it. This is for the mesh sizing which we will go into later.
- Assigning **31m** to the horizontal distance between the **Y-Axis** and the line of the rectangle farthest from it. Because the chord is taken as **1m** from the website. And **30m** is for the edge to be far from the Airfoil so there's no interference with our simulation results.
- Same thing for the Arc, so that no interference happens, we assigned a radius of **20m**.
- Trimming the line of the rectangle closest to the **Y-Axis** from **Modify** > **Trim** to open up the domain and give it the desired **C type** shape.

5. **The Fifth Step** is to **Generate** the domain from **Concept** > **Surfaces from Sketches**. Then we select all the arc and the rectangle and pick **Operation** > **Add Frozen** so that when it's generated it is considered as the fluid (Air) surrounding it.

Finally, we need the Airfoil surface to be considered as what we want to study in our simulation. We do that by going to **Create** > **Boolean** > **Subtract** as the operation, the Airfoil as the **Tool Body** and domain as the **Target body**. We obtain what is shown in Fig (III-6).

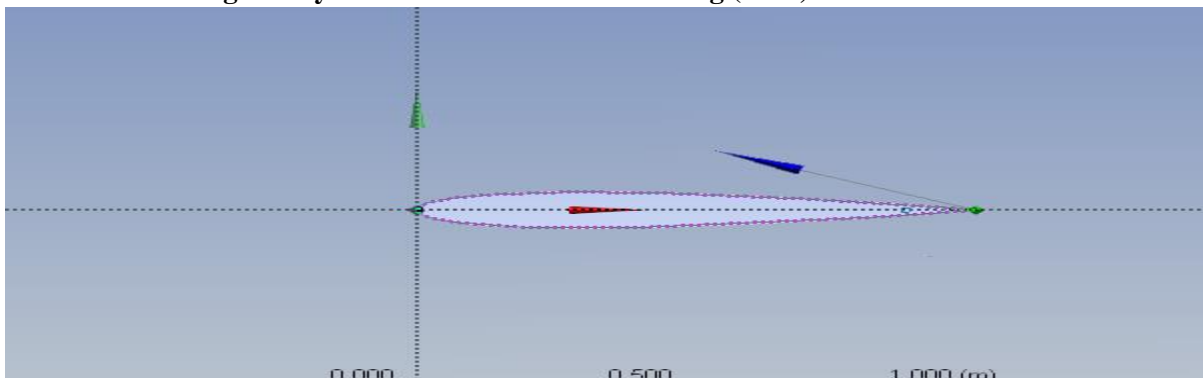


Fig (III-6). Separating the Airfoil from the Domain body.

6. **The Final part** is Splitting the domain for some **Edge Sizing** to help gain more control in the meshing and more room to adjust it. **It goes as follows:**
 - Starting from **Tools > Face Split** with **Face Split Type** as **By Plane** so that we split it with respect to a the **ZX Plane** so that the domain is split horizontally as shown in Fig (III-7).

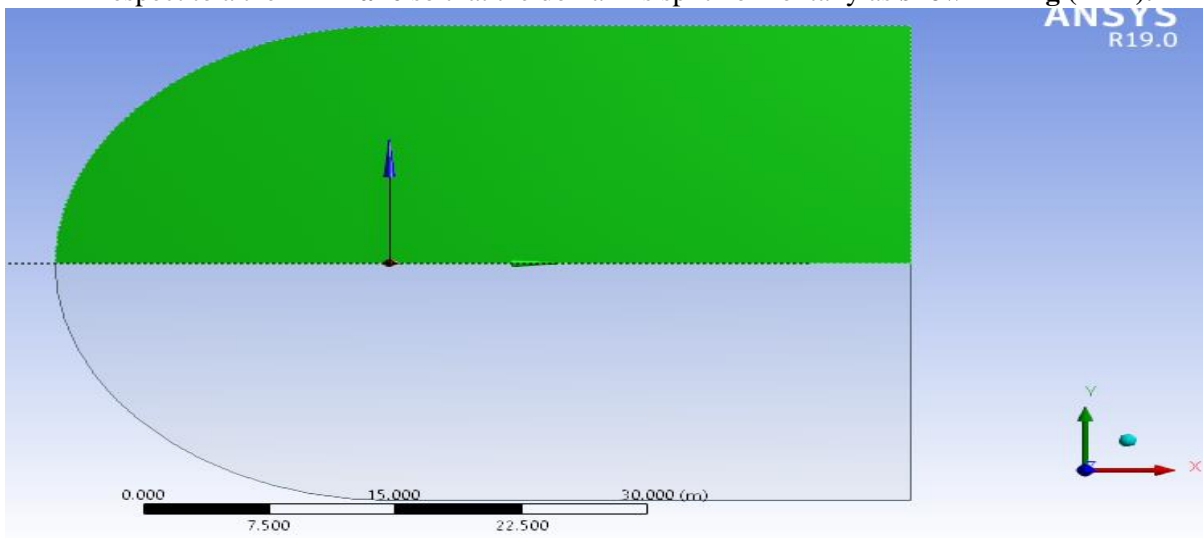


Fig (III-7). Domain after the First Face Split with Respect to the ZX Plane.

- Splitting the domain vertically depending on a **New Plane** because we want our sizing to be around the trailing edge so that we can refine it there to obtain better results in the Airfoil wake. The coordinates of the new plane are: 1 for X to account for the chord line and **0** value for **Point Y** and **Z**. for vertical splitting, **Normal** coordinates are **1** for **Z** and **0** in **X** and **Y**.
- With the **Target Face** being both split up parts of the domain.
- For the edge sizing around the leading edge, we made another Plane with the same **Normal** coordinates for vertical splitting but with **0.1** in the **Point X** and **0** in **Y** and **Z**. so that it coincides perfectly with the edge of the rectangle (the reason for the **0.1m** distance before).
- With the **Target Face** being the circle side of the domain.

7. **Lastly**, a minor last step is setting the **Fluid/Solid** to **Fluid**. As shown in Fig (III-8). And also setting the **Line Body** as **Supressed** because we won't be needing it in our meshing.

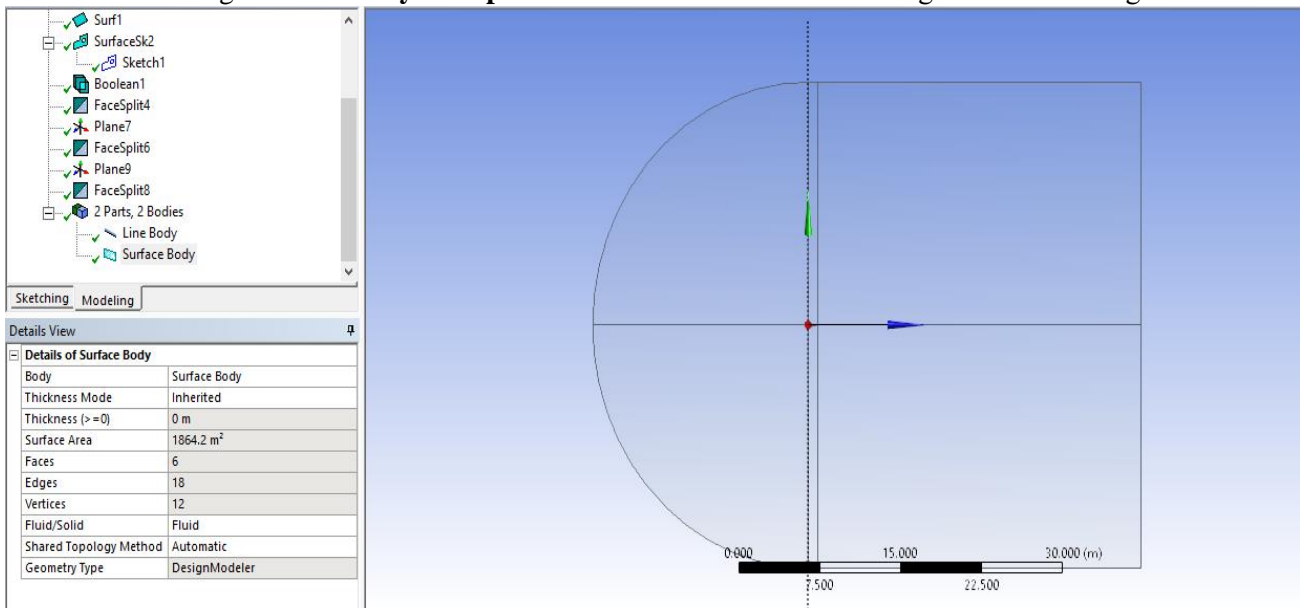


Fig (III-8). Final look at the Geometry of NACA 0012.

- **This process is the same for all our Airfoils, with the only change being the Airfoil Data.**

III.1.3. Preparing the Mesh on Ansys Mesh Creator:

The goal in this step is to create the mesh around the lines we created and around the Airfoil and domain to make sure it is well aligned and distributed around the places we are interested in studying. And that is a process that requires:

1. **First**, Configuring the **Edge Sizing**, from **Mesh > Insert > Sizing**.

The first Sizing is on by the horizontal edges of the domain parallel to the wake; the mesh is concentrated around the trailing edge and parallel to it for better results around those areas. With the type of sizing as **Number of Divisions** set to **100 Divisions** for better control, the **Behaviour** set as **Hard**; because if you set it as **Soft** than you are basically telling **Ansys** that it is malleable, but when it's **Hard** it means it has to stick to our chosen number of divisions. Finally, the **Bias Type** which is basically how we want our cells to be distributed is **from small to large spacing between cells** since we want them to be more concentrated around the Airfoil while the **Bias Factor** is **500** to set the distance between each cell.

2. **The Second Sizing** is about controlling the mesh **surrounding the Airfoil and on the outlet**, to have higher concentrations of cells around it, on its nose and parallel to its tail.

The configuration is the same except that the **Number of Divisions** is **200** because it's a more sensitive area that requires more details to get better results around the Airfoil surface. And the **Bias Factor** which is **50000** to be more accurate

3. **The Third Sizing** revolves around the Airfoil's rear surface and the edges of the domain parallel to it. The **Number of Divisions** is **200** even though the space is smaller because we want better results here, and the **Bias Type** is set to **No Bias** for equal distributions of cells along the Body and the domain surrounding it.
4. **The last step of the Sizing** is configuring the mesh for the Leading edge and the Cercle of the Domain surrounding it. The **Number of Divisions** is **100** here because it's a smaller region and doesn't require much cells for detailed results.
5. **Next**, is to insert a **Face Mesh** to map between the edges and create a **Quadrilateral Mesh** all for the sake of getting better Data from our Cells near the studied Airfoil. From **Mesh > Face Meshing >** selecting all the domain.
6. **Finally**, generating to obtain the final Mesh as shown in Fig (III-9) and Fig (III-10).

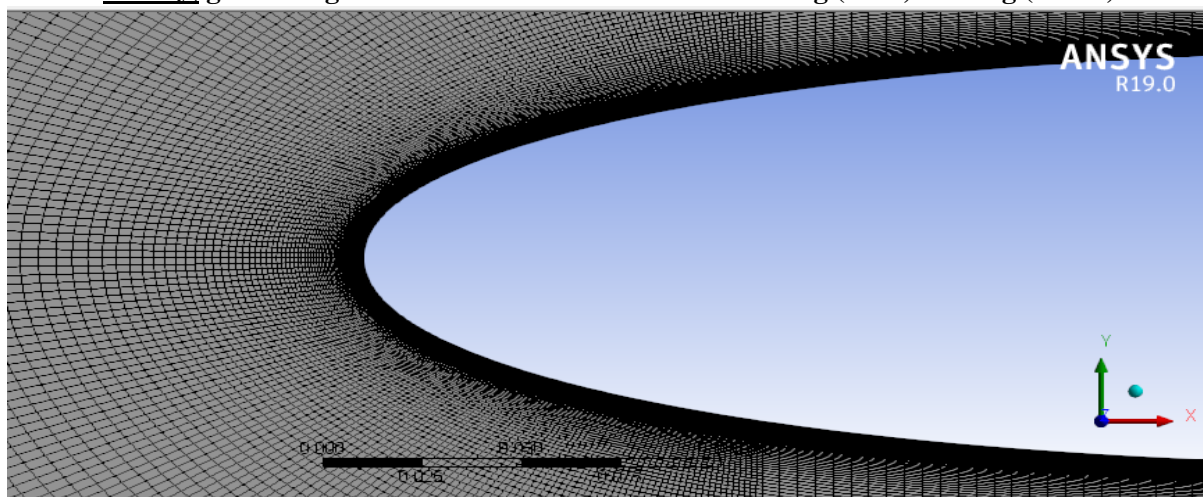


Fig (III-9). Mesh Refinement around the Airfoil Nose.

1. **The Last task** is creating **Named Selections** which is basically naming the domain parts so that the **Fluent Solver** can understand them. It's a simple process that consists of selecting each required part and then right clicking and choosing **Named Selection**. We created 3 selections: Inlet, Airfoil-Wall shown in fig (III-11), and the Outlet.

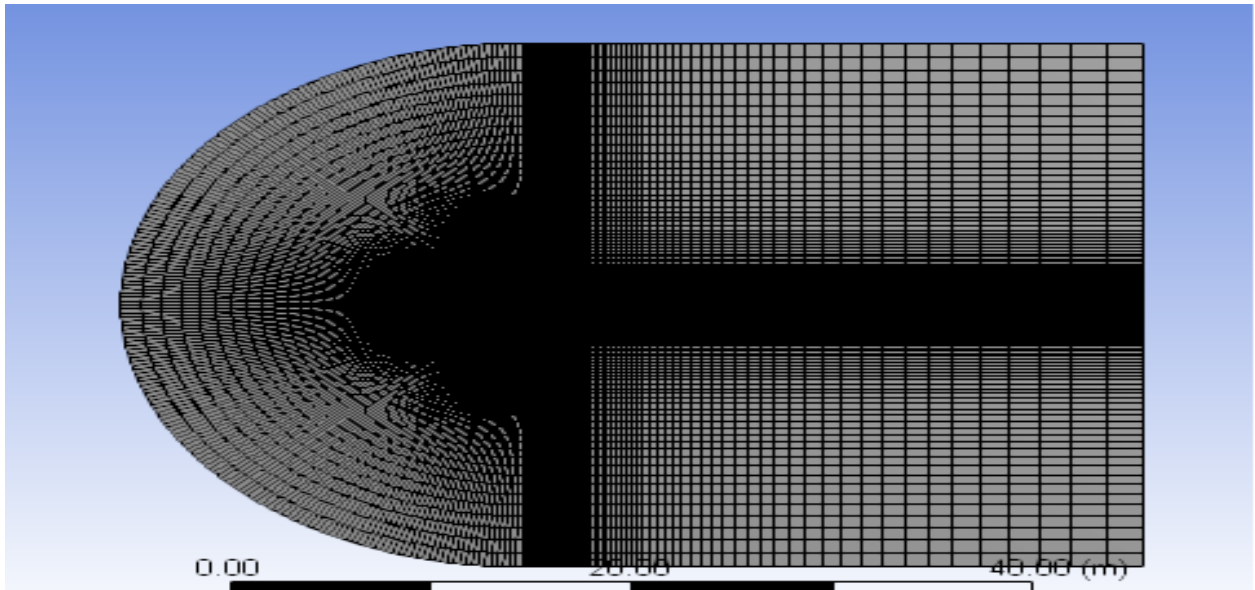


Fig (III-10). Final look at the desired Mesh.

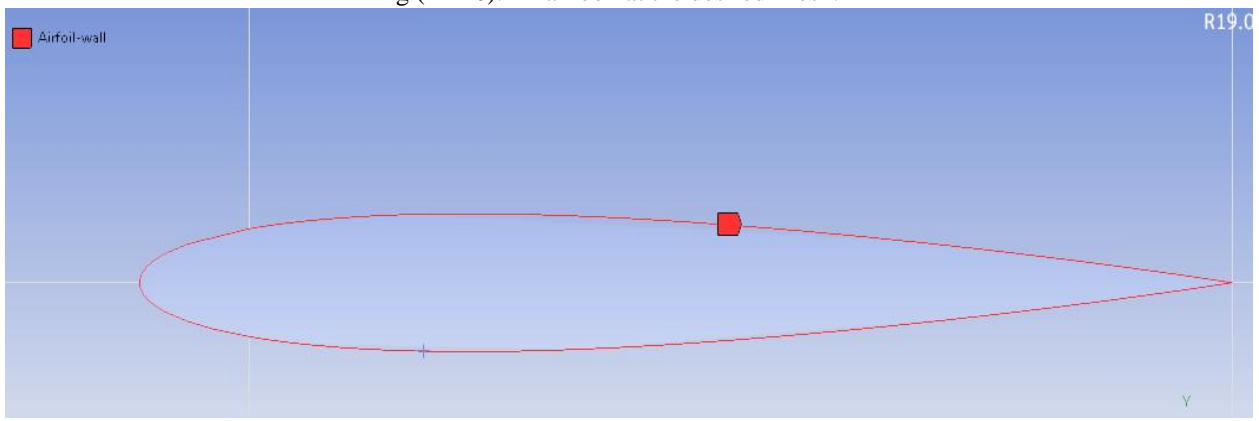


Fig (III-11). The Named Selections of the Airfoil-Wall.

III.1.4. Setting Up and Launching the Simulation on the Fluent Solver:

This is a pretty straightforward step, since all we have to do is **Update** the mesh and configure the simulation in the most efficient way in order for the solution to converge and then launch it and let it do the work. Yet there are a few key points we need to take care of **which are:**

- 1- Launching **Fluent** requires first launching **Setup** from the **Workbench** main panel. And then to check **Double Precision** for more accurate results, and setting up the number of Processors we want our computer to use (**Parallel option**) as portrayed in Fig (III-12).

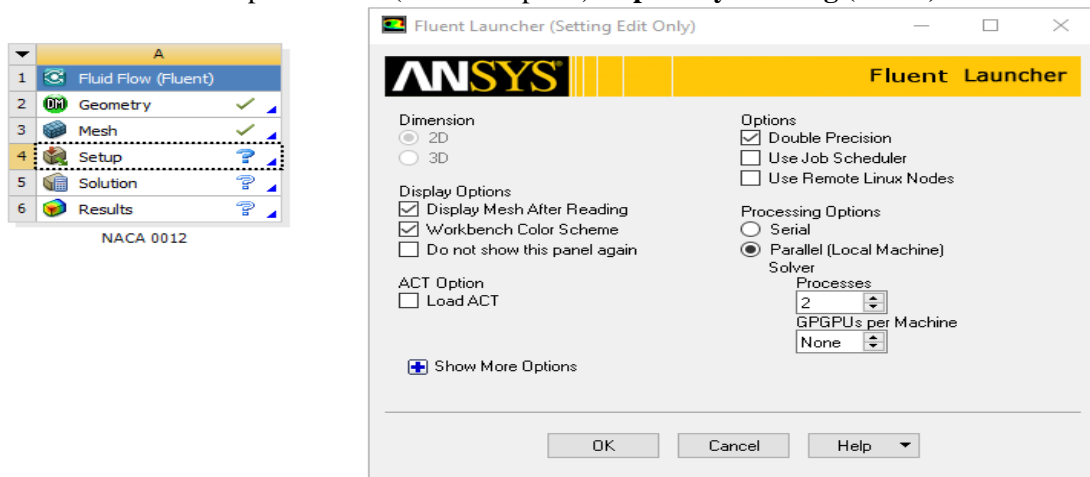


Fig (III-12). The Fluent Launcher Configuration.

2. After the Solver processes the mesh, we proceed to check it and change what we need to change leaving the rest as default because it already serves our purpose, like for instance: we leave the **Solver Type** in the **General** option as **Pressure-based** because it's a subsonic incompressible flow and its **Time** as **Steady** because we are dealing with a flow that doesn't vary over time.

The main changes we made are:

- In the **Models** section under **Viscous** which enables us to choose the turbulence model we want to work with, we went with the **K- ω SST model** because it's a good robust model for attached flows and also works well with separation so we thought it's a good choice since we are going to be changing the angle of attack later on.
- We made sure our chosen **Material** is a **Fluid** and that it's **Air** under atmospheric conditions.
- Next is the **Boundary Conditions**, we made sure the **No Slip Shear Condition** is checked in the **Airfoil-Wall** section meaning we assume the velocity at the wall is **zero** and we left the **Outlet** parameters set to constant pressure downstream.

As for the **Inlet**, we need to set the **Velocity Specification Method** to **Magnitude and Direction**. **Magnitude being 28m/s** we can simply modify our Angle of Attack from this section by changing the velocity components and for the purpose of computing everything simultaneously we used a **Parameter set**. Hence, the need to set a **new input parameter** in **Velocity Magnitude** and setting it to **28m/s**; the speed of our real-life Wind Tunnel. And doing the same for the **X** and **Y-Components** of our flow setting **X** to 1 and **Y** to 0 to account for the initial Angle of Attack we used which is **0**.

- We also went to **Reference Values** and set it to **compute** from the **Inlet**.
- The **Methods** are basically two types, **Simple** which solves for the pressure and velocity separately and **Coupled** which does it at the same time.

We chose **Coupled** because it diverges faster and set all the other settings to **Second Order** because it's more accurate than **First Order**.

- The next step is to go to **Report Definitions**, and add what we wanted to plot and get the result of in our simulation.
- We start by defining the **Lift** and **Drag Coefficients** by checking **Report Plot** and **Plot to Console** to give us the **C_D** and **C_L** graphs and **Create Output Parameter** so that it exports our results to the **Parameter set**. We also need to click the **Airfoil-Wall** to indicate that it's what we want the drag and lift to be studied on. But the thing is it's going to give us the **Normal** and **Axial Forces** instead so we label them as **Axial-Coeff** and **Normal-Coeff** we will explain that later on.
- And then we define the **Pitching moment** the same way except for setting its position as **0.25m** essentially at the center of Pressure since the chord is **1m**. Lastly, we added a definition for the **Static Pressure** around the Airfoil to set it later as a convergence condition. And named it **Surface-Int** since to add it we added a **Surface Integral Report** and basically did the same setting as the others.
- In **Residual Monitors**, since we are going to depend on Static pressure around the Airfoil as a convergence criterion we unchecked all the other factors here but still kept them as graphs to plot just to check on their development.
- And in the **Convergence Conditions** section we set the static pressure that we defined earlier as the criterion and add it with a **Stop Criterion** of **1e-07** for maximum accuracy. We named it **Surf-Monitor** and checked **Print** to see its evolution.
- Finally, before launching the calculation we have to initialize each cell with a value. We went with the **Hybrid Initialization** because it basically converges faster. The panel on which we can do this whole process is shown in Fig (III-13).

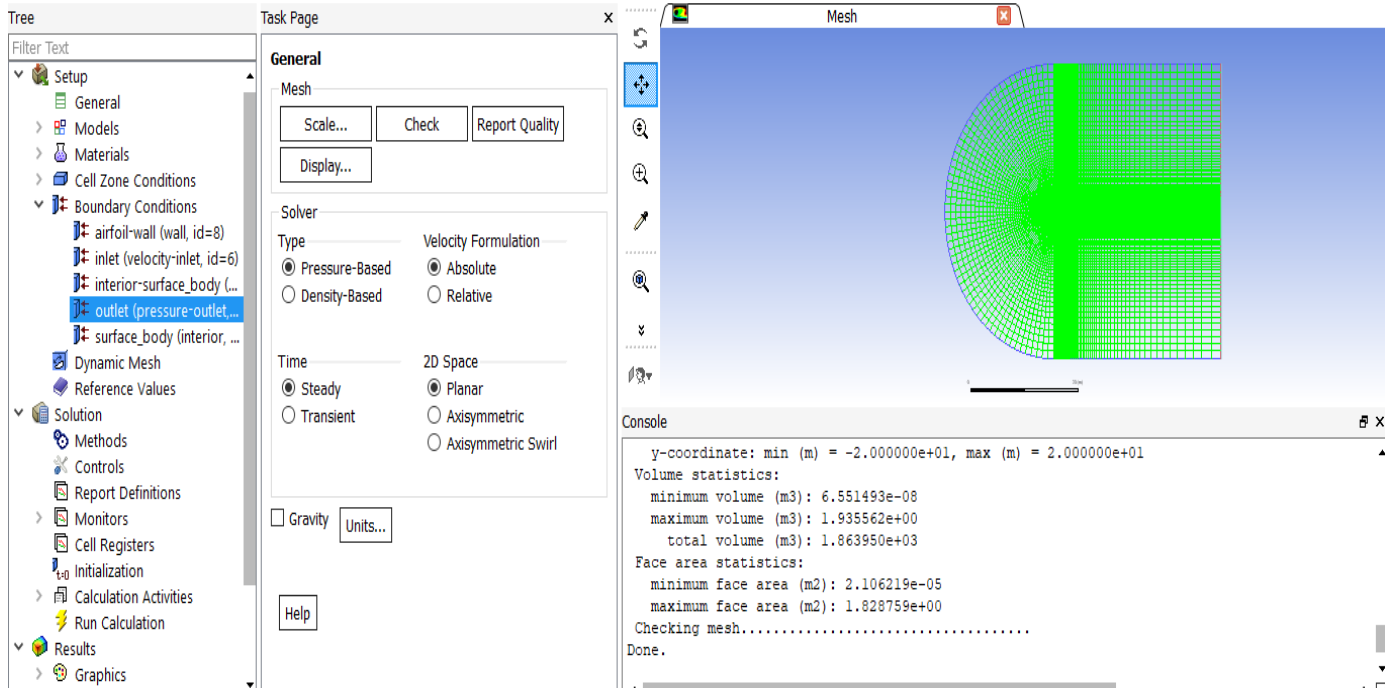


Fig (III-13). Main Panel for Configuring and Launching the Simulation.

- We now can launch our simulation. Since we confirmed we don't have any errors from **Check case**, we set the **Number of Iterations** to **1000** to give it enough room to work and converge properly and then finally **Calculate**.

The Results are shown in Fig (III-14). And note that the meshing process and this configuration is the same for all our studied Airfoils.

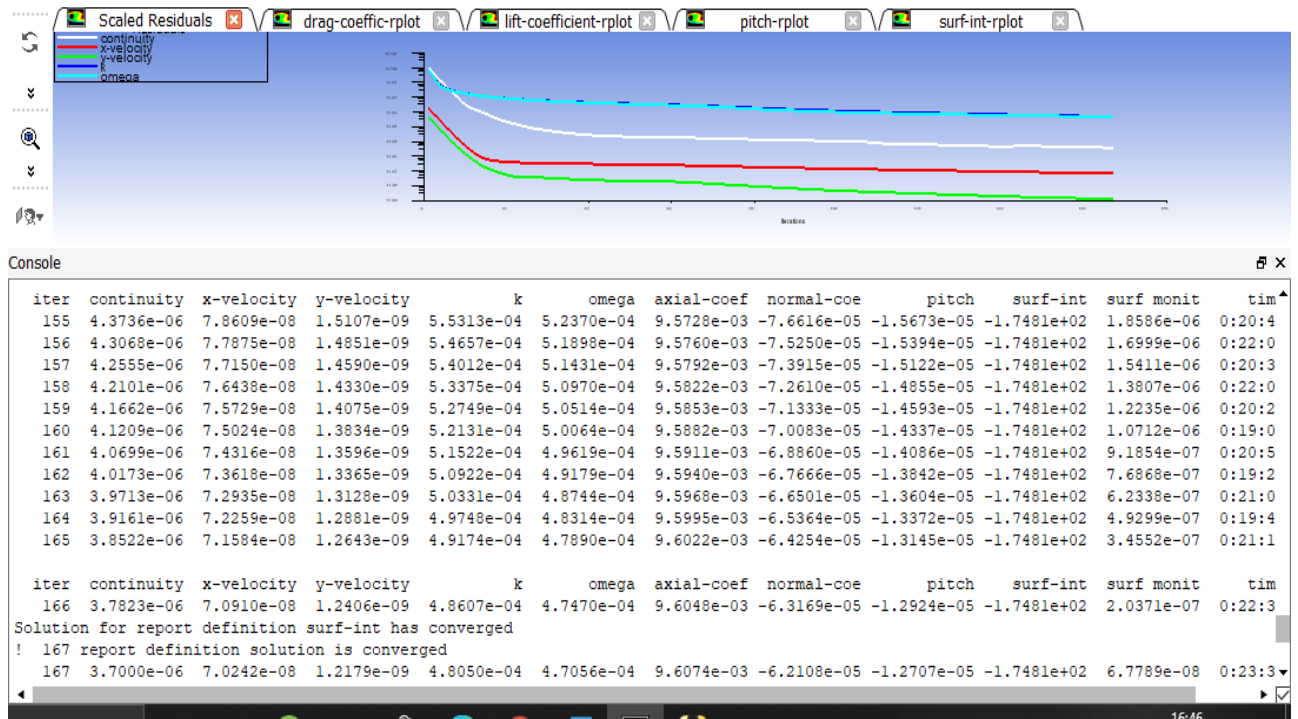


Fig (III-14). Simulation results after convergence for NACA 0012.

III.1.5. Results and Parameter sets:

Now that we have our simulation results for 0 angle of attack, all that is left to do is input our values and let ANSYS do the same for the rest of them. But first we need to go to **Results** to set the forces exerted on the Airfoil as output parameters. We can also get velocity and pressure contours around the Airfoil surface but we'll get to that later.

Time to explain why the simulation would give us the Axial and Normal Forces instead of Lift and Drag:

Lift and **Drag** are defined as the components of R that are perpendicular and parallel to the **Velocity** flow. While the **axial** and **normal forces** are defined as the components of R that are perpendicular and parallel to the **chord line**. And since, we rotated the flow direction instead of rotating Airfoil to change the Angle of Attack for each time (it would give us the same results like the Wind Tunnel principle). The values of Drag and Axial force and Lift and Normal force would change for different angles of attack unlike for 0 AoA where would get the same results. So, in order to get our Lift and Drag coefficients, we need to adjust it according to the equations (II.6) and (II.7) describing the relationship between Drag/Lift and the Normal and Axial Forces.

One more thing is how we change the **X and Y components** of the Flow. We simply put the **X component** as **Cos (α)** and the **Y component** as **Sin (α)** since we want to input the direction vectors for our flow. With **α** being the **Angle of Attack in Degrees**.

- So, we go to **New Output Parameter** and set a **New Expression**. We input the equation: $((P26 \times P1) - (P27 \times P2))$ and name it as **Lift**. Since it's the same as (II.6) or $L=N.Cos(\alpha)-A. Sin(\alpha)$. with **P26** as the **Normal Force**, **P1** as the **X Component** or **Cos(α)**, **P27** as The **Axial Force** and **P2** as the **Y component** or **Sin(α)**. as shown in Table (III-2).

Outline of All Parameters				
	A	B	C	D
1	ID	Parameter Name	Value	Unit
2	Input Parameters			
3	NACA 0012 (A1)			
4	P1	Xcomponent	1	
5	P2	Ycomponent	0	
6	P3	Inlet Velocity	28	m s ⁻¹
7	P12	AoA	0	
*	New input parameter	New name	New expression	
9	Output Parameters			
10	NACA 0012 (A1)			
11	P6	Pitching Moment	-1.2707E-05	
12	P24	axial-coeff-op	0.0096074	
13	P25	normal-coeff-op	-6.2108E-05	
14	P26	Normal Force	-0.029824	N
15	P27	Axial Force	4.6135	N
16	P28	Lift	-0.029824	N
17	P29	Drag	4.6135	N
18	P30	Lift-Coeff	-6.2108E-05	
19	P31	Drag-Coeff	0.0096074	
*	New output parameter		New expression	

Table (III-2). The Input and Output Parameters concerned with the results.

- The same thing was done to **Drag** and **Lift-Coeff** and **Drag-Coeff** since: $Cl = Cn \cos(\alpha) - Ca \sin(\alpha)$ (III.1) and: $Cd = Ca \times \cos(\alpha) + Cn \sin(\alpha)$ (III.2).

III.1.6. Results Discussion and Comparison with Known Data:

- After finalizing the work and obtaining the results, now it's time to turn the DATA into graphs to discuss it and compare with the already existing DATA.
- 1- We decided to increase our DATA size and study it from angle of attack -12 to 22 degrees. Which gave us a more apparent graph of its changes, we drew graphs using Microsoft Excel of the coefficients of Lift and Drag Vs the AoA in addition to CD/CL Vs AoA/Cl vs Cd
- 2- we obtained the results shown in Fig (III-15) and Fig (III-16) and Fig (III-17).

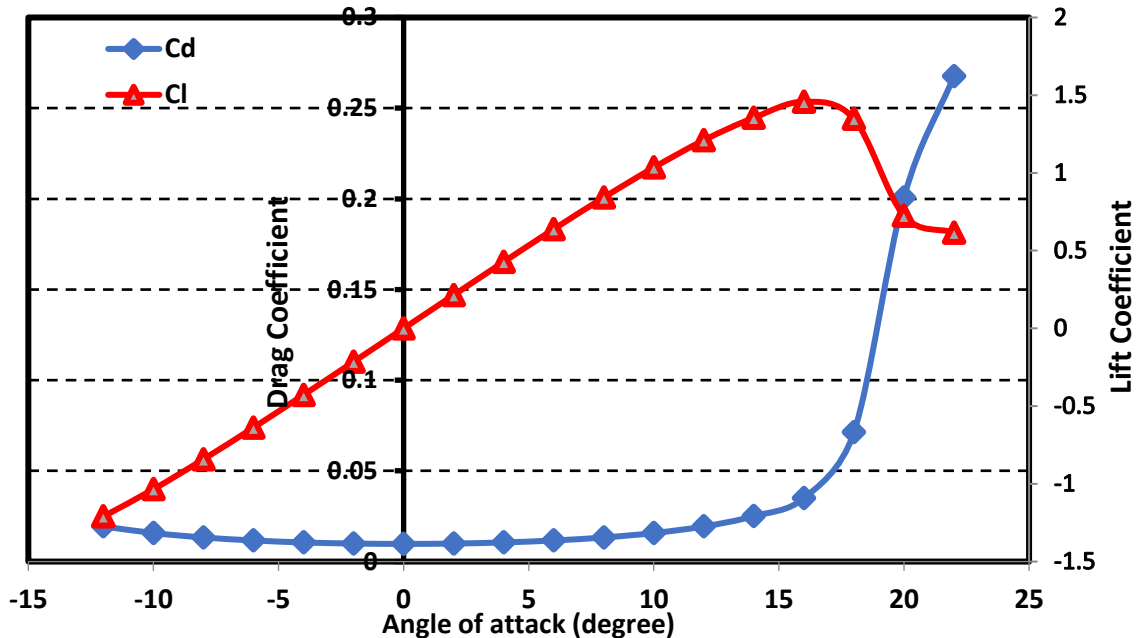


Fig (III-15). Lift and Drag Coefficients Versus the Angles of Attack (-12 to 22 degrees).

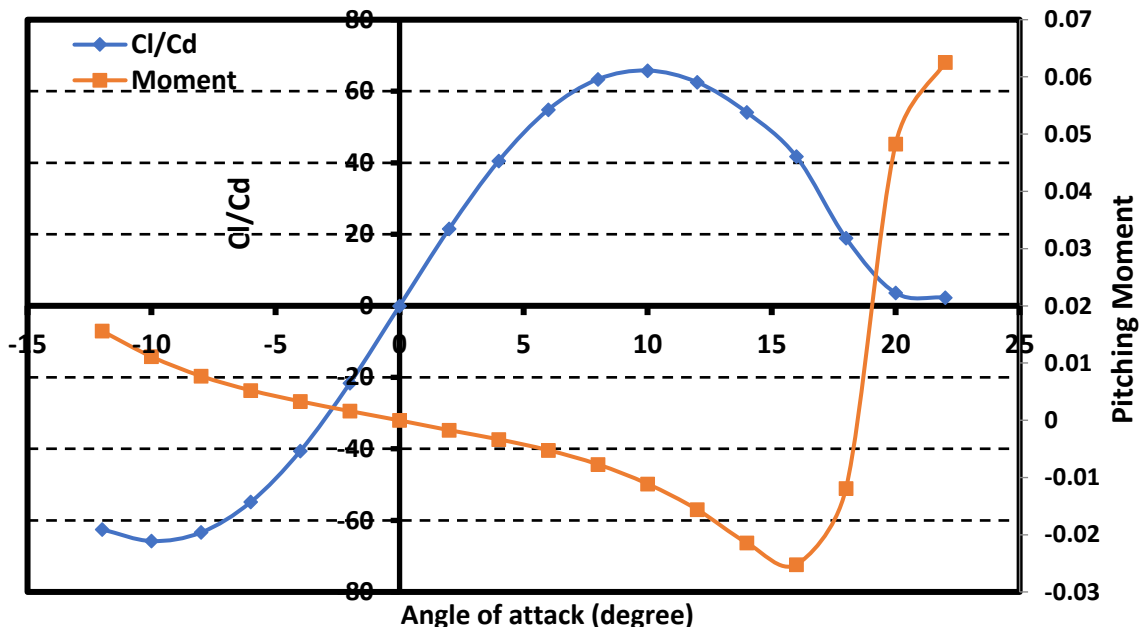


Fig (III-16). CL/CD and the Pitching Aerodynamic Moment Versus the Angle of Attack (-12 to 22 degrees).

- We note that Cl keeps on increasing as the AoA increases until it reaches a certain value around 18 and 20 degree where it falls drastically. That is Cl max/Stall for NACA 0012.
- As we increase the AoA, Drag takes a dive around 0 degrees, then start increasing again to the point where it increases drastically following the fall of Lift on the Stall point.
- The pitching moment values even though they seem to be fluctuating, they are still around the 0 value which is consistent since it's a symmetrical Airfoil.

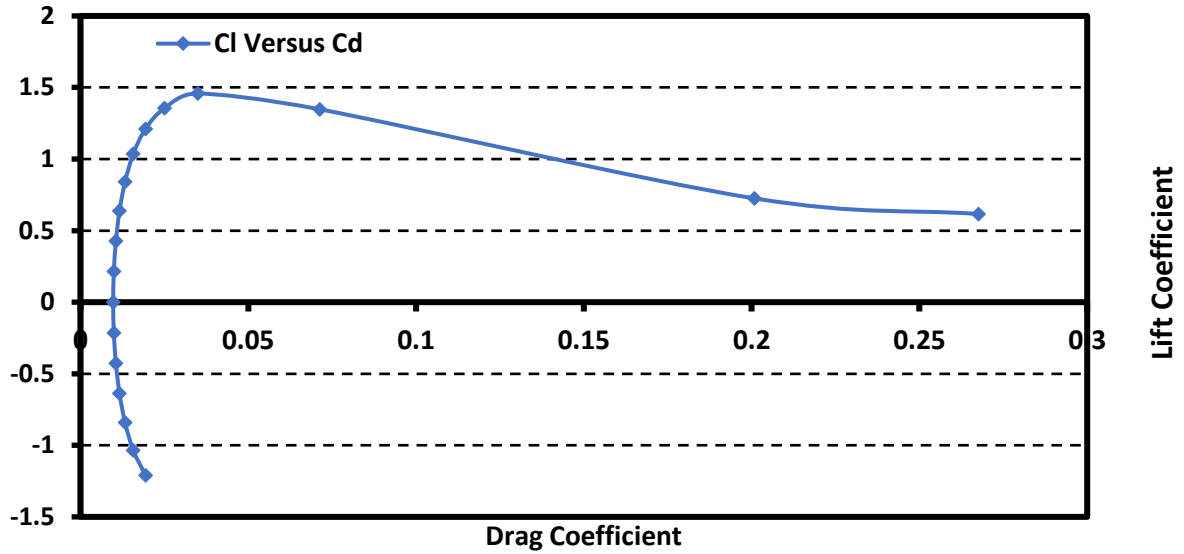


Fig (III-17). Lift Coefficient Versus Drag Coefficient.

- We can use the Cl VS Cd graph (or the polar) to find the best climb rate or sink rate as well as the best glide ratio (it determines how well our Airfoil can function in a glider in terms of distance and the drop in altitude) which we can find by drawing a line straight from the origin tangentially to the curve then read Cl/Cd which is our glide ratio.
- 3- The numerical results we obtained are shown in Table (III-3)

AoA	Lift Coeff	Error	Drag Coeff	Error	Moment	Cl/Cd
-12	-1.21028	-3.8162%	0.019363	6.3901%	0.015607	-62.5053
-10	-1.03472	-4.5108%	0.015732	7.0204%	0.011113	-65.7696
-8	-0.8419	-6.5074%	0.013288	10.733%	0.007713	-63.3582
-6	-0.63815	-1.9588%	0.011633	18.704%	0.005231	-54.8585
-4	-0.42802	-0.6683%	0.010552	31.900%	0.003302	-40.5637
-2	-0.21472	-1.5948%	0.009939	44.043%	0.001601	-21.6048
0	-0.00012	-0.0120%	0.009741	47.590%	-2.45e-05	-0.01216
2	0.21409	1.8835%	0.009945	44.130%	-0.00173	21.52745
4	0.427859	0.7057%	0.010556	31.950%	-0.00334	40.53377
6	0.638149	1.9589%	0.011633	18.704%	-0.00523	54.8564
8	0.841901	6.5177%	0.013288	10.733%	-0.00771	63.35662
10	1.034703	4.5124%	0.015729	7%	-0.01111	65.78506
12	1.210314	3.8288%	0.019363	6.3901%	-0.0156	62.50691
14	1.354985	2.7150%	0.025053	7.5236%	-0.02141	54.08377
16	1.45821	0.48997%	0.034954	1.3159%	-0.02521	41.71802
18	1.347687	3.7641%	0.071257	5.8796%	-0.01191	18.91313
20	0.725372	N/A	0.200803	N/A	0.048273	3.612357
22	0.61592	N/A	0.267661	N/A	0.062519	2.30112

Table (III-3). Airfoil Data for the NACA 0012.

- The real-life counterparts are obtained from Airfoiltools.com which gets it from the XFOil Software specialized in Aerodynamic testing. As shown in Fig (III-19).
- We noted an error of 0.01 for some points and 0.1 in some other points which is mainly due to the weak computing power we had access to. But overall, the results were good and more details on the validation are portrayed in the graphs in Fig (III-18).
- The graphs clearly demonstrate that even though there was a small error, the results are still valid due to the high similarity between the two cases, even though Drag Coefficient values are allowed to have high error percentage because the study is made under inviscid conditions which generate Drag very close to 0.

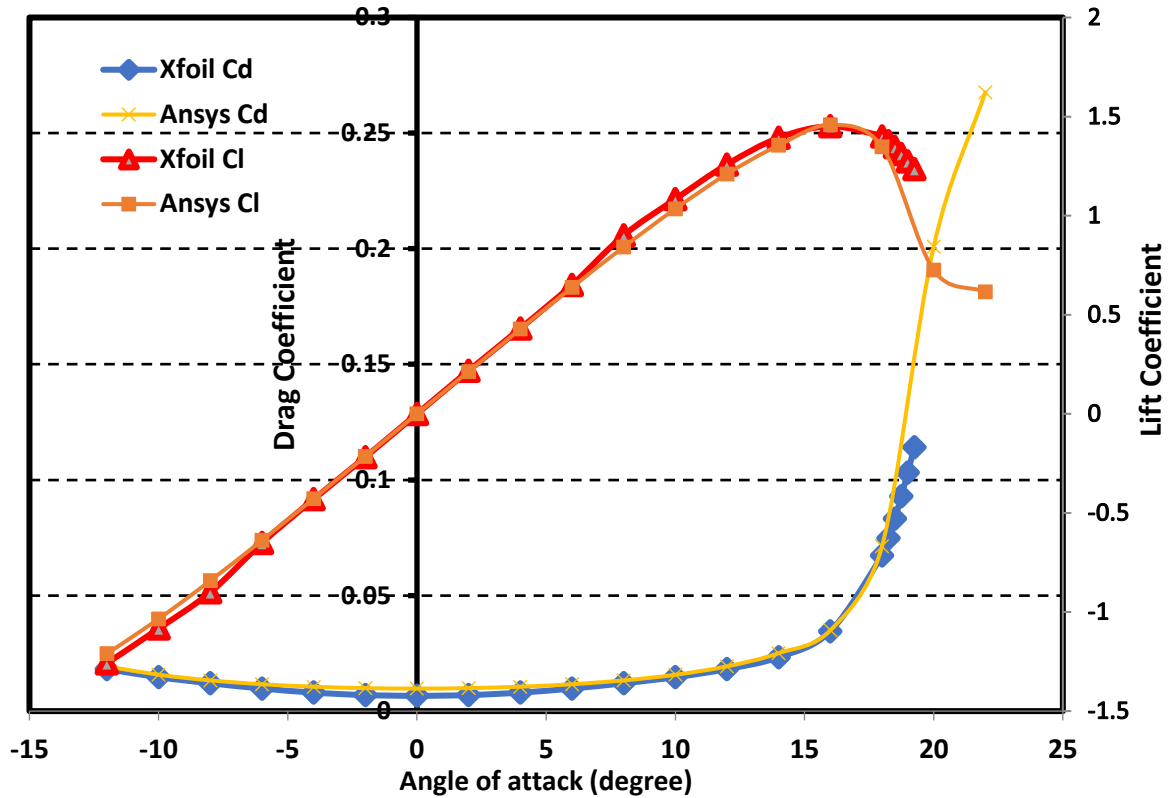


Fig (III-18). Comparison between our NACA 0012 Ansys Simulation Results and Standard Xfoil Data.

4- Finally, to fully show the extent of the data we retrieved from our simulation, a few Contours and Plots were made using the Fluent Post-Processor varying with respect to different Angles of Attack, some of them are **Shown in Figs (III-20,21,22,23,24,25,26,27)**.

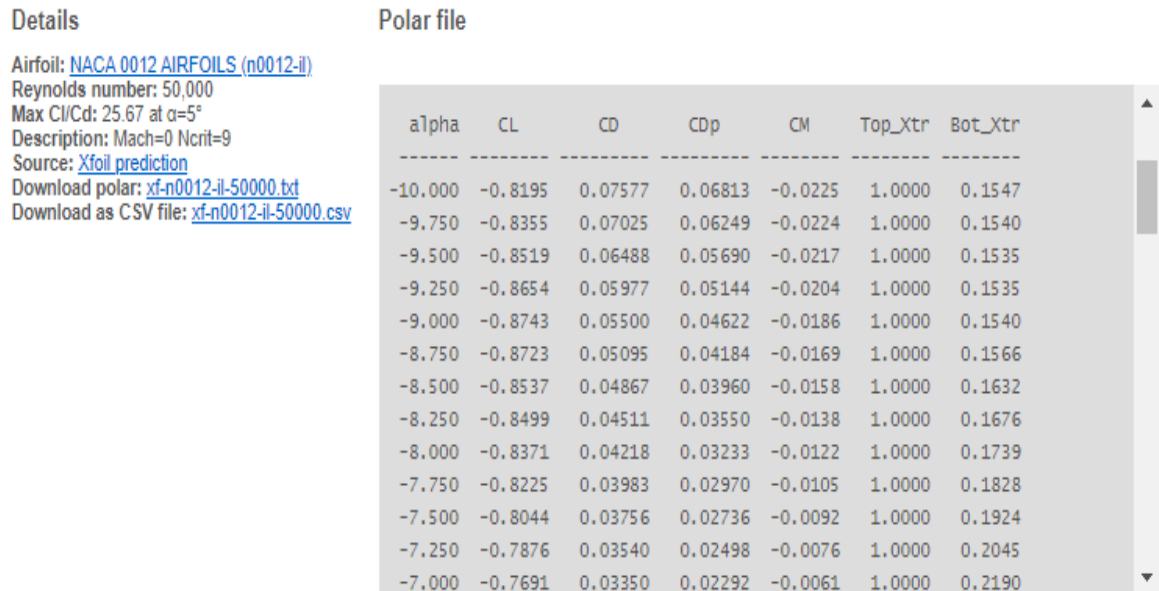


Fig (III-19). Xfoil Results from Airfoiltools.com for NACA 0012.

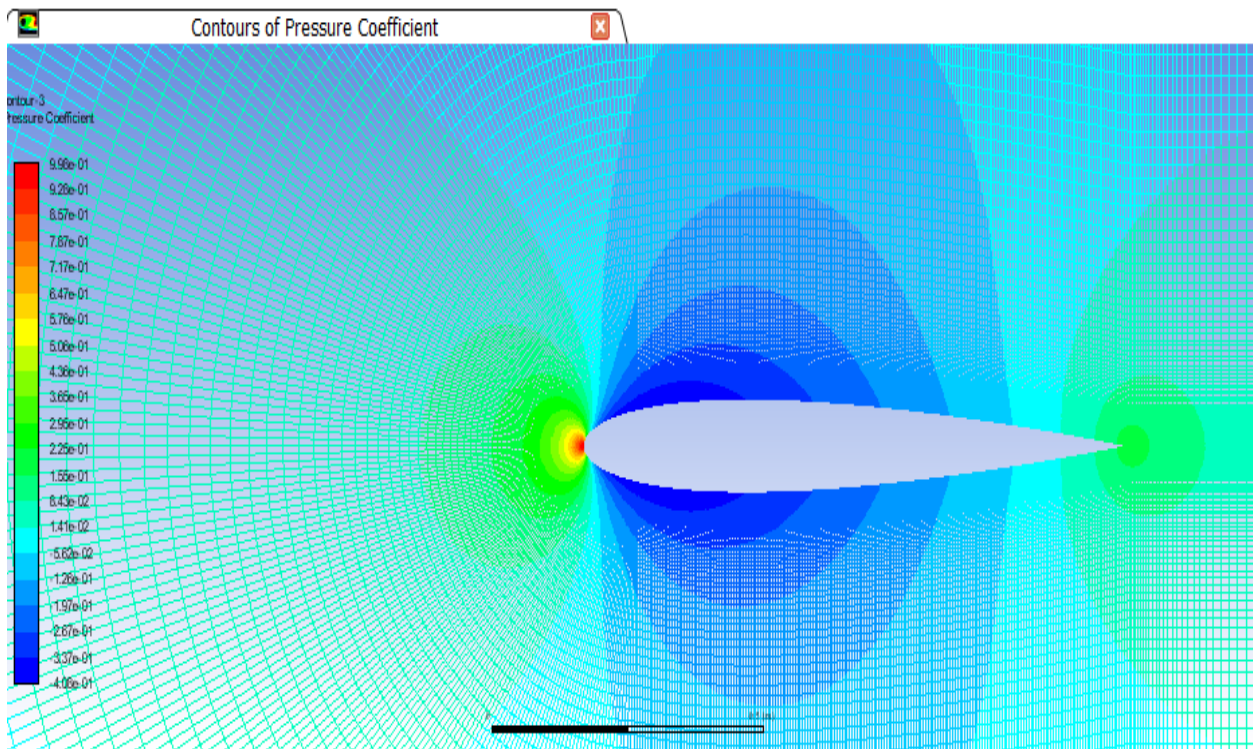


Fig (III-20). Pressure Coefficient Contours for NACA 0012 at 0 angle of Attack.

- We notice that the highest C_p is around 1 at the nose which is theoretically accurate with equal pressure distribution at 0 AoA with the symmetrical NACA 0012.

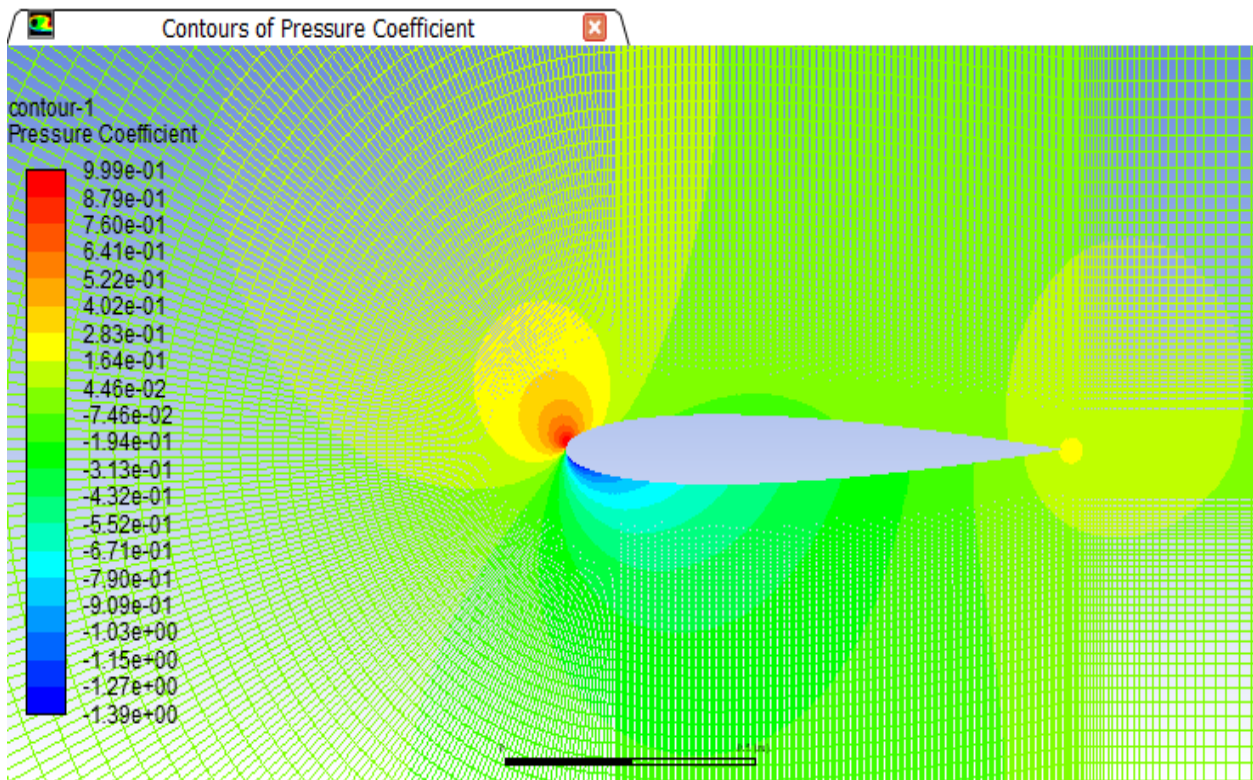


Fig (III-21). Pressure Coefficient Contours for NACA 0012 at -12 Angle of Attack.

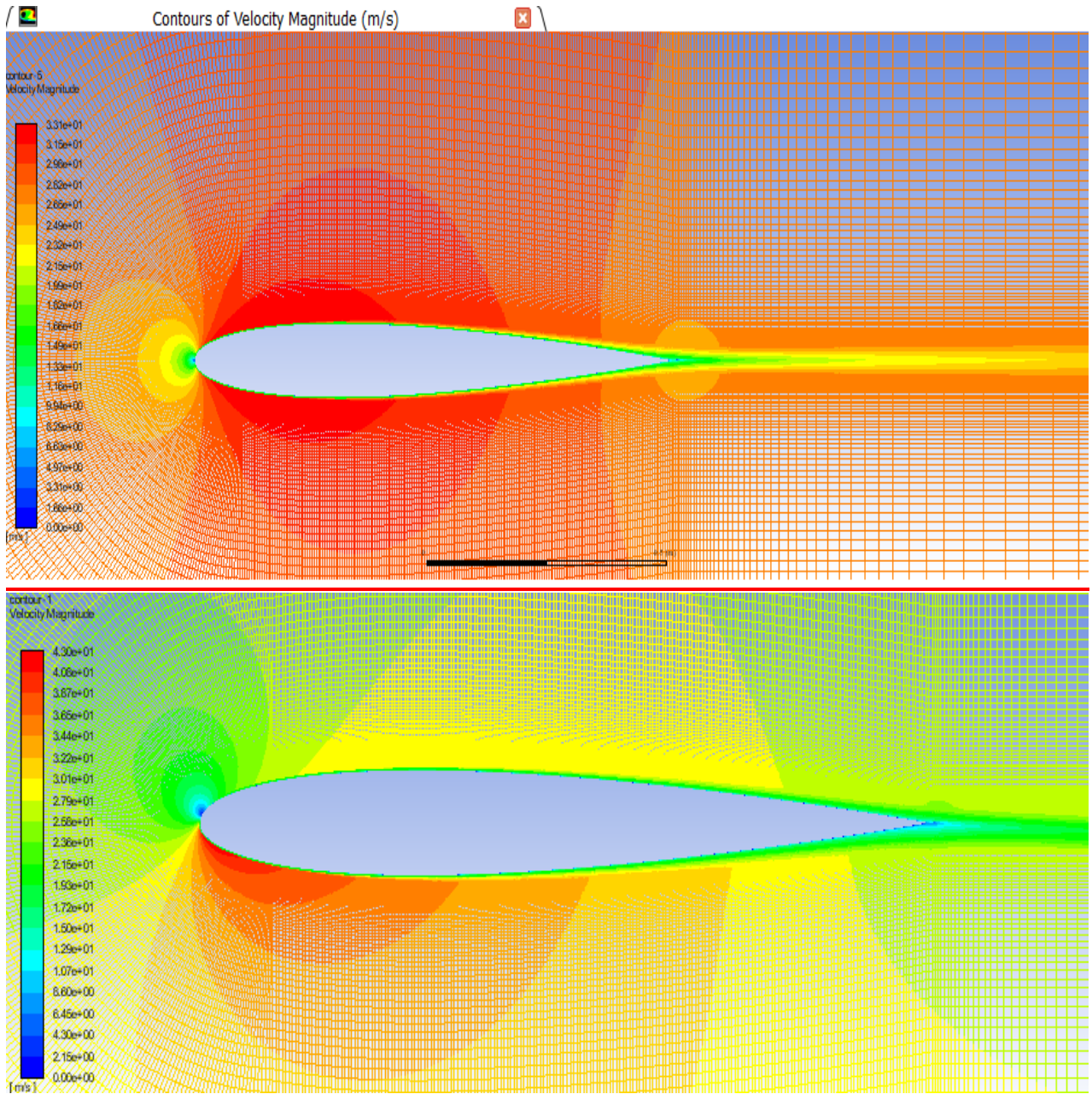


Fig (III-22). Velocity Magnitude Contours for NACA 0012 at 0 angle of Attack (Top) and -12 AoA (Bottom).

- As expected, we notice stagnation points around the nose where velocity is around 0 and flow acceleration at the top and bottom at 0 AoA with the opposite going on at 12 AoA.

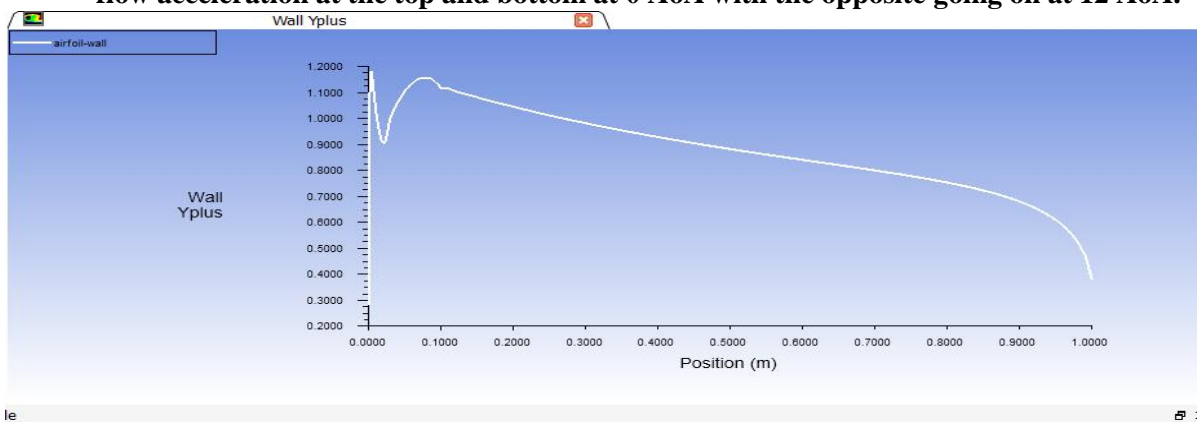


Fig (III-23). Y+ values Plots for NACA 0012 at 0 angle of Attack

- This the main validation criterion for our simulation and since the Y^+ value is around 1, it proves that the results are good and the mesh is precise.

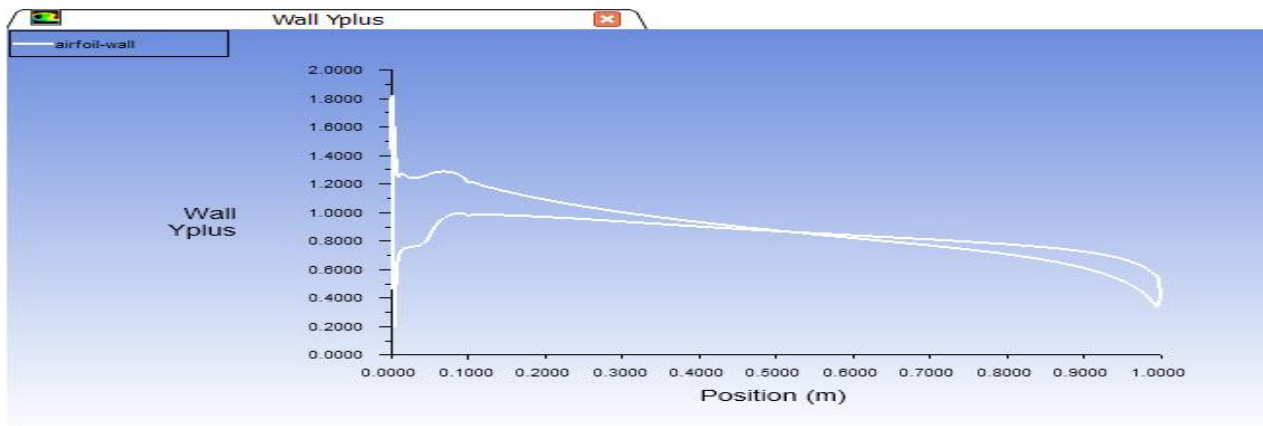


Fig (III-24). Y^+ values Plots for NACA 0012 at -12 Angle of Attack.

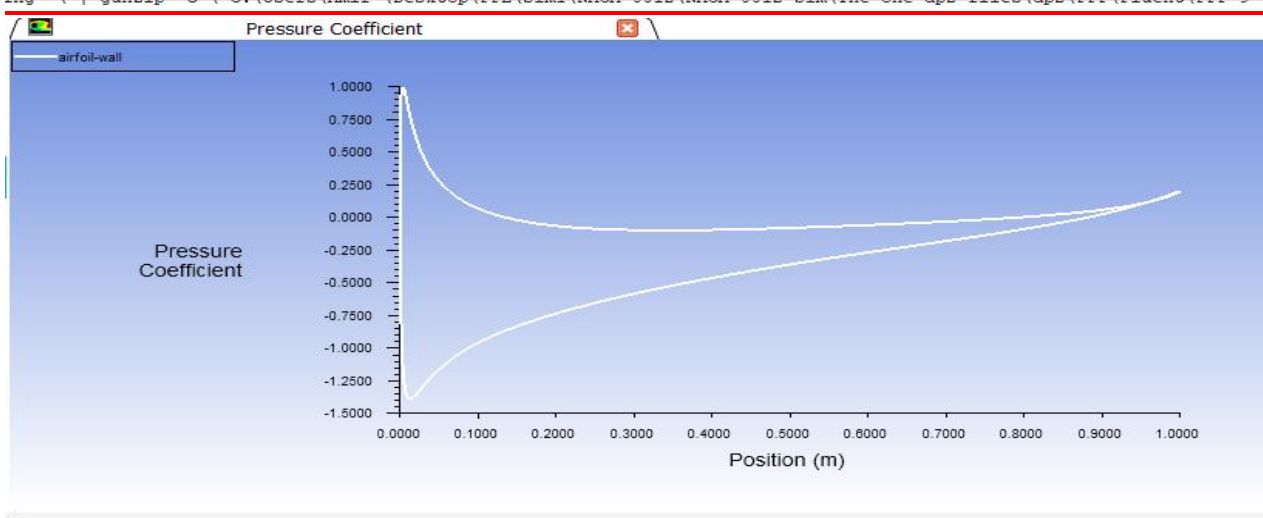
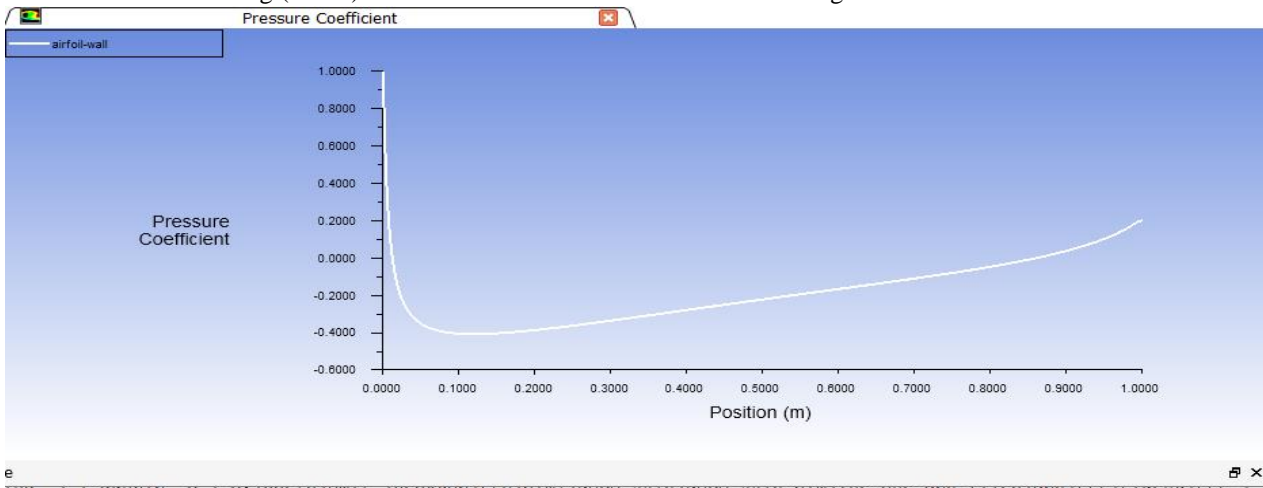


Fig (III-25). Pressure Coefficient Plots for NACA 0012 at 0 angle of Attack (Top) and -12 AoA (Bottom).

- We notice (0AoA) values at the top of the plot around 1 which is consistent with the stagnation point then we get the negative pressure as the flow accelerates that gets back up as it decelerates around the trailing edge.

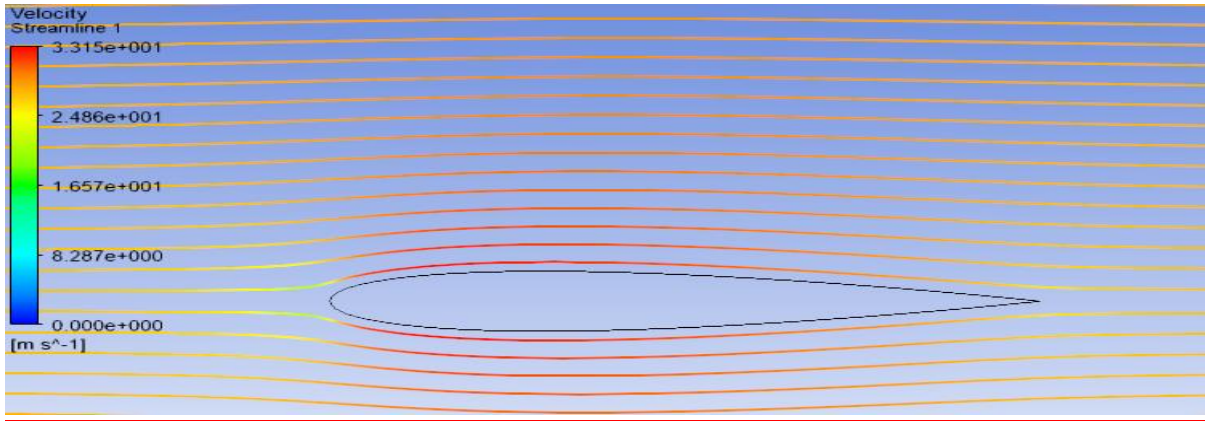


Fig (III-26). Velocity Streamlines for NACA 0012 at 0 angle of Attack

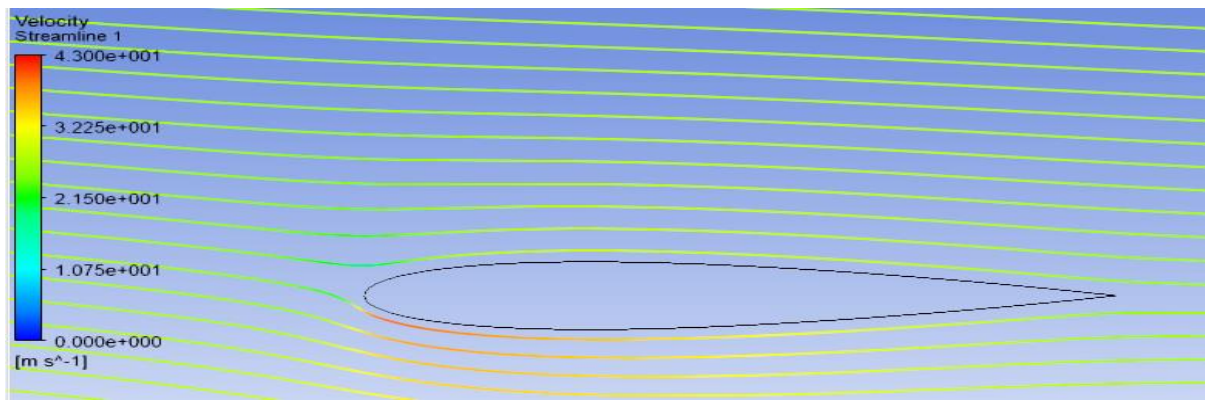


Fig (III-27). Velocity Streamlines for NACA 0012 at -12 AoA.

- All these comments can be applied for the other Airfoils NACA 0015, 4412.

III.2. Numerical Simulation on NACA 0015 Airfoil:

NACA 0015 same as NACA 0012 is a symmetrical Airfoil of the NACA 4-digit series, so basically it means that it has 0 maximum camber. The difference is that it's thicker with a maximum thickness (t) of 15% at 30% of the chord. As shown in Fig (III-28) taken from airfoiltools.com.

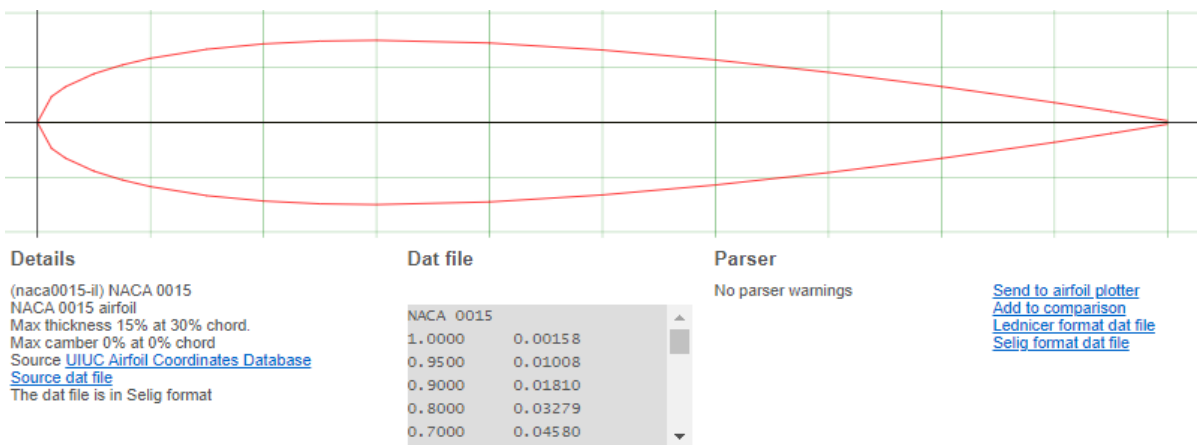


Fig (III-28). NACA 0015 DATA from Airfoiltools.com.

III.2.1. Geometry and Mesh:

Since the same process is followed in this Airfoil, only the results will be shown. Starting with the final geometry and mesh of NACA 0015 Shown in Fig (III-29) and Fig (III-30).

As was done in the previous Airfoil, a high concentration of cells was implemented around the Airfoil and its wake and wall for maximum accuracy.

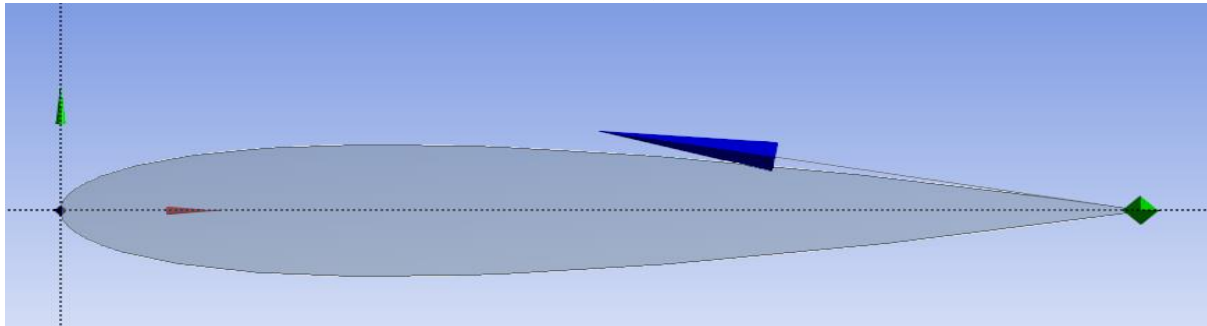


Fig (III-29). Final look at the NACA 0015 Airfoil after importing the DATA File.

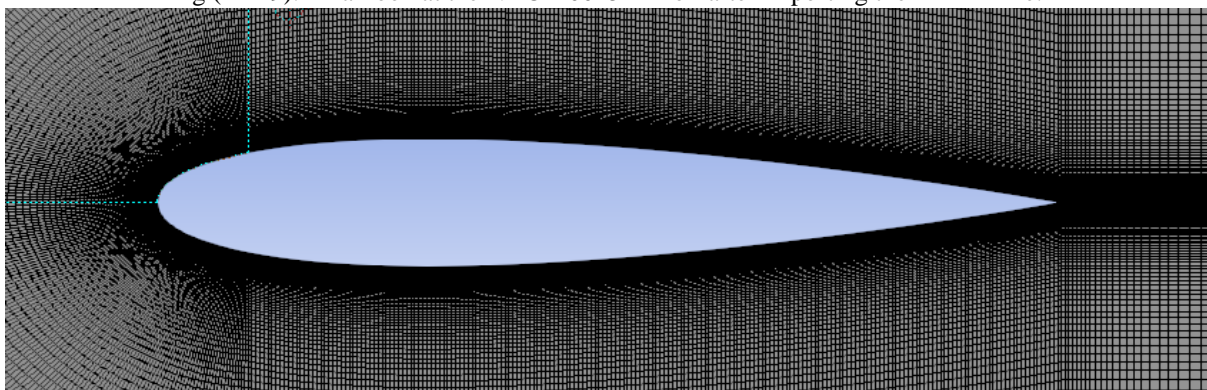


Fig (III-30). Complete Mesh of the NACA 0015 Airfoil.

III.2.2. Simulation on Fluent and Results:

- The same conditions were followed in this simulation giving us the results in Fig (III-31). After convergence we followed (II.6), (II.7) for the forces and (III.1), (III.2) for the coefficients, whilst calculating X and Y.

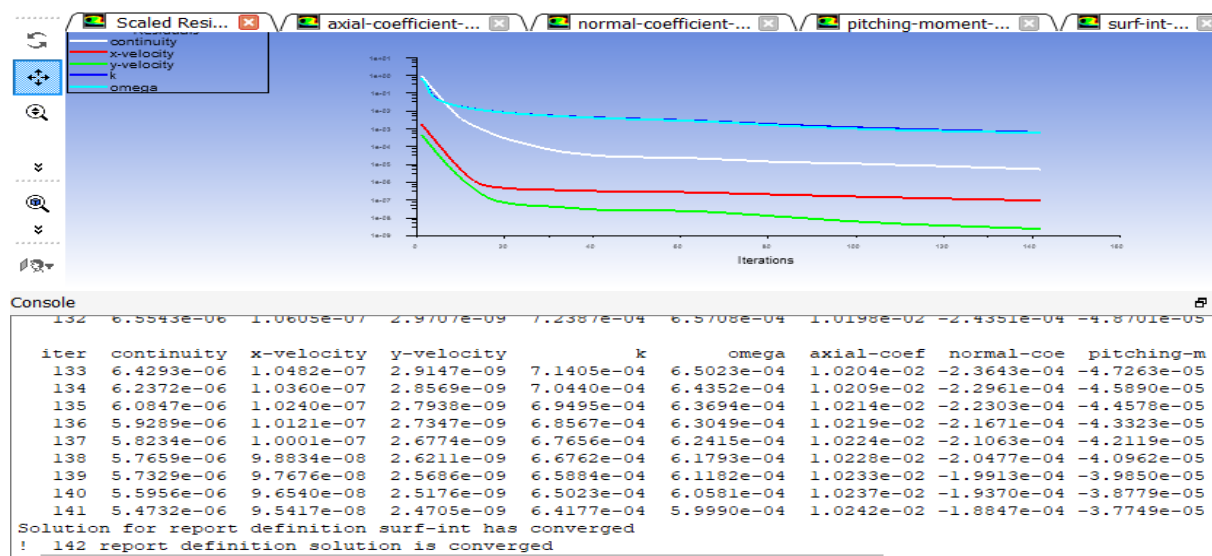


Fig (III-31). Solution Convergence and Forces/Moment Result from ANSYS Fluent for NACA 0015.

III.2.3. Results Discussion and Comparison with Known Data:

Finally, the analysis of the obtained results is shown in Fig (III-32), Fig (III-33), (III-34), (III-35).

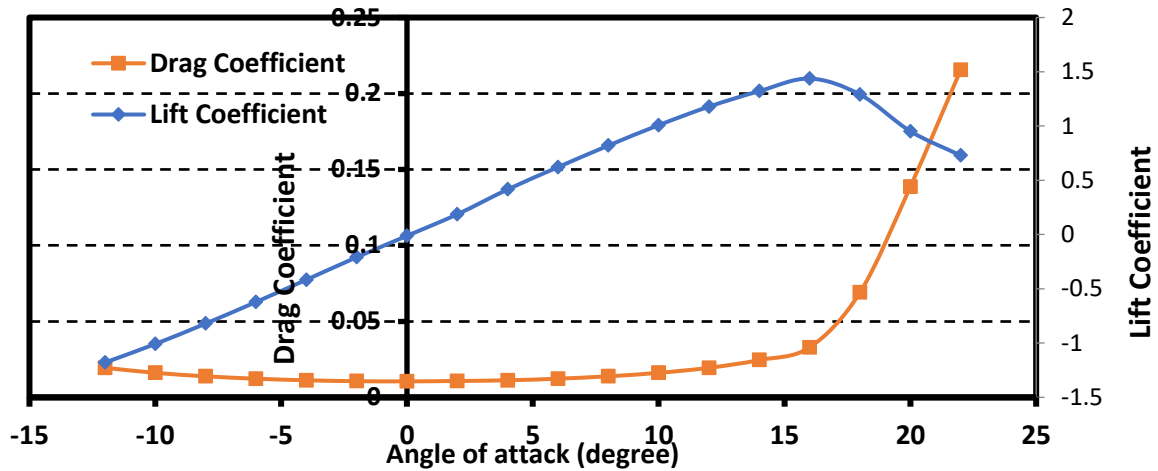


Fig (III-32). Lift and Drag Coefficients Versus the Angles of Attack (-12 to 22 degrees).

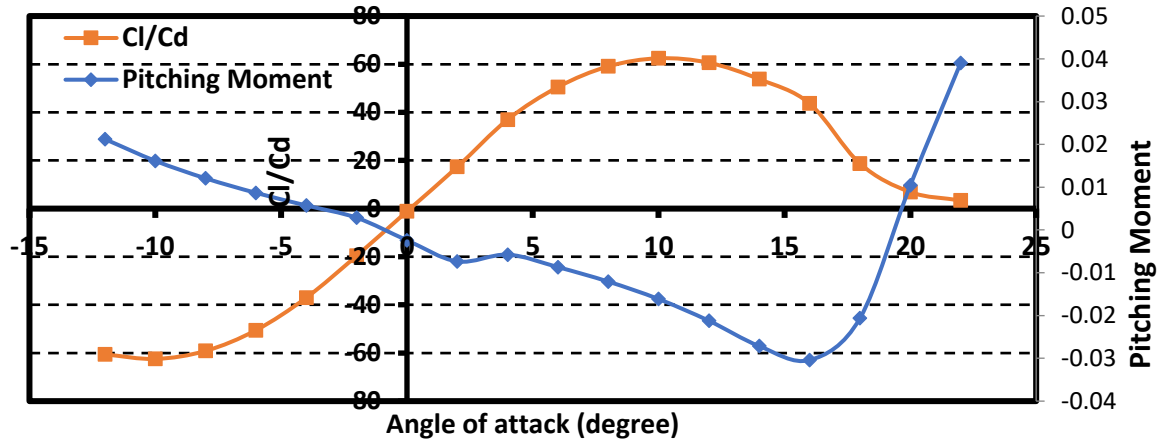


Fig (III-33). CL/CD and the Pitching Aerodynamic Moment Versus the Angle of Attack (-12 to 22 degrees).

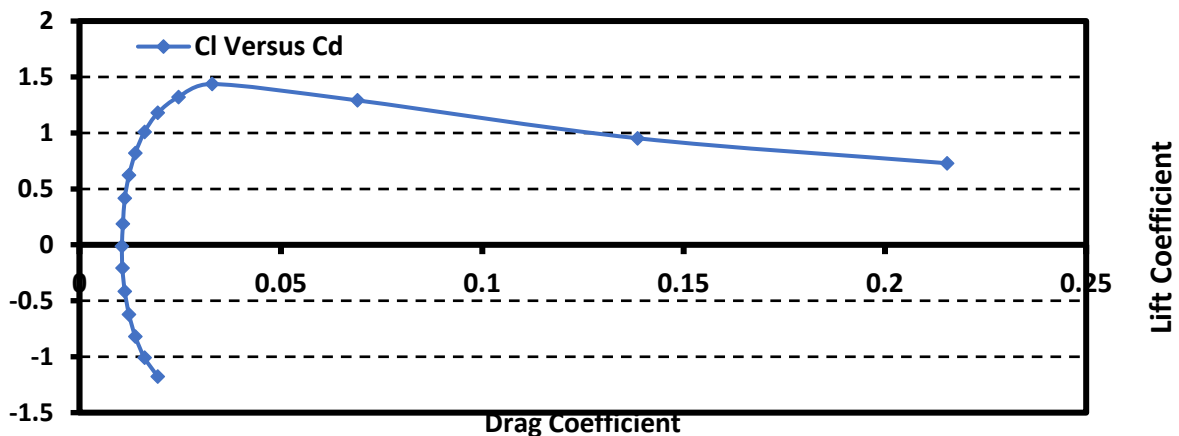


Fig (III-34). Lift Coefficient Versus Drag Coefficient.

- **Cl increases with AoA until 20 AoA (Cl max/Stall) when it falls. It is similar to NACA 0012 but with more tolerance before the sudden stall yet less lift in comparison.**
- **As we increase the AoA, Drag takes a dive around 0 degrees, then increases again and we notice relatively similar results to NACA 0012.**
- **The pitching moment graph may seem to differ from NACA 0012 but the values are still basically the same as they still move around 0. Seeing as how it's a symmetrical Airfoil.**
- **We can use the Cl VS Cd graph (or the polar) to find the best climb rate or sink rate as well as the best glide ratio same for all Airfoils.**

5- The results for NACA 0015 are also relatively similar in comparison with the data and graphs we obtained from airfoiltools.com made from XFOil which is consistent with real-life data.

AoA	Lift Coeff	Error	Drag Coeff	Error	Moment	Cl/Cd
-12	-1.179	-5.2098%	0.019462	10.579%	0.021237	-60.5787
-10	-1.00817	-8.0304%	0.016141	10.554%	0.016155	-62.4589
-8	-0.81991	-4.3836%	0.013869	17.533%	0.012072	-59.119
-6	-0.62129	-3.6012%	0.012295	25.459%	0.008678	-50.5313
-4	-0.4164	-4.5392%	0.011252	35.566%	0.005732	-37.0075
-2	-0.2088	-2.8837%	0.010656	38.389%	0.002858	-19.5952
0	-0.01192	-1.1919%	0.010539	42.297%	-0.0024	-1.13134
2	0.187141	6.4295%	0.0108	38.461%	-0.00735	17.32736
4	0.416257	4.5719%	0.011255	35.602%	-0.00576	36.98272
6	0.621267	3.6197%	0.012299	25.500%	-0.00868	50.51265
8	0.81995	4.3901%	0.013875	17.584%	-0.01206	59.09682
10	1.008192	8.0368%	0.016143	10.568%	-0.01615	62.45253
12	1.179097	5.2325%	0.019461	10.573%	-0.02122	60.58821
14	1.321506	2.8375%	0.024582	10.233%	-0.02715	53.75956
16	1.437333	0.0602%	0.032927	1.3138%	-0.0304	43.65277
18	1.290852	11.232%	0.069045	29.297%	-0.02063	18.69571
20	0.952393	N/A	0.138601	N/A	0.010437	6.871489
22	0.72915	N/A	0.21543	N/A	0.039035	3.384617

Table (III-4). Airfoil Data for the NACA 0015.

- We notice that our results are not very far from their real-life counterparts obtained from Airfoiltools.com which gets it from the XFOil Software specialized in Aerodynamic testing same as NACA 0012.
- We noted an error of 0.01 for some points and 0.1 in some other points which is mainly due to the weak computing power we had access to. But overall, the results were very satisfactory and complied with data obtained from XFOil that is consistent with Tunnels.

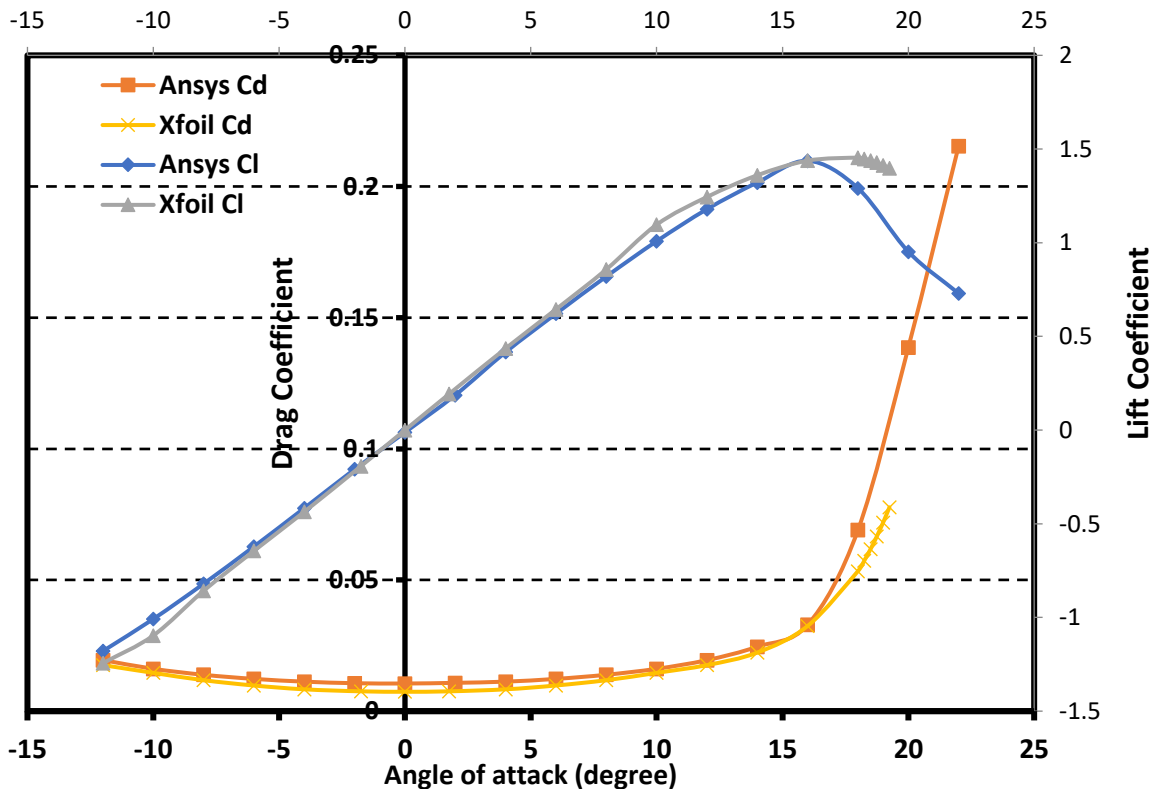


Fig (III-35). Comparison between our NACA 0015 Ansys Simulation Results and Standard XFOil Data.

Then comes the contours and the plots presented in the same way as the NACA 0012:

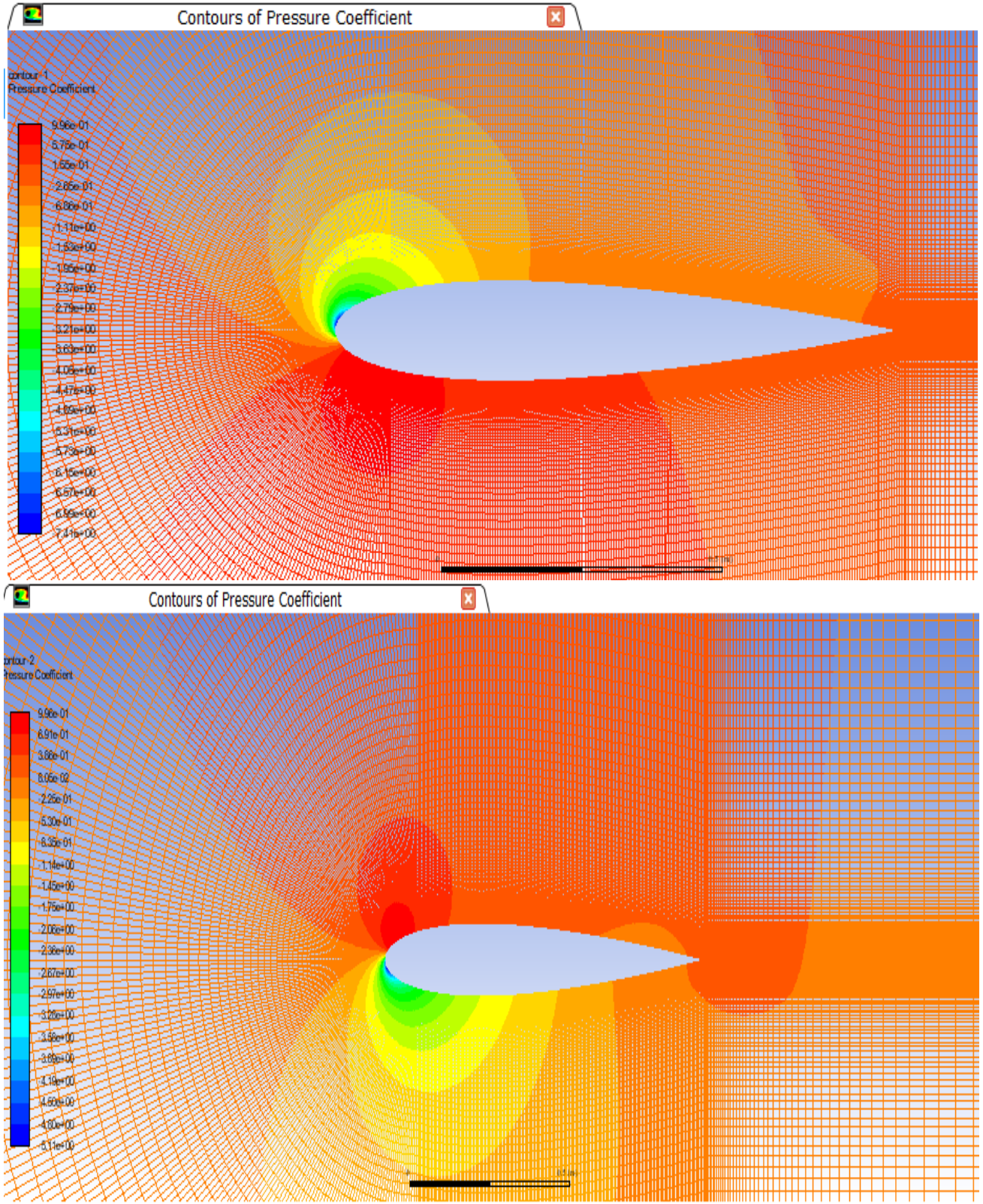


Fig (III-36). Pressure Coefficient Contours for NACA 0015 at -12 AoA (Top) and 18 AoA (Bottom).

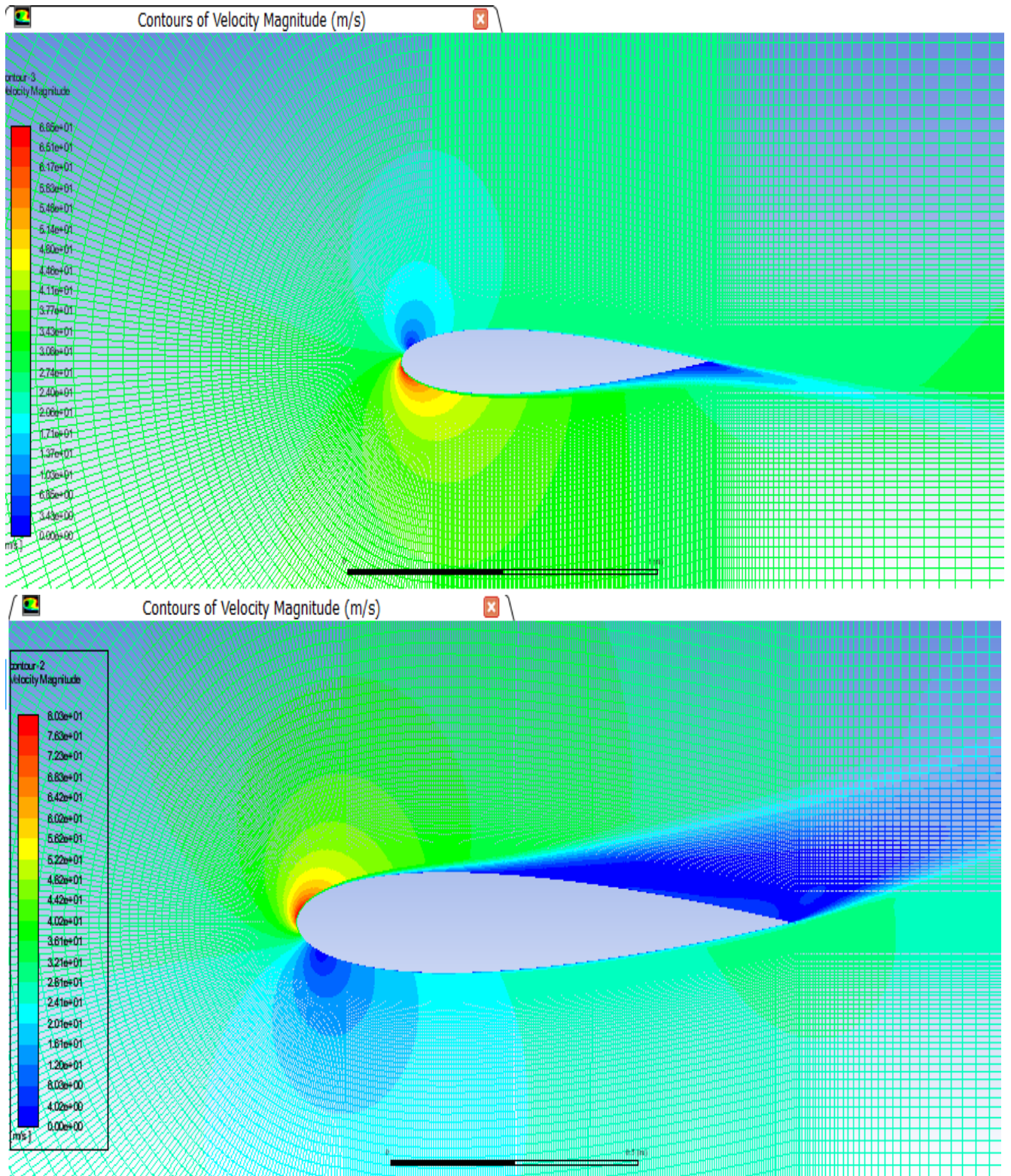


Fig (III-37). Velocity Magnitude Contours for NACA 0015 at -12 AoA (Top) and 18 AoA (Bottom).

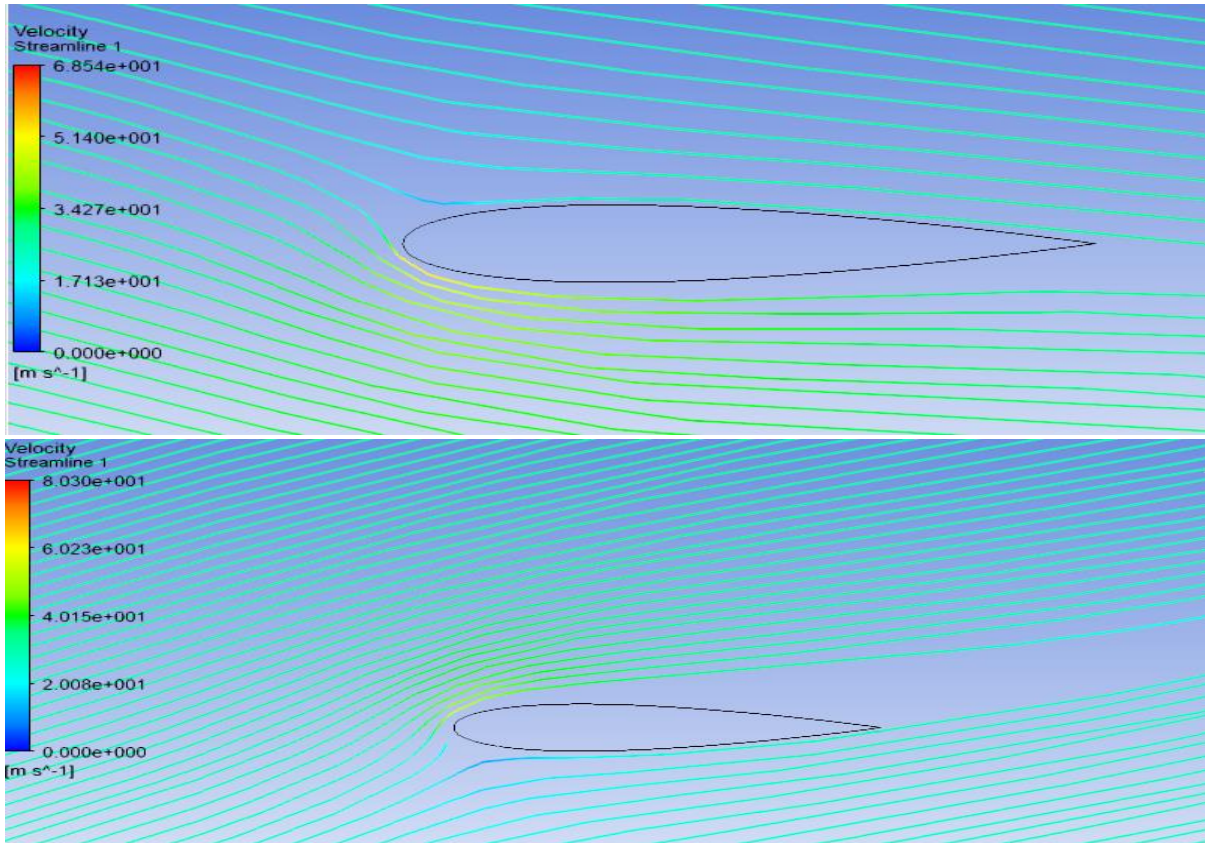
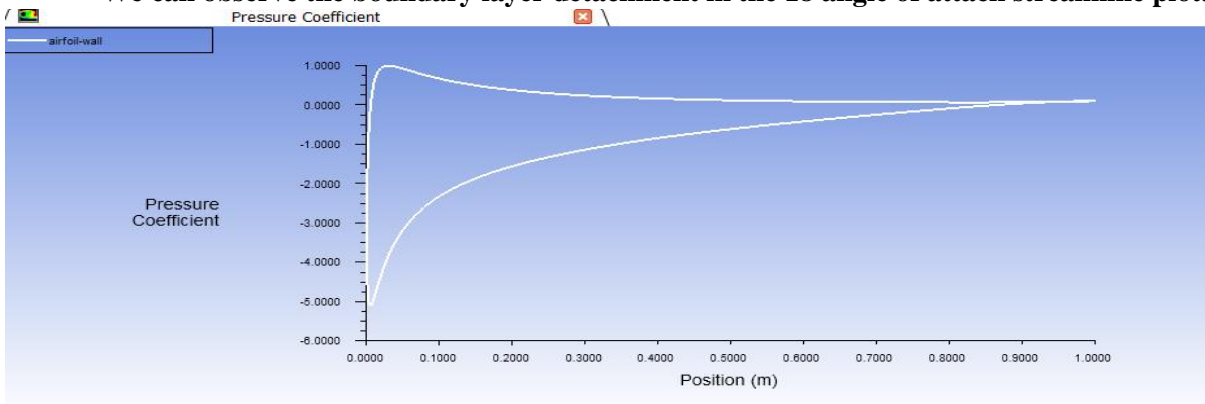


Fig (III-38). Velocity Streamlines for NACA 0015 at -12 AoA (Top) and 18 AoA (Bottom).

- We can observe the boundary layer detachment in the 18 angle of attack streamline plot.



- Fig (III-39). Pressure Coefficient Plots for NACA 0015 at -12 angle of Attack.

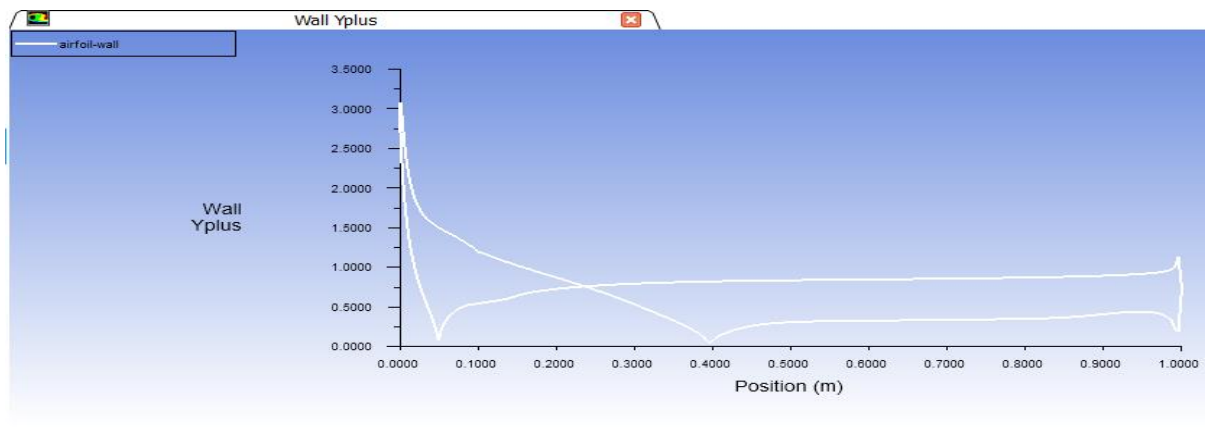


Fig (III-40). Y+ values Plots for NACA 0015 at 18 Angle of Attack.

III.3. Numerical Simulation on NACA 4412 Airfoil:

NACA 4412 is a cambered Airfoil of the NACA 4-digit series, it has 4% maximum camber at 40% chord. With the same thickness as NACA 0012, the difference is that it's more bent towards the leading edge. As shown in Fig (III-41) taken from airfoiltools.com.

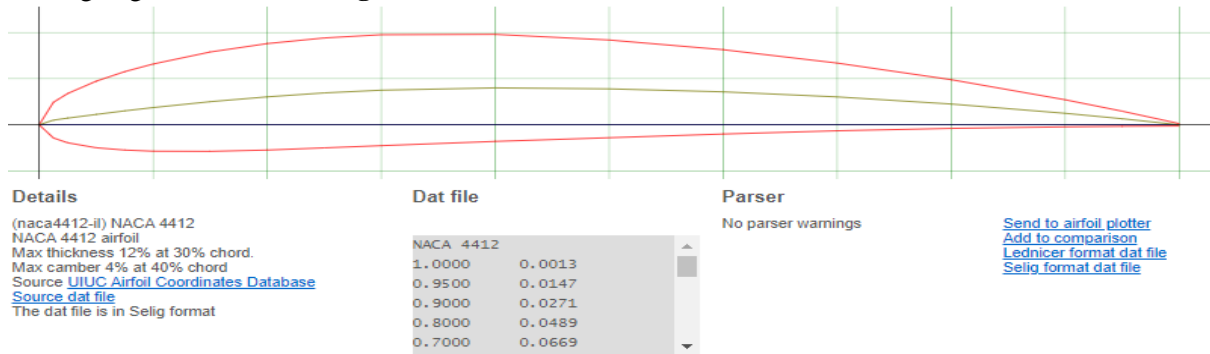


Fig (III-41). NACA 4412 DATA from Airfoiltools.com.

III.3.1. Geometry and Meshing:

With this Airfoil, the same process was followed with slight changes in the mesh process because the same methods would create problems when trying to make a structured mesh. Only the results are shown starting with the final geometry and Mesh **Shown in Fig (III-42), (III-43)**.

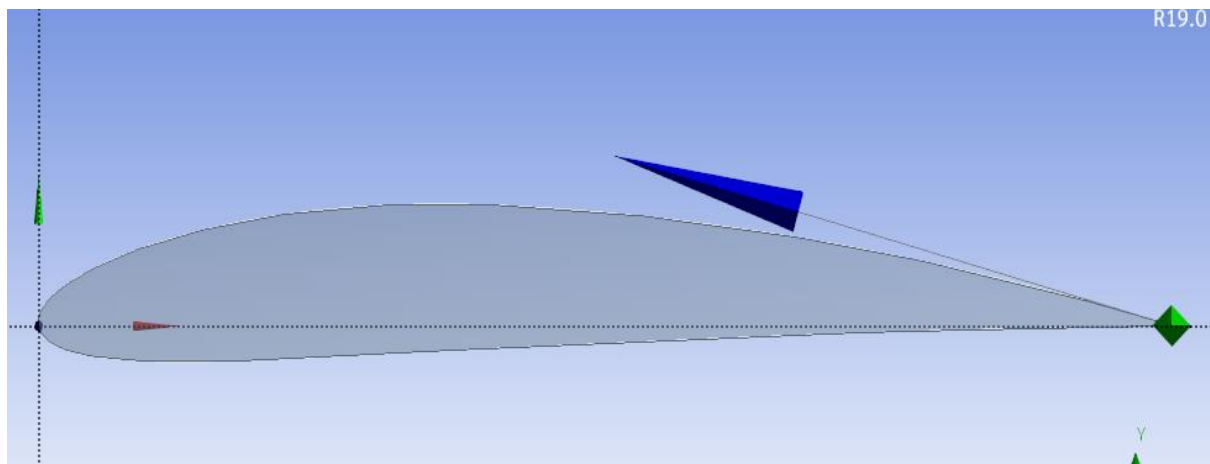


Fig (III-42). Final look at the NACA 4412 Airfoil after importing the DATA File.

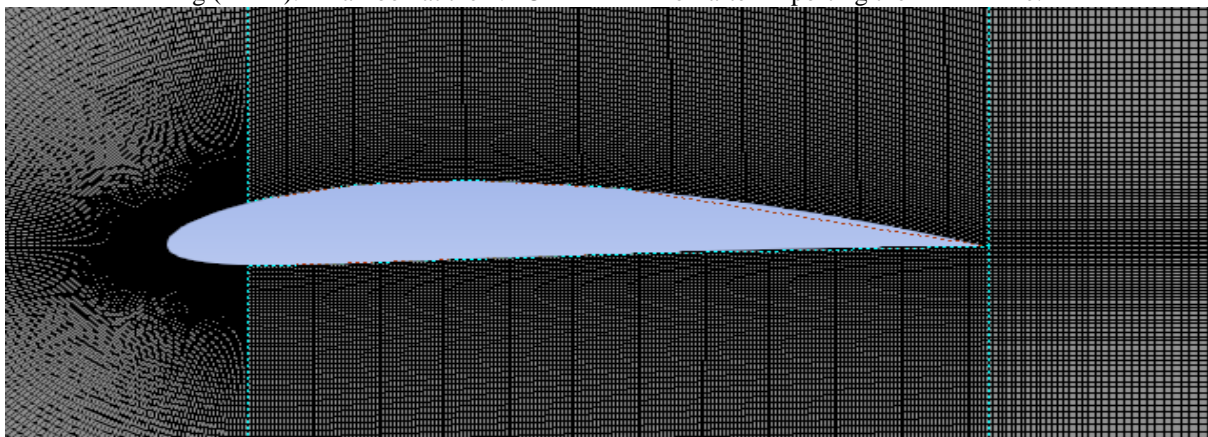


Fig (III-43). Meshing of the NACA 4412.

III.3.2. Simulation on Fluent and Results:

Some variations in the setup were made to avoid flow return in the outlet such as downgrading the methods to **first order** which stabilized it and also setting the **convergence criterion** limit to **1e-05**. We then obtained the convergence and the results for the initial 0 AoA as shown in Fig (III-44).

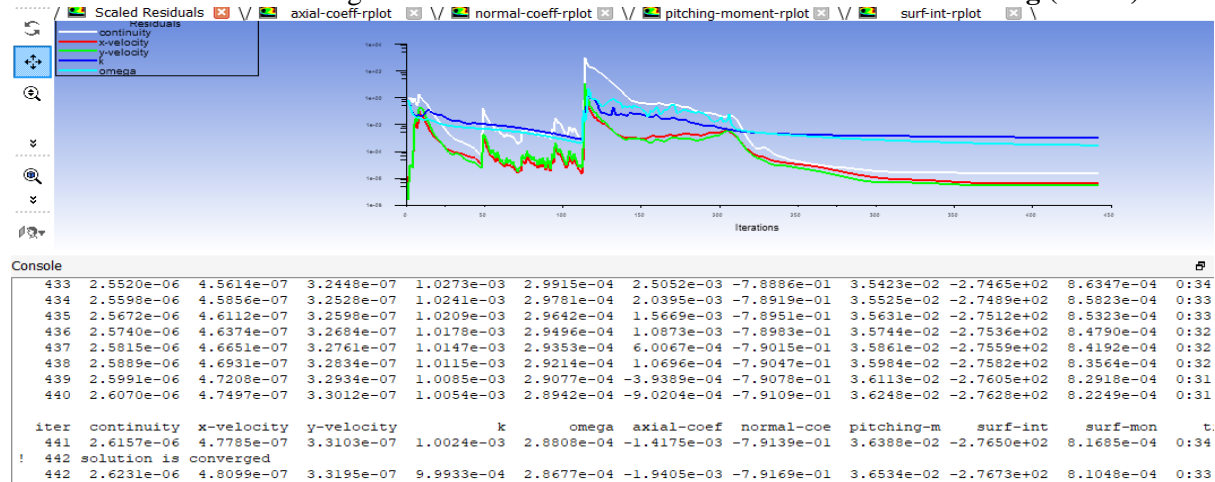


Fig (III-44). Solution Convergence and Forces/Moment Result from ANSYS Fluent for NACA 4412.

III.3.3. Results Discussion and Comparison with Known Data:

The graphs for the results were plotted as shown in in Fig (III-45), Fig (III-46) and (III-47).

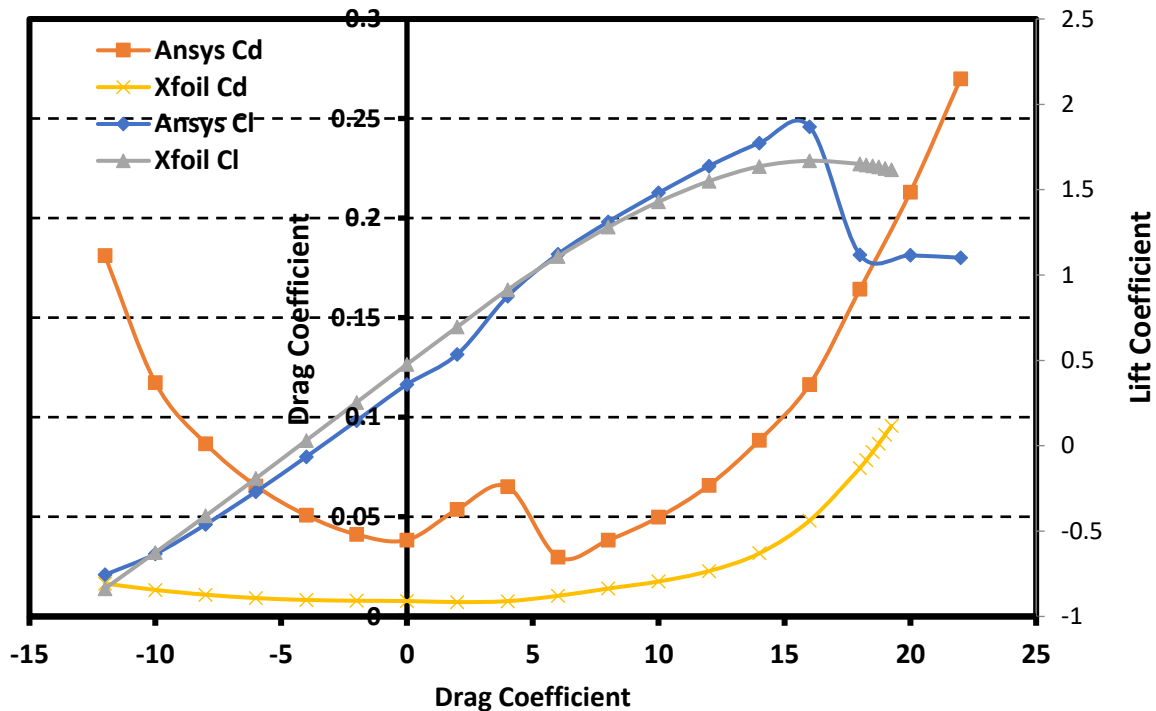


Fig (III-45). Lift and Drag Coefficients Versus the AoA (-12 to 22 degrees) with comparison to Xfoil Data.

- Unlike, symmetrical airfoils, the cambered NACA 4412 starts producing lift at -2 AoA, and it gives way more lift in its Clmax AoA falls sooner slightly at around 16 AoA.
- The same phenomenon for Drag happens here, but we notice more Drag accompanied with the extra Lift the cambered Airfoil produces with its lowest point around 0/4 AoA.
- Since, it's a cambered Airfoil, it's natural that the moment around the center of pressure is not equal to 0 like in NACA 0012 and 0015. But it still remains constant, since it coincides with the Aerodynamic center at a value of approximately 0,1 N.m.
- CL Vs Cd values and graph are very similar to real-life data which validates the results, we also note optimum values around 6 AoA followed by 0 AoA.

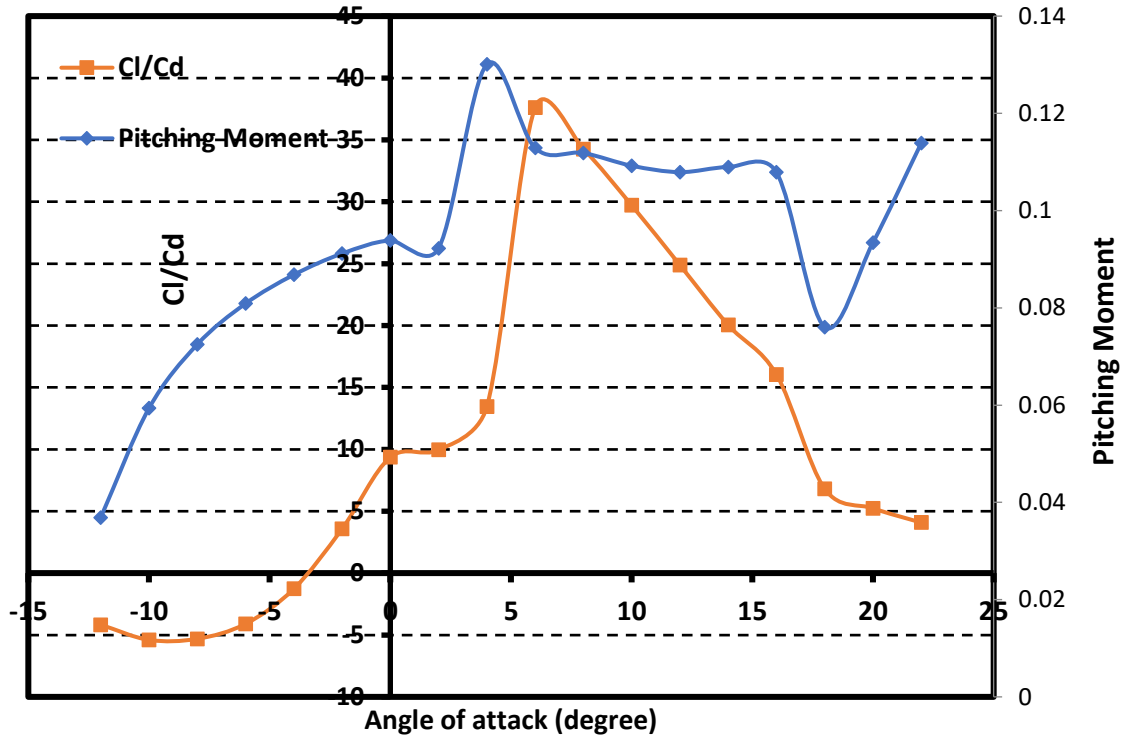


Fig (III-46). CL/CD and the Pitching Aerodynamic Moment Versus the Angle of Attack (-12 to 22 degrees)

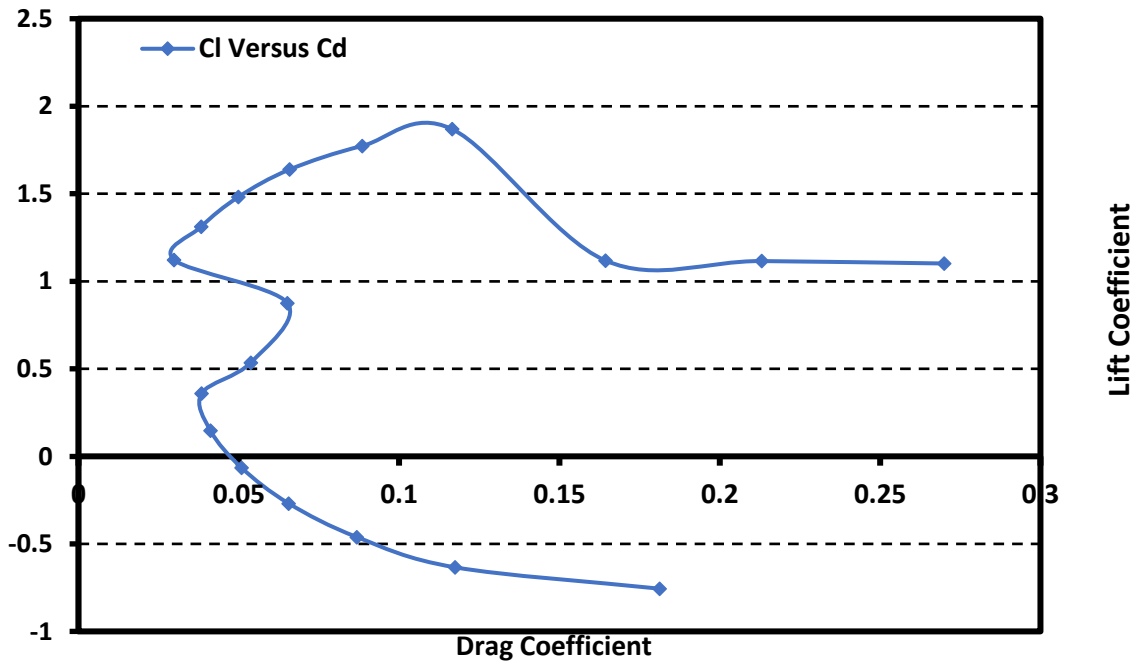


Fig (III-47). Lift Coefficient Versus Drag Coefficient for NACA 4412.

AoA	Lift Coeff	Error	Drag Coeff	Error	Moment	Cl/Cd
-12	-0.75583	-9.6761%	0.181181	998.06%	0.036881	-4.17166
-10	-0.63392	-1.4434%	0.117467	783.21%	0.059348	-5.39663
-8	-0.46092	-12.200%	0.08681	696.42%	0.072483	-5.30957
-6	-0.26886	-40.911%	0.065559	612.59%	0.080873	-4.10107
-4	-0.06461	306.42%	0.050822	512.31%	0.086802	-1.27124
-2	0.146937	42.287%	0.041157	420.97%	0.091168	3.570166
0	0.359223	24.738%	0.038387	398.53%	0.9385	9.357949
2	0.535823	23.058%	0.053779	646.93%	0.092258	9.963485
4	0.87586	4.1938%	0.065146	746.05%	0.130069	13.44457
6	1.122349	10.403%	0.029832	189.63%	0.112884	37.62176
8	1.312391	2.4825%	0.03831	173.64%	0.111856	34.25675
10	1.481613	3.6600%	0.04986	183.29%	0.109231	29.71543
12	1.638716	5.7372%	0.065854	188.83%	0.10791	24.8839
14	1.773053	8.3442%	0.08846	179.05%	0.108935	20.04365
16	1.869299	11.960%	0.1165	141.70%	0.10788	16.04542
18	1.118528	32.251%	0.164336	120.28%	0.076058	6.806361
20	1.115546	N/A	0.213066	N/A	0.09343	5.235676
22	1.101631	N/A	0.270005	N/A	0.113884	4.080043

Table (III-5). Airfoil Data for the NACA 4412.

-Big percentage errors for the Cd were noted mainly due to trickiness of cambered airfoils, the small values at hand and the weak computing power.

But overall, the results were good (judging from Cl and the graphs in Fig (III-45)). Drag is supposed to be inaccurate and close to 0 (Inviscid model).

Contours and Plots of different properties for NACA 4412 are shown in Figs (III-48,49,50).

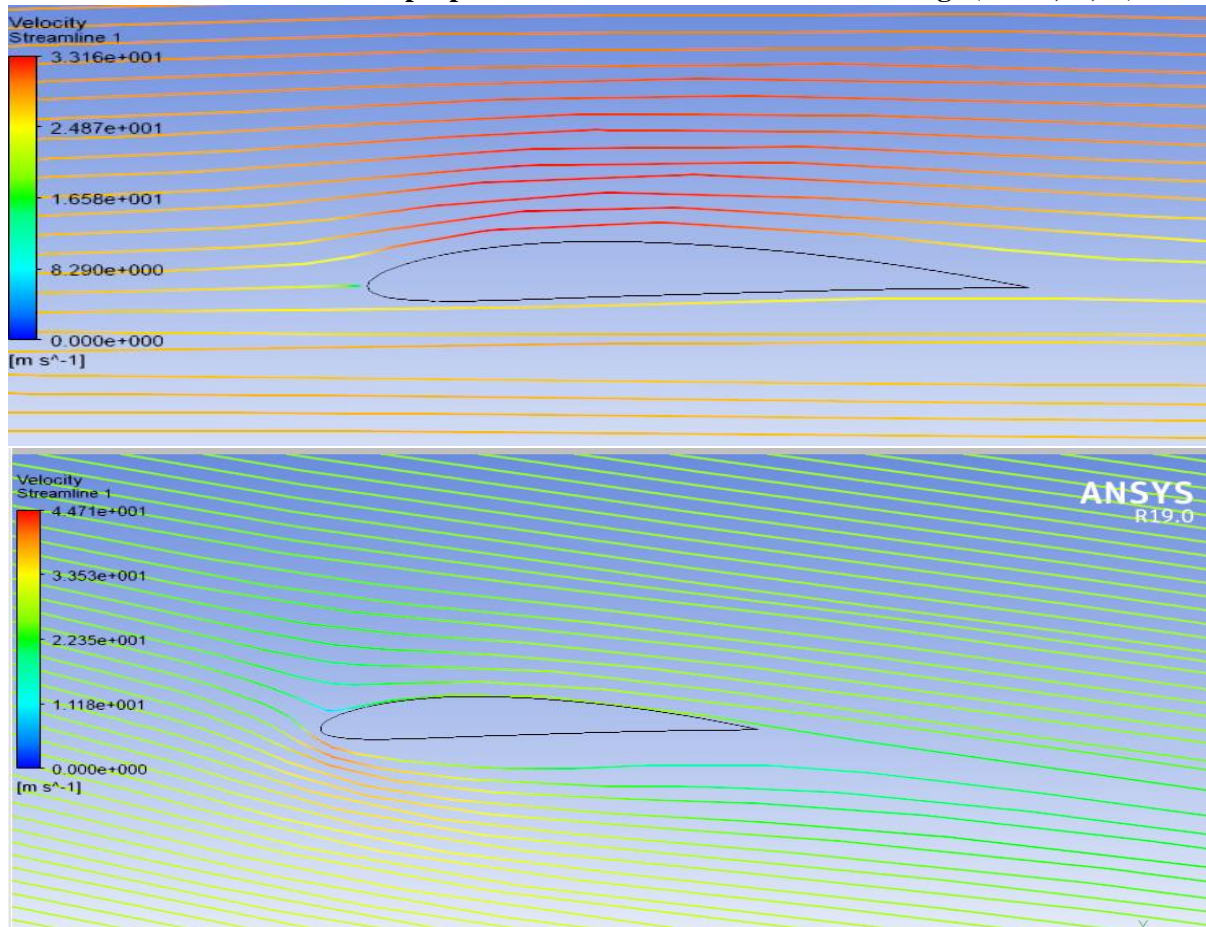


Fig (III-48). Velocity Streamlines for NACA 4412 at 0 AoA (Top) and -12 AoA (Bottom).

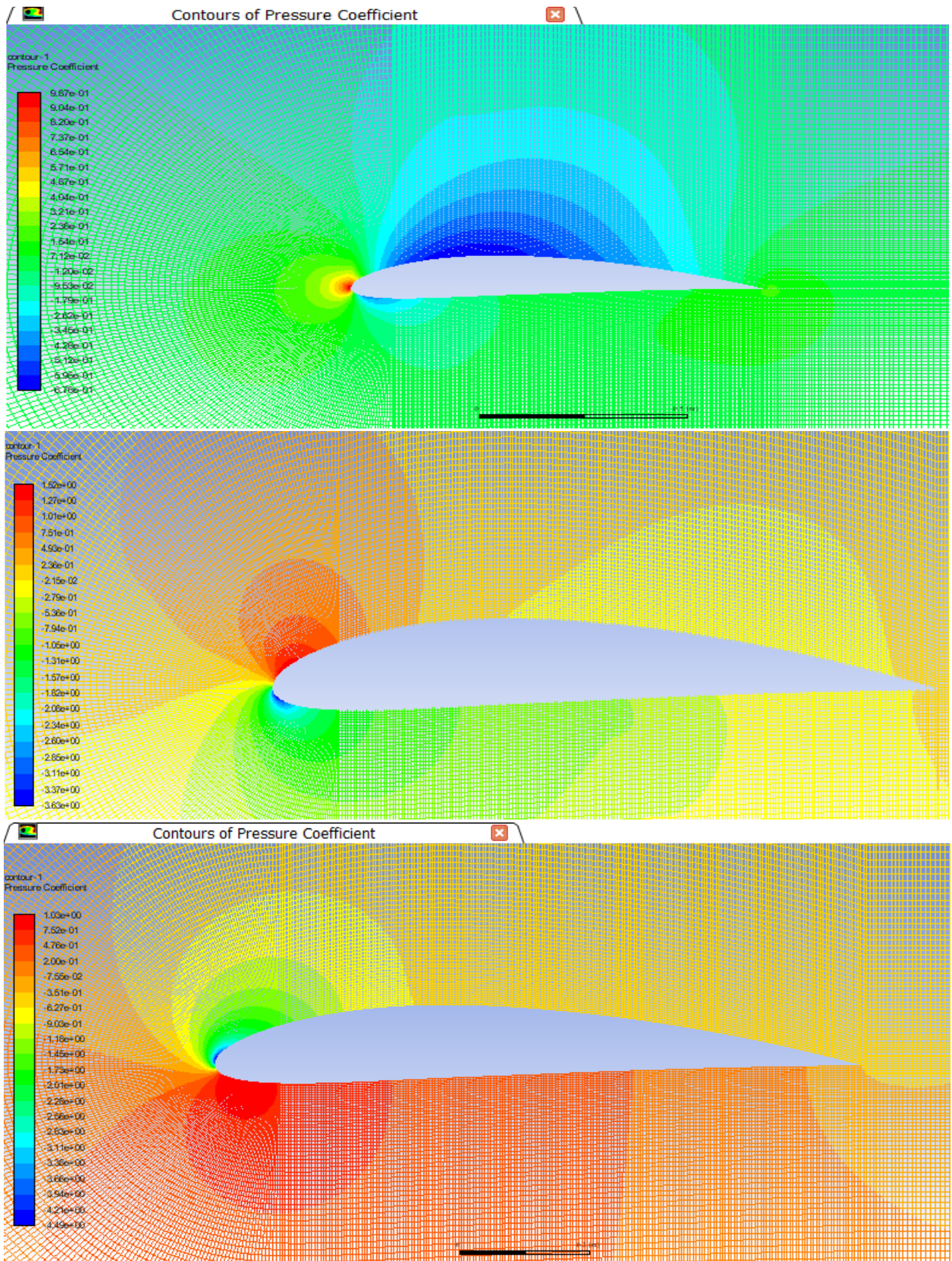


Fig (III-49). Pressure Coefficient Contours for NACA 4412 at 0 AoA (Top)/-12 AoA (Mid)/18 AoA (Bottom).

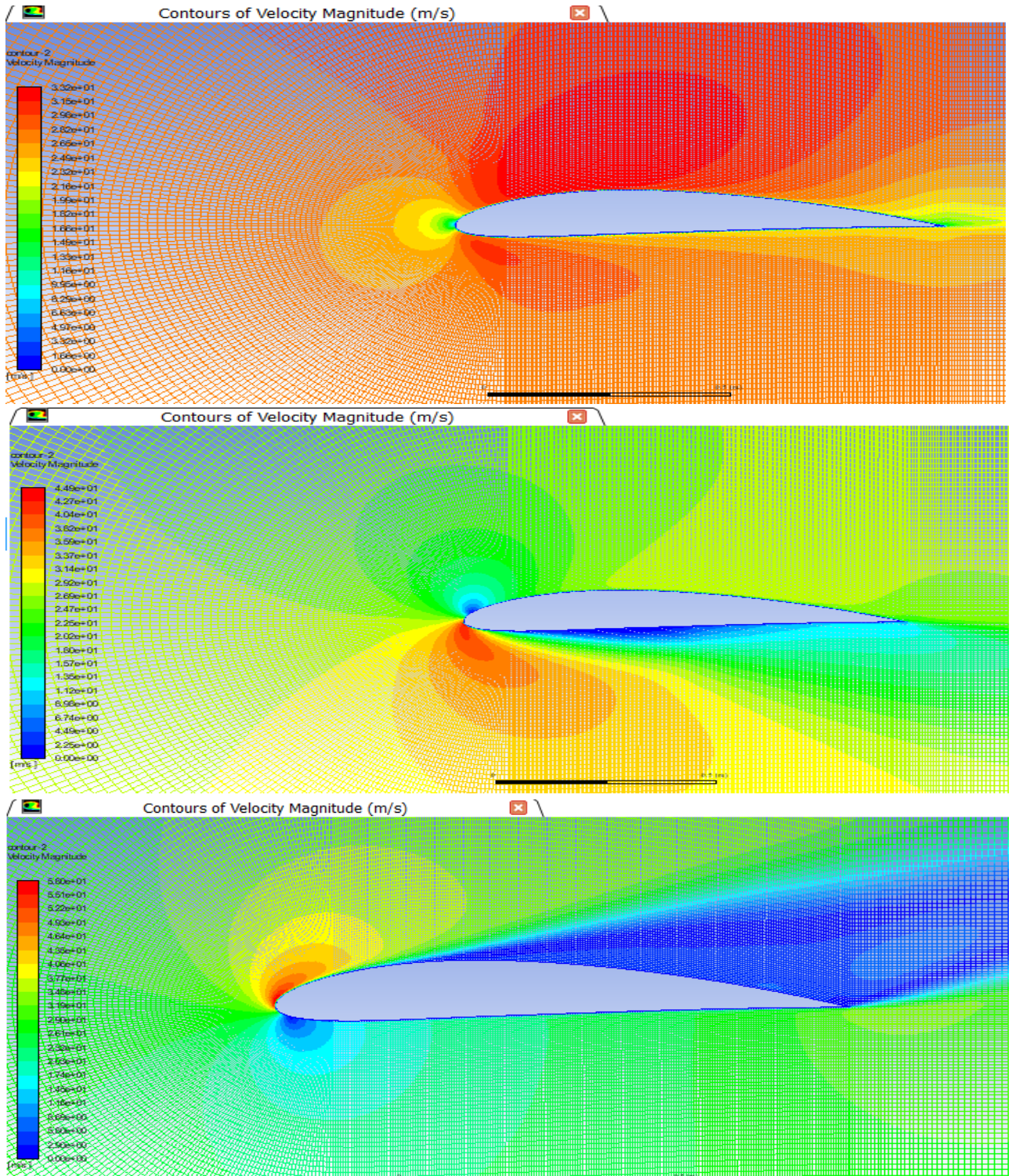


Fig (III-50). Velocity Magnitude Contours for NACA 4412 at 0 AoA (Top)/-12 AoA (Mid)/18 AoA (Bottom).

III.4. CONCLUSION:

Using Ansys Software, three Airfoils were studied; NACA 0012, NACA 0015, NACA 4412. In the end, All the aerodynamic results were obtained and validated by previous experiments and studies.

And now that they are somewhat satisfactory and compliant with real-life data obtained from XFOil that is consistent with Wind Tunnels results. All that is left is to do our proper testing and installation to compare and show the precision of our digital instruments in the next Chapter dedicated to Production and Wind Tunnel testing.

IV- INTRODUCTION:

This final chapter will be on the test set-up and production phase of our work, it will present data acquisition system for testing Airfoils and a detailed description of the proposed system design; including hardware and software implementations.

They say that need calls for invention and creativity, and since the design of wind tunnels presents us with many challenges, we thought about a solution to install the measuring equipment in the most optimal way which also requires the best selection of sensors.

The purpose of this chapter is to present an experimental setup and real-time data acquisition system for determining various aerodynamic parameters such as Lift, Drag, Pitching moment, Incidence angle (AoA)... Etc. based on what we needed, the solution of using this economical and low-cost system provides the engineer with precise values of those properties.

In order to do that, we went through lots of variations of designs on “SolidWorks”. Each design had its advantages and inconveniences, which led us finally to the option we deemed the best for this experiment which is presented in these next pages.

They will mainly approach:

- A Detailed Description of the Electronic Measuring Equipment used.
- The Design of the customised Measuring Equipment Support using SolidWorks
- The Conception and Production of the Airfoils/Wings/Equipment Support and the Methods employed in the Process.
- The Testing Phase: Process and Difficulties.
- Results: Comparison and Conclusion.

IV.1. Description of the Electronic Measuring Equipment:

A variety of electronic and digital devices were used to improve the precision of the results obtained and to automate the process, each has its own purpose and usefulness. They are:

IV.1.1 Electronic circuit for Data Acquisition:

IV.1.1.1 General description:

Before the design of the system, some important requirements were made. The system must be very low-cost with accurate measurements. The proposed low-cost data acquisition system is designed to measure the aerodynamic forces of airfoils. These parameters can be used for the design of aircrafts. By using this system, the user can get all the information about the motor, such as the lift force generated by any specified airfoil at different Angles of Attack.

The proposed hardware system is based on: PIC18 microcontrollers, high precision load cell sensors, an angle sensor (MEMS Accelerometer) and a high sensitivity airspeed sensor. So, a very high-performance microcontroller was selected for the control and the acquisition. The variation of the Angle of Attack can be controlled by an accelerometer (to measure the angle) and the electronic circuit is connected to the sensors, and is used for real time data acquisition. The circuit is connected to a personal computer (PC) via an FT232RL module and a USB cable. This communication, along with a program developed in LabView, allows displaying all the measurements.

Fig (IV-1) describes the overall system architecture.

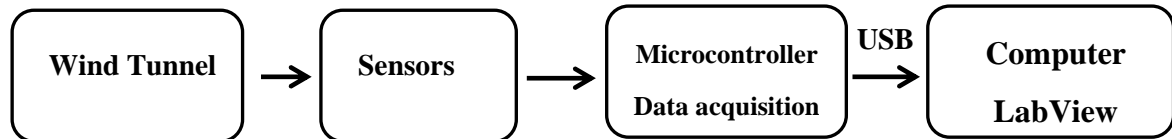


Fig (IV-1). System architecture.

In order to obtain all the measurements, four kinds of sensors were integrated in the system:

- PIC 18 Microcontrollers.
- Load cells, to measure the lift/drag forces.
- Air speed sensor,
- MEMS accelerometer sensor to measure the incidence angle and for Airfoil adjustment.

IV.1.2. Hardware:

IV.1.2.1. PIC 18F4620 Microcontroller:

1- Description:

Our electronic circuit is based on a Microchip PIC microcontroller (μC). The PIC microcontroller providing complete control in a single chip, it has special function registers, power on reset, interrupts, user RAM for program data storing, EPROM program memory, timer circuits, instruction set, low power consumption, and on-board Auto-D converters. [18]

PIC microcontrollers universal Board is a powerful development platform. It is ideal for developing embedded applications involving high speed wireless communication, USB based data logging, real time data monitoring and control and interactive control panels [19]

We worked with microcontrollers (μC) consisting of hardware and software tools, it supports the development and transfer of program code (using MicroC software) from a computer to the microcontroller, and evaluation of its execution on rapid prototyping hardware. PIC18 microcontrollers family offers high computational performance at an economical price with the addition of high-endurance. On top of these features, the PIC18 microcontrollers introduce design enhancements that make these microcontrollers a logical choice for many high-performances, power sensitive applications. **Fig (IV-2) shows the microcontroller architecture.**

2- Characteristics: [20]

- Voltage: 5 Volt; Current: 25 mA.
- The microcontroller has 44 pins (Input/output, analog/digital).
- Operating frequency: 40 MHz.
- Can be powered by USB or external power source.
- Processing analog and digital signals.
- 13-Channel (10-Bit) Analog-to-Digital (A/D) Converter.
- The electrical circuit using 18F4620 microcontroller can be connected to a PC using serial communication (UART TTL).
- 03 Timers.
- Serial and parallel communication (UART, ...).
- Enhanced Capture/Compare/PWM (ECCP) modules.
- Three Programmable External Interrupts.
- Flash program memory of 64Kbyte program memory.
- Data memory of 1024 bytes.

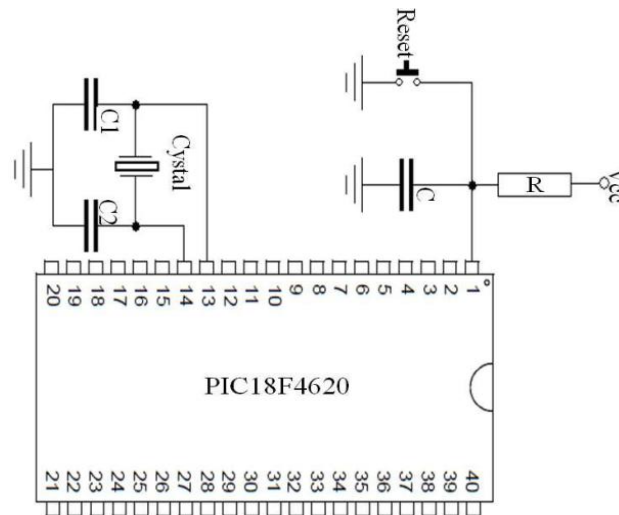


Fig (IV-2). Microcontroller architecture.

IV.1.2.2. Degraw Load Cell with an HX711 Electronic module:

1- Description:

A load cell is a force sensing module which can be used to measure the weight and the force. Load cells transform the force acting on them into electrical signals. The measuring is done with very small resistor patterns named “strain gauges” which are very small and flexible circuit boards. The gauges are bonded onto a beam or structural member that deforms when force is applied, which deforms the strain gauge. As the strain gauge is deformed, its electrical resistance changes in proportion to the force. The generated electrical signal by the load cell sensor is very small and needs an additional amplification of the signal. For high precision measurements, the load cell sensor comes with an HX711 electronic module that uses 24-bit high precision analog to digital converter chip, on the other hand, it facilitates the communication between the load cell and the microcontroller in our designed electronic circuit [21]

Fig (IV-3) shows the load cell and its electronic module.

2- Characteristics:

- **Data accuracy:** 24 bits (24 bits analog to digital converter chip).
- **Refresh frequency:** 10-80 Hz.
- **Voltage:** 2.7V - 5VDC.
- **Current:** less than 10 mA.



Fig (IV-3). Load cell (left), and electronic module of load cell (right).

IV.1.2.3 GY61-ADXL335 Accelerometer (for AoA measurement):

1- Description:

In order to measure the AoA, the accelerometer GY61-ADXL335 was selected. This sensor is a MEMS (Micro Electro Mechanical System) accelerometer. It measures the acceleration range $\pm 3 g$ in three orthogonal axes labeled the X, Y and Z direction. This accelerometer is an acceleration sensor capable of measuring linear acceleration in three axes and has a good resolution (up to 13-bit) at its acceptable sensitivity. It can read in the range of 0.5 Hz to 1600 Hz for the X and Y axes while the Z axis has a range of 0.5 Hz to 550 Hz. Inside the accelerometer, there is an on-board 3.3V voltage regulator to power the sensor so the voltage should be between 3.3V and 6V DC. This accelerometer is compatible with most of the microcontrollers (5 volts). **Fig (IV-4)**, shows the accelerometer sensor.

2- Characteristics:

- Model: Three-axis magnetic field accelerometer module (compact size, low power supply).
- Accelerometer has on-board 3.3 V voltage regulator.
- Analog voltage output centered at 1.65 V.
- Operating voltage: 3.3 V – 5 V.
- Analog interface.
- Sensitivity: 300 mV/g.

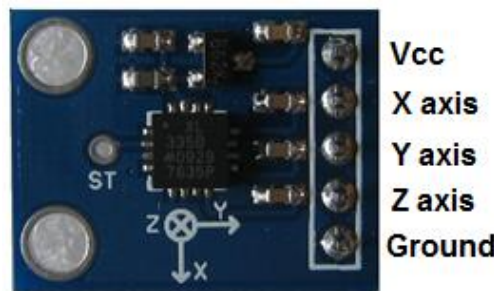


Fig (IV-4). Accelerometer sensor

Pin Definitions:

- VCC: 3.3V or 5V.
- X_OUT: Analog Output.
- Y_OUT: Analog Output.
- Z_OUT: Analog Output
- GND: Ground.

IV.1.2.4 NXP MPXV7002Dp Air Speed sensor:

1- Description:

Airspeed sensors typically rely on a pitot tube connected to 2 pressure sensors in each of its ports (dynamic at the tip and static at the side) and a temperature sensor. When air passes through it is able to measure the difference in pressure from the ports and when using the measured temperature, it can easily estimate the current airspeed which is how the NXP MPXV7002DP works, it calculates all those parameters digitally with more efficiency and precision. It's a state-of-the-art monolithic silicon pressure sensor designed for a wide range of applications especially those using a microcontroller with A/D inputs.

2- Technical Characteristics:

- ✓ Ideally suited for Microprocessor/Microcontroller-based systems.
- ✓ 5.0% maximum Error over 0° to 85°C
- ✓ Thermoplastic (PPS) Surface Mount Package.
- ✓ Temperature Compensated over 10° to 60°C.
- ✓ Patented Silicon Shear Stress Strain Gauge.
- ✓ Designed to measure Positive and Negative Pressure with an offset at 2.5V instead of 0V.
- ✓ Provides an accurate, high level analog output signal proportional to the applied pressure.
- ✓ Allows pressure measure up to 7Kpa through each port.

3- Role:

The purpose of employing it in our work is as always to reach maximum accuracy and precision in our readings, since its highly compatible with microcontroller systems and provides a state-of-the-art technology that can give us proper and detailed airspeed data to use in our study. The sensor kit is portrayed in Fig (IV-5).



Fig (IV-5). The NXP MPXV7002Dp Airspeed Sensor Kit.

IV.1.3. Software:

LabVIEW contains a comprehensive set of tools for acquiring, analyzing, displaying, and storing data, as well as tools to help you troubleshoot code you write. LabVIEW can be used to communicate with hardware such as data acquisition, devices, instruments, electronic circuits [22]

In the present design, LabVIEW was used to receive data from our electronic circuit (Load cell, airspeed sensor, accelerometer sensor), and then display in real time the results and the curves.

IV.1.4. Description of the data acquisition system:

We connect X, Y and Z analog output of the accelerometer to three analog inputs (pin 2, 3 and 4) of the 18F4620 microcontroller. To activate the accelerometer sensor, Vcc port of the sensor should be connected to 5-volt power, GND (ground port of the sensor) to the ground. The digital data and clock outputs of the electronic module of load cell are connected to digital pins (21 and 22) respectively. Furthermore, to calibrate the load cell a command by push bottom was added to the circuit, this last was connected to the digital pin 23 of the microcontroller. At the beginning of each measurement, this

calibration command allows us to start measuring the force from zero. The airspeed sensor is connected with the microcontroller via pin 15.

For high accuracy measurements of aerodynamic forces, a 20MHz oscillator was used in our electronic circuit. It is connected to pin 13 and 14 of the microcontroller. The oscillator used to manage the speed at which the processor executes instructions, activate the timers, detect the signals, the baud rate of serial communication signals, the amount of time needed to perform an analog-to-digital conversion. In order to connect the microcontroller to PC by UART communication, FT232RL FTDI serial module adaptor was used. **Fig (IV-6)** shows the connection of FT232RL FTD module with microcontroller (pin 25 and 26). This communication can be done using four signals: TXD, RXD, GND and VCC. The TX pin (pin 25 of microcontroller) to transmit the information to PC, RX pin (pin 26 of MCU) to receive the information from PC. For good data transmission/reception, the baud rates of the microcontroller and the personal computer PC must be the same value (9600 bits per second). The accelerometer measures acceleration along the three axes (X, Y, Z). It provides analog voltage output proportional to the three values of acceleration. Then, these three voltages can be converted to a digital signal and received by the microcontroller. The generated MicroC program in the microcontroller processes the data received from the accelerometer to find out the angles along the three axes.

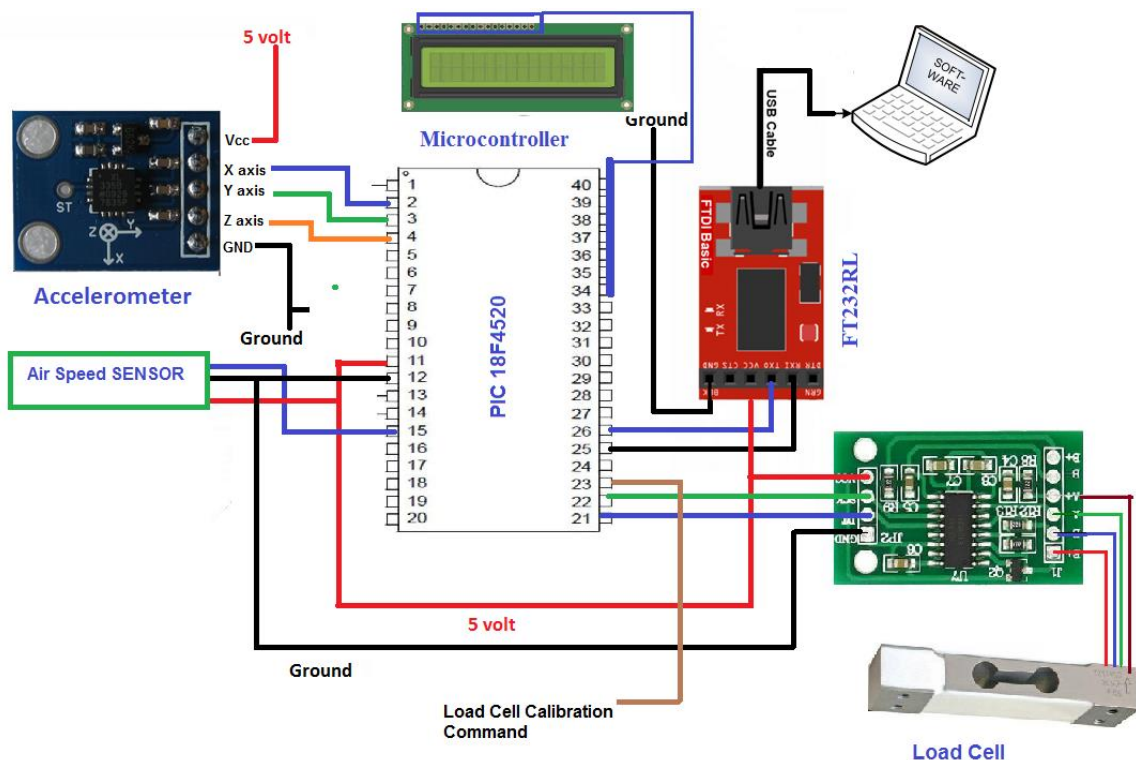


Fig (IV-6). Data acquisition electronic circuit

In order to investigate the results, a Visual Instrument LabVIEW interface was created. The developed LabVIEW interface allows the user to display real-time results, real-time curves and charts, store the data. After the test run, the results can be exported in a format that will be capable of being read by Microsoft EXCEL software. Then, we can perform an investigation on the tested airfoil.

Fig (IV-7) shows the LabVIEW interface. For the validation, many tests have been performed using external electronic equipment.

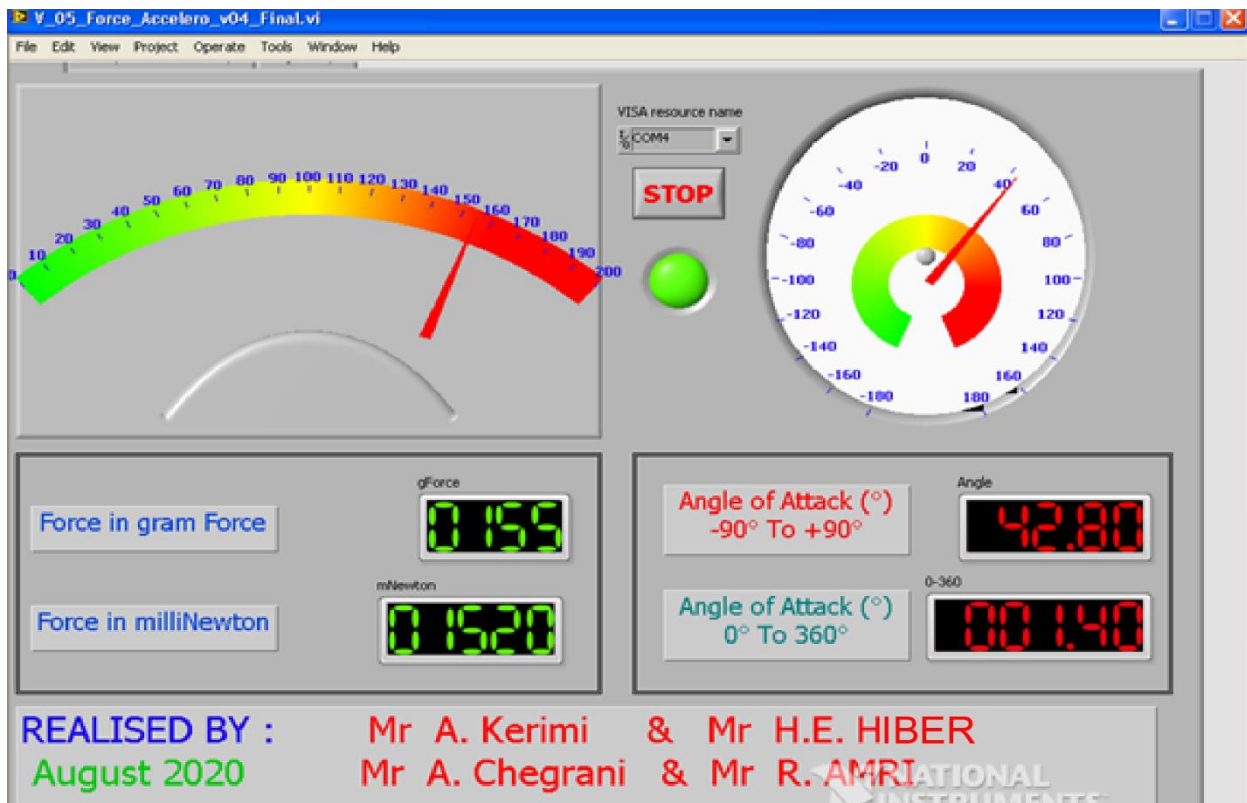


Fig (IV-7). LabVIEW Interface

IV.1.5 Experimental testing:

IV.1.5.1. Experimental measurement setup:

The test setup is shown in Fig (IV-8).

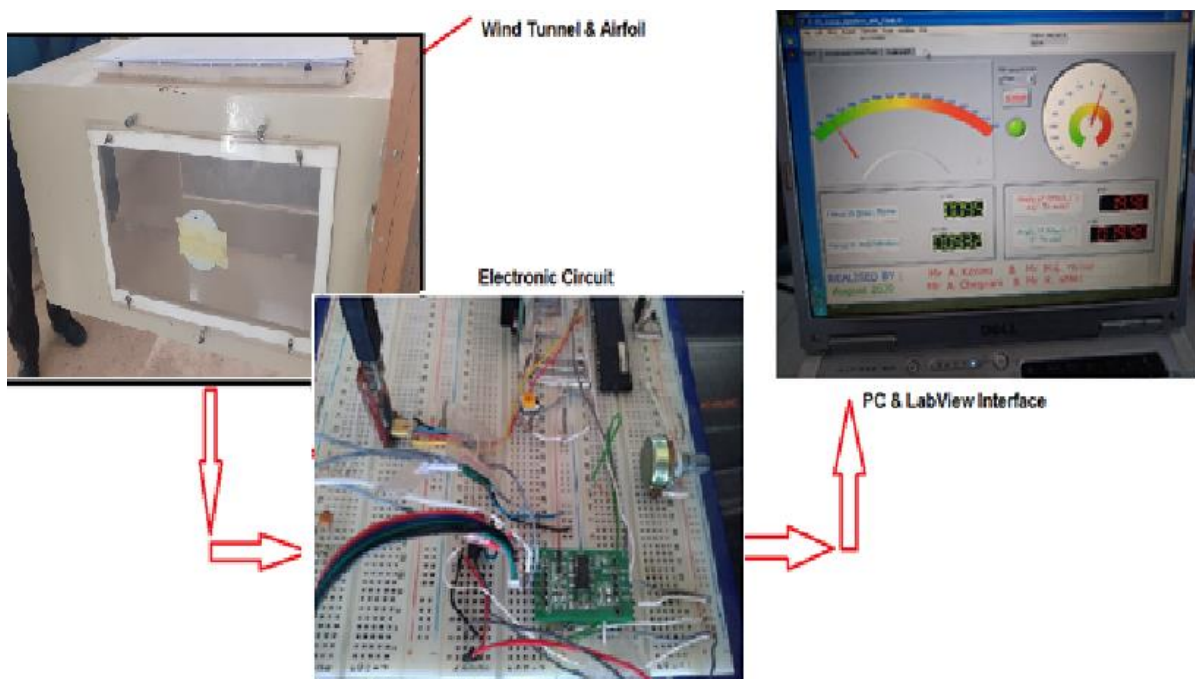


Fig (IV-8). The Test set-up.

IV.2. The Conception and Design Process on SolidWorks:

In the beginning it was just an idea and in order to bring that idea to reality we needed to look at it from all angles and have a glimpse of what we wanted it to look like so we used SolidWorks to design our prototypes as shown in Fig (IV.9)

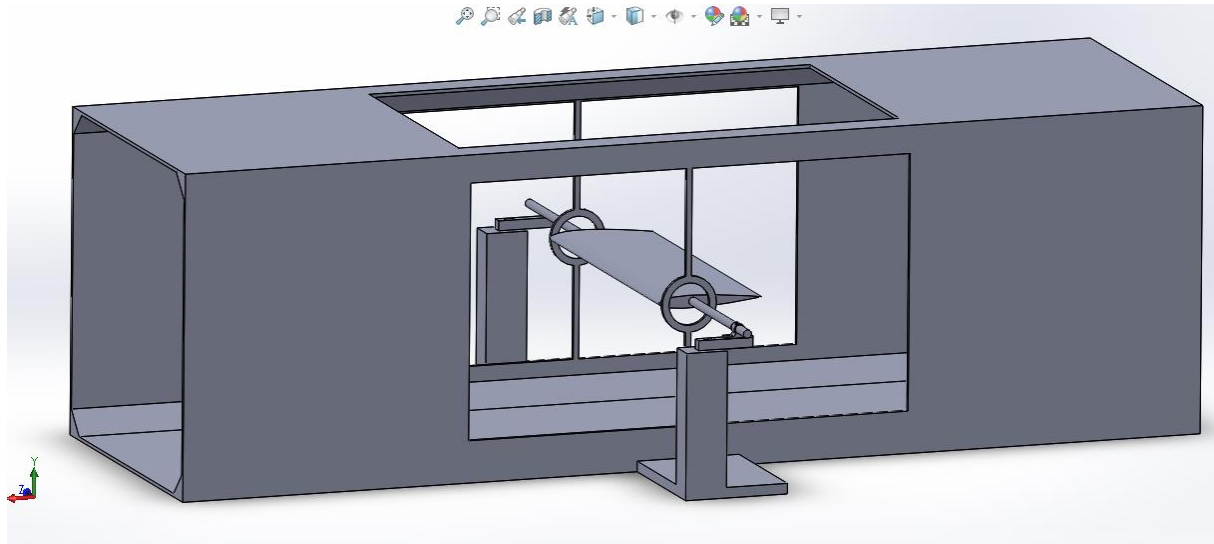


Fig (IV-9) The Preliminary Prototype of the Test Chamber Model.

Then we started adding and removing things, adhering to the laws of material resistance and fluid dynamics. The simpler the model, the less problems and the better results will be read.

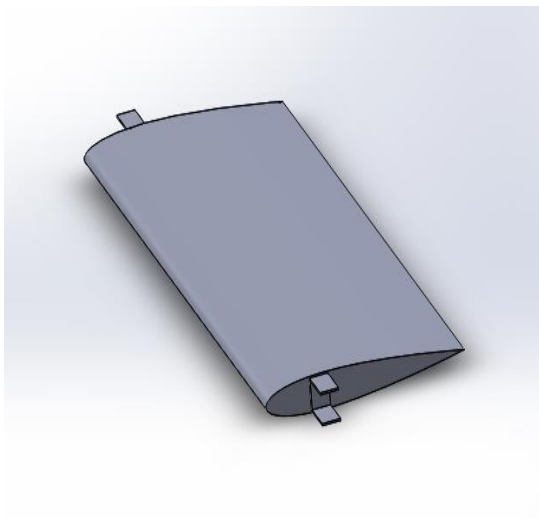


Fig (IV-10) The Wing Model

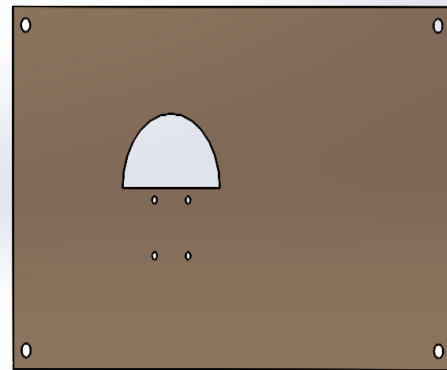


Fig (IV-11) The plexiglass Panel Model

- **The different pieces were all designed and modified on SolidWorks. The resulting models are shown in Figs (IV-10,11,12,13,14,15). And then the assembly was made into what is shown in Fig (IV-16).**



Fig (IV-12) The Holder

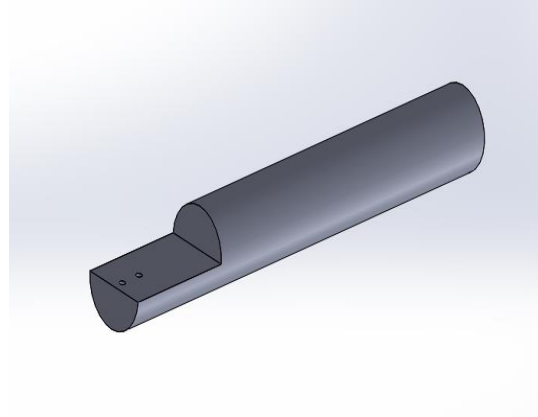


Fig (IV-13) The Stand

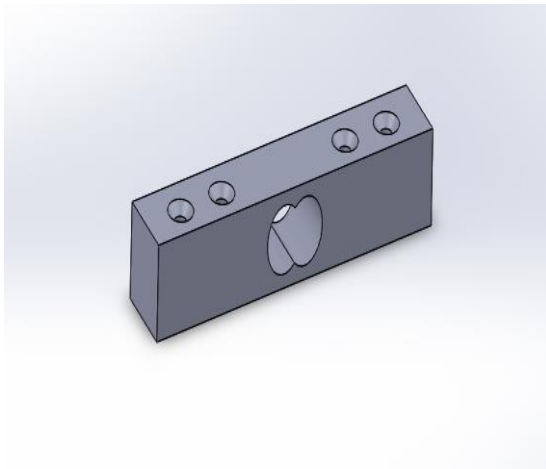


Fig (IV-14) The Load Cell Model

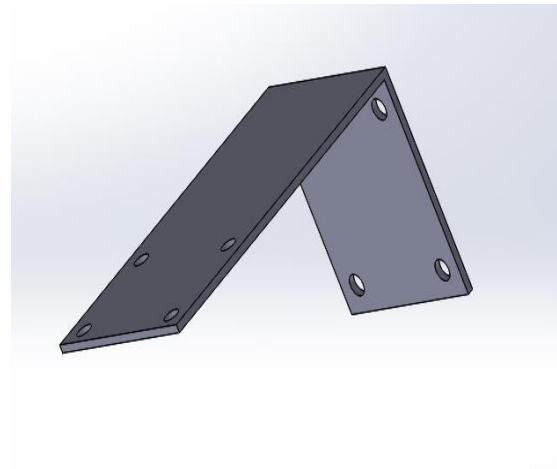


Fig (IV-15) The Platform Model.

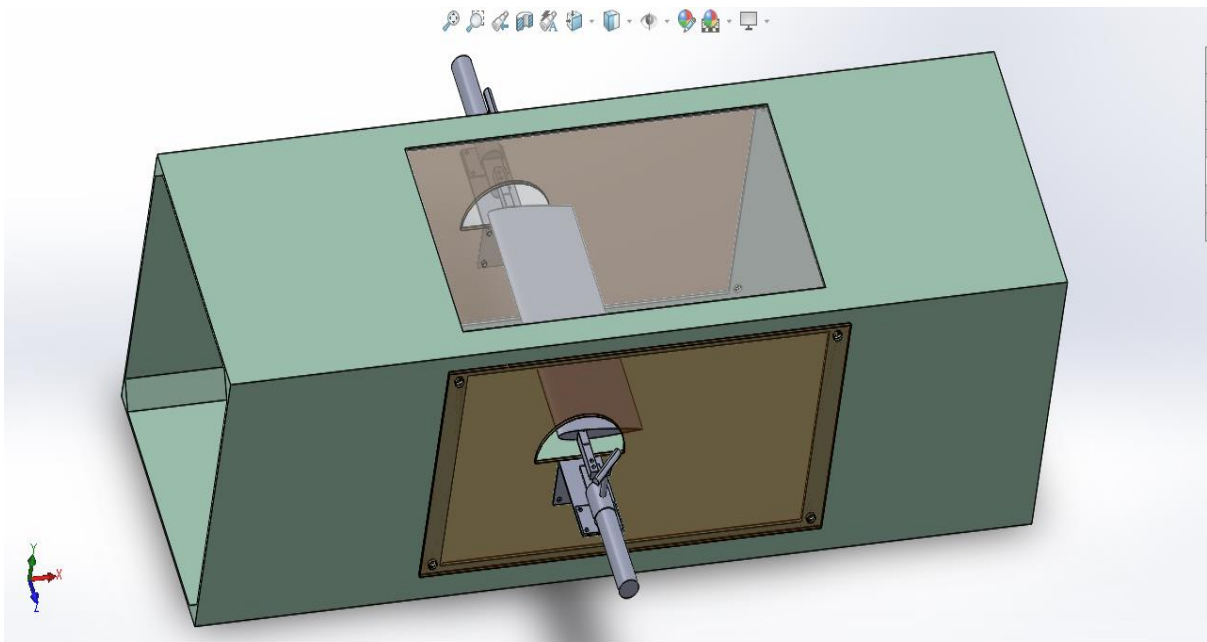


Fig (IV-16) The Assembly of all the Pieces into the Wind Tunnel.

- The final step was to design the whole Wind Tunnel with making the rest of it on SolidWorks also then performing the assembly with the Test Chamber model as Shown in Fig (IV-17).

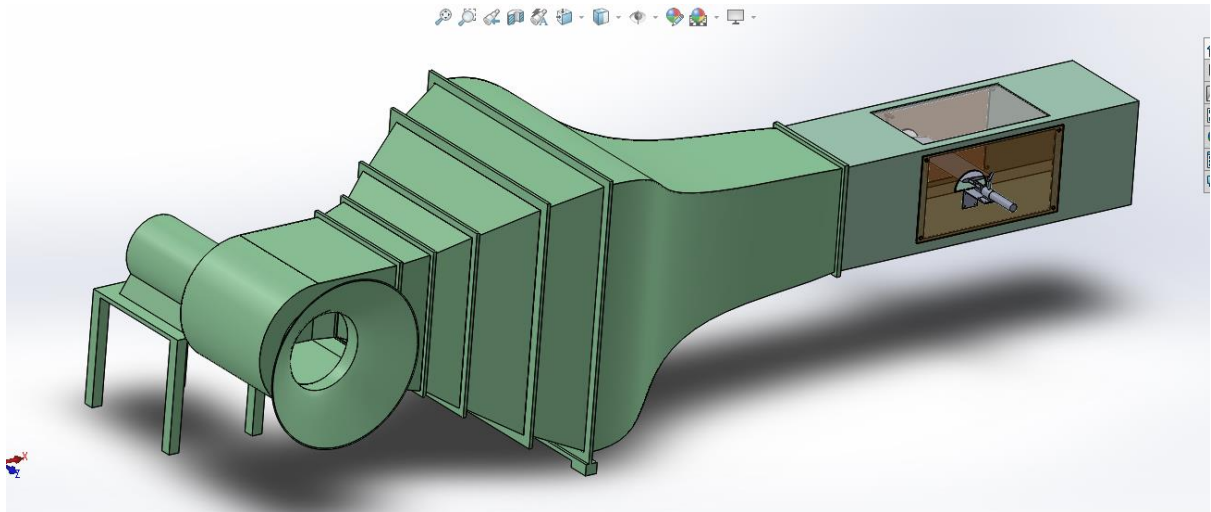


Fig (IV-17). Final look at the Wind Tunnel Design on SolidWorks.

IV.3. Conception and methods of Production:

IV.3.1. Core Materials for the Airfoils/Wings:

The materials used in the process are a combination of aluminium, iron and wood for the different parts of the platform holding the load cells described in detail in this part,

While we depended on Composite materials for the wings for the wings for the purpose of having light smooth and solid bodies to work on.

IV.3.1.1 Composite materials:

The choice to employ Composite materials came after reviewing the need for the studied bodies to have design flexibility, low weight, durability and high Impact resistivity which are ones of the many advantages Composites provide.

Light weight was the main reason for using them. they can also be much stronger than other materials. For example: reinforced carbon-fiber can be up to five times stronger than 1020 grade steel and only one fifth of the weight.

The advantage in strength and weight isn't the only perk. Thermal and chemical resistance as well as Electrical insulation properties makes Composite material gain an edge over conventional ones for the multiple properties it can have not often found in single-compound materials. [23]

IV.3.1.1.1 Definition:

Composite materials are a material made from two or more constituent materials with significantly different physical or chemical properties that, when combined, produce a material with characteristics different from the individual components. [24]

- **The main families of composites include organic matrix composites (OMC), metal matrix composites (MMC) and ceramic matrix composites (CMC)**



Fig (IV-18) A close-up picture of Glass Fiber Bundles.

IV.3.1.2. Reinforcements:

Composite reinforcements describe all methods of improving the mechanical properties of composite materials. The choice of reinforcement is important for the properties of the finished part. Such as load-carrying capacity, strength, impact resistance and flexural stiffness.

The role of the reinforcement in a composite material is fundamentally one of increasing the mechanical properties of the neat resin system. All of the different **fibres** used in composites have different properties and so affect the properties of the composite in different ways.

However, individual **fibers** or **fiber bundles** can only be used on their own in a few processes such as **filament winding**. For most other applications, the **fibers** need to be arranged into some form of sheet, known as a fabric, to make handling possible. Different ways for assembling **fibers** into sheets and the variety of **fiber** orientations possible lead to there being many different types of fabrics, each of which has its own characteristics. [23]

IV.3.1.3. Fibers:

Fibers are the composite's primary source of strength and stiffness. They must be especially treated with chemicals called sizing, those chemicals make them compatible with the intended matrix and ease their processing so much.

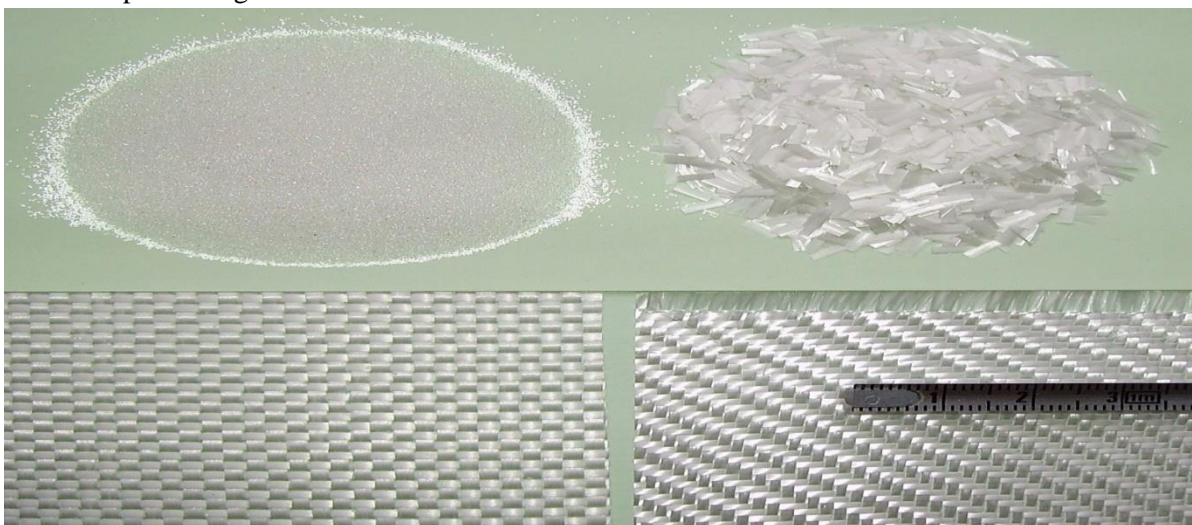


Fig (IV-19) Different States of Fibers.

a- Glass Fiber:

The majority of all fibers used in the composites industry are glass. Fiber glasses, known as glass fiber, are the oldest and, by far, the most common reinforcement. This material is produced from very thin glass wires melted from molds which is called the Pultrusion Process. Some glass fiber properties are shown in Table (IV-1).

An example of the final glass fiber sheets we used are shown in Fig (IV-20). [25]

- Textile grade glass fibers are made from silica (SiO_2) sand melted at 1720°C (3128°F).

Fiber type	Tensile strength (MPa) ^[10]	Compressive strength (MPa)	Density (g/cm ³)	Thermal expansion ($\mu\text{m}/\text{m}\cdot^\circ\text{C}$)	Softening T ($^\circ\text{C}$)	Price (\$/kg)
E-glass	3445	1080	2.58	5	846	~2
S-2 glass	4890	1600	2.46	2.9	1056	~20

Table (IV-1). Some Glass Fiber Properties. (3)

The choice we made came in accordance with the full consideration of its advantages and limitations such as:

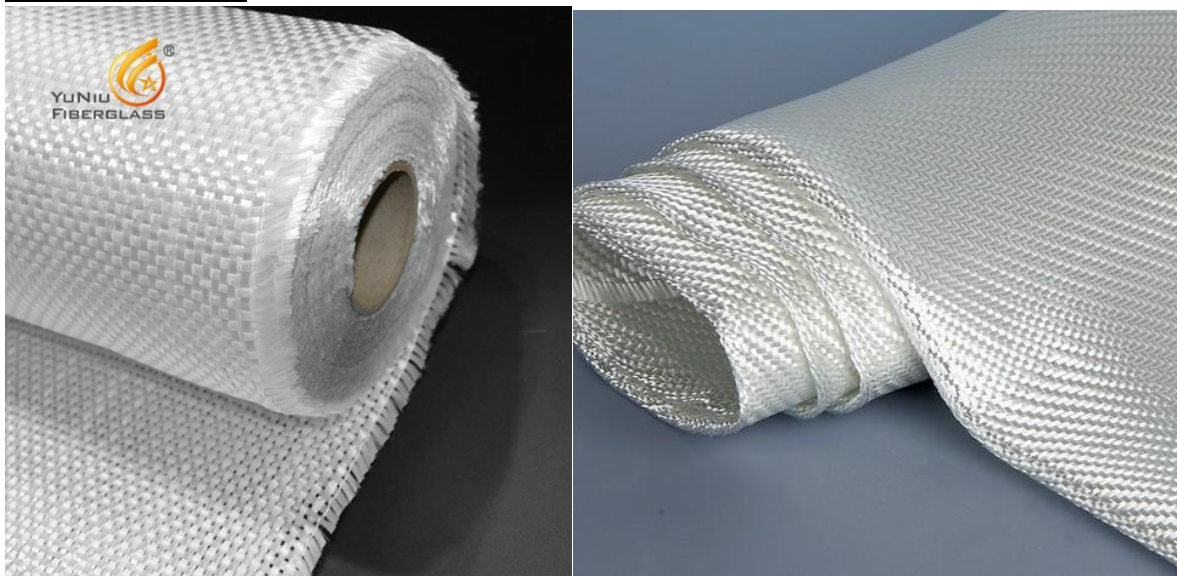


Fig (IV-20) Glass Fiber sheets.

b- Advantages and Limitations:

- Main advantages:
 - ✓ Good thermal and electrical resistance.
 - ✓ Good resistance to chemicals and moisture.
 - ✓ Good compatibility with organic matrices.
 - ✓ Low cost.
- Main limitations:
 - ❖ Medium mechanical characteristics including elastic stiffness.
 - ❖ Low impact strength.

IV.3.1.4. The Matrix:

The matrix is a binder that keeps the dispersion of fibers in place, protecting them physically and chemically, providing in addition the mechanical connection between the reinforcing elements. [26]

It comes in many forms: Metallic, Ceramic or Organic (the type that we used).

within the organic matrices, the two types of resins that are currently used are:

- Thermoplastic resins.
- Thermosetting resins (Polyester resins, Epoxy resins, Phenolic resins, Thermo stable resins...)
- **We employed the Thermosetting resin called the Epoxy resin**

It is the most used in aeronautics; it has good adhesion to the fibers and good mechanical and thermal properties that can resist a temperature of up to 170 ° c. [26]

IV.3.1.5. Molding:

It is the applying the Glass Fiber with the resin reinforcement, 2 types of processes are known:

- Open mold by Contact Projection.
- Closed mold by Thermosetting / polymer injection, under vacuum.

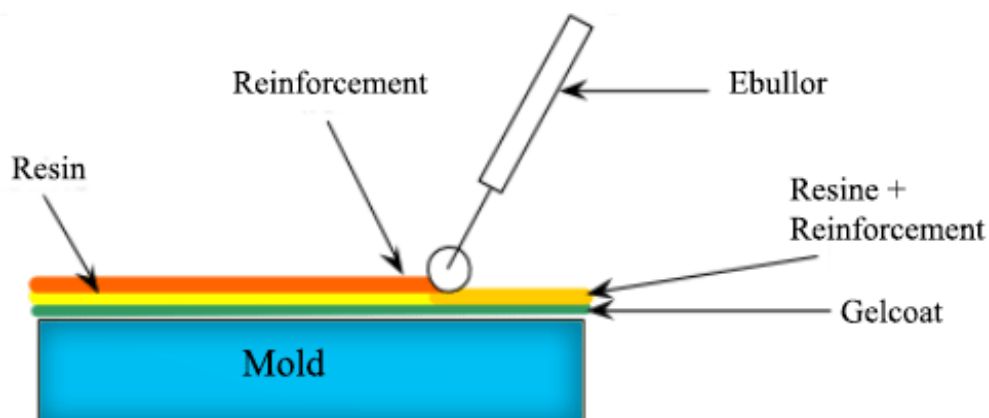


Fig (IV-21) Description of the process of Molding using Glass Fiber and Resin Reinforcement.

IV.3.2. Materials used in the Support Items:

In order to build the platform that holds our load cells and the rest of the electronic equipment, we needed light materials that the plexiglass enclosing the test chamber can carry without any problems and while holding steady for data acquisition precision integrity

Another requirement was to reduce noise when the wind tunnel is operating due to the vibrations which can be harmful to our test results and equipment, thus avoiding errors in obtaining the results on one hand.

On the other hand, the choice was to have materials that are easily found and that are malleable for the purpose of modification or change if the need for it arises. All these factors led us to the use of aluminium plates and wooden rods and panels for the platform. With the test chamber closing doors made out of PlexiGlass as **Shown in Fig (IV-22).**

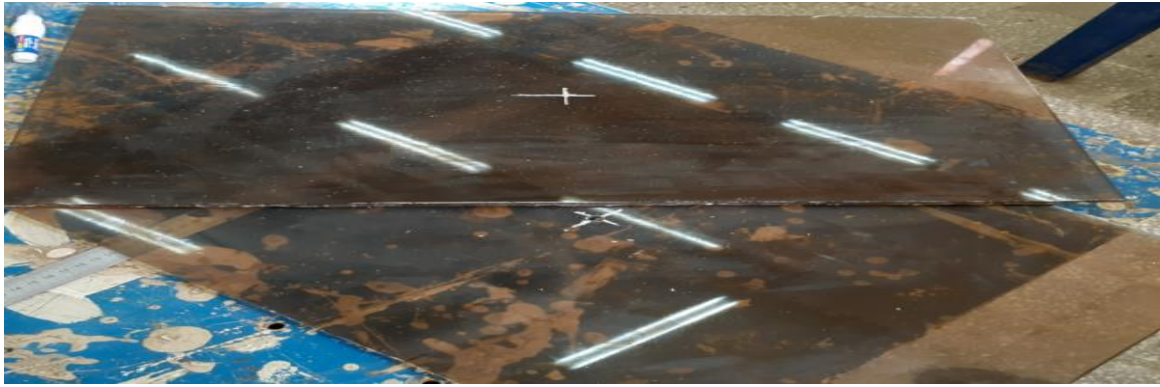


Fig (IV-22). PlexiGlass Board.

IV.4. Production and Realisation:

The production stage is what prepared us for the testing phase. We made sure we designed the best possible solutions and tools for optimal results and maximum precision.

IV.4.1. Wing construction:

The Airfoils were printed from SolidWorks on a piece of paper then cut and glued on an aluminium panel. The piece of aluminium was polished into the shape of our Airfoil. Then it was prepared to be nailed on a piece of polyester because of its lightness and so that we can easily cut it and model it into a wing using heat wires to ensure a precise texture for the correct aerodynamic properties to be kept.

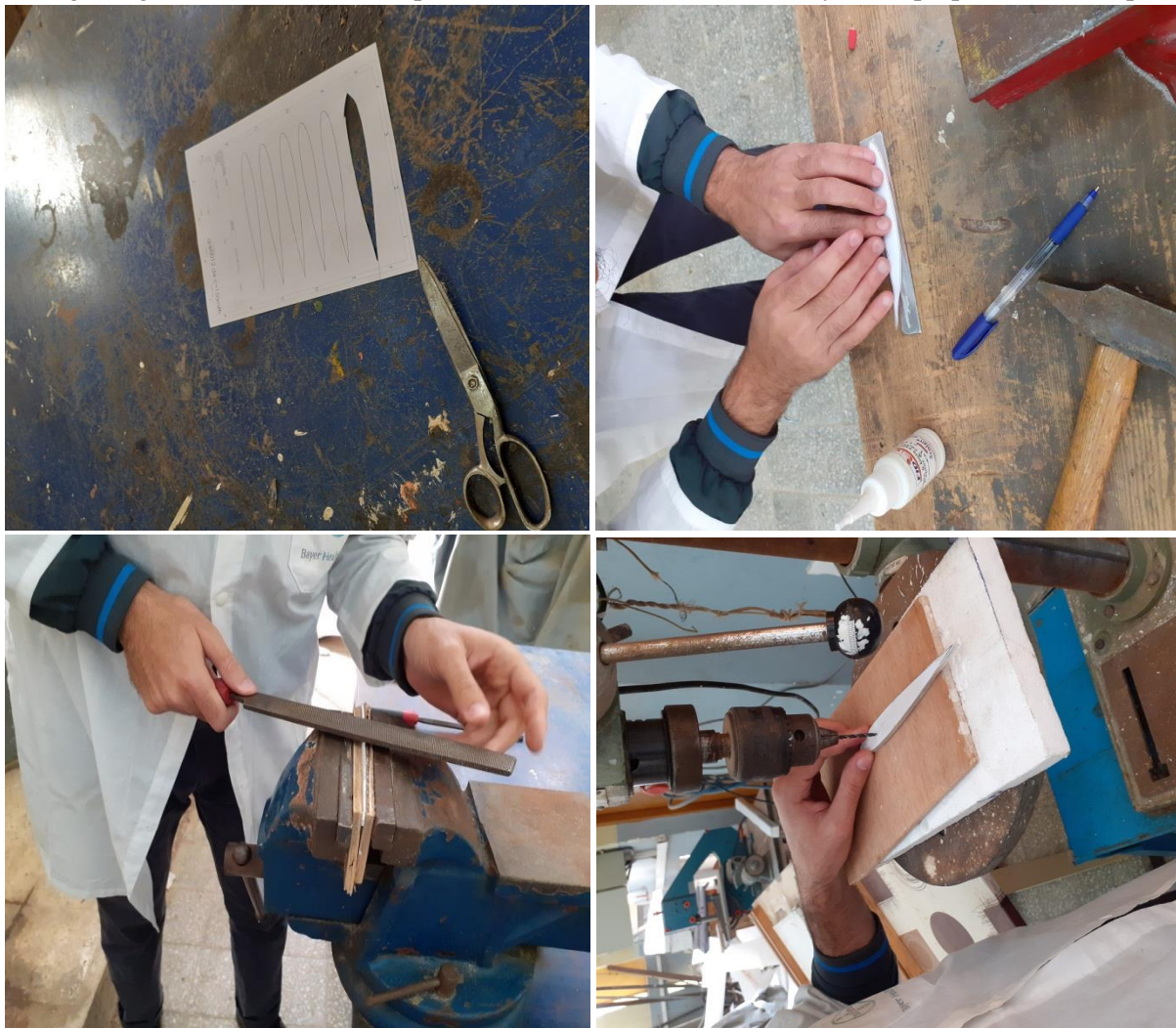


Fig (IV-23) Construction of the Airfoil Surface.

- As shown in Fig (IV-24). Hot wires were used to cut the wing into a precise shape for it to be ready for the Glass Fiber reinforcement Process Shown in Fig (IV-25).



Fig (IV-24) The Process of Shaping the Wing.

The Glass Fiber piece was cut according to the wing size and weighed in order to prepare the matrix. The matrix was made from a mixture of the Epoxy resin and a Catalyst (hardener).

Such as: Glass Fiber weight = Epoxy resin weight + 1/2 of the Epoxy weight for the Catalyst.



Fig (IV-25) Preparation of the Glass Fiber and Epoxy Mixture and the Matrix.

The Glass Fibers were glued by the matrix (Epoxy resin + catalyst) on the polyester wing then pressured using a polyester mold and a heavy weighted object as shown in Fig (IV-26).



Fig (IV-26) Attaching Glass Fibers to the Wing Surface.

- After 72 hours, the wing dried up and we started the process of removing the impurities followed by the polishing process. Shown in Fig (IV-27).



Fig (IV-27) Impurities Removal and Polishing Process.

The polishing of the Glass Fiber wing is the key to getting rid of any residuals left on the surface, followed by the application of polyester putty then more polishing gave us the highly smooth surface we wanted to reach so that air can follow without any obstruction during the testing phase.

Finally, comes the painting job which is also very important for observing the Wing inside the Wind Tunnel. The good visualisation provided by the white colour contributes to even more precision.

The process is shown in Fig (IV-28).



Fig (IV-28) The Painting of and the Final look at the Wing.

IV.4.2. Design and Production of the Measuring Equipment Support:

The support pieces were printed from SolidWorks with their actual measurements. The aluminium was cut to make the platform that holds the other parts and was attached to the plexiglass board. The wooden rods were accordingly to allow us to make the stand that holds the loadcell.



Fig (IV-29) The Preliminary Steps in the Design of the Support Pieces.

In addition, some pieces were custom made such as the holder that contains the wooden rod (meaning the stand) for stability taking into consideration the size of the wind tunnel and the weight standards for the platform resistivity. While the rest of the pieces were made exactly as they were designed on SolidWorks (The platform, The stand).

A final look at the pieces is shown in Fig (IV-30).



Fig (IV-30) Final Look at the Designed Pieces after the Paint job.

IV.5. CONCLUSION:

After Concluding the conception and design of our pieces. It was apparent that the tests would go smoothly since the electronic equipment goes well with the produced support items.

The wing presented a highly smooth surface which would in return affect the precision of the study since air would flow without any obstruction along its surface. And because of the design; the wing is held on both ends by the test chamber walls which enables us to ignore the vortices effect along the edges. So, our study on the wings is the same as the study on their Airfoils

This is where the simulation results come in as they serve as a comparison point between the theoretical studies, the numerical results and the experimental data.

The preliminary outcome of the numerical simulations, the smoothness and precision of the designed parts and the bleeding edge technology of the electronic sensors predict high precision data from the upcoming experimental results.

Unfortunately, due to the inability to proclaim the Airspeed sensor, we were unable to perform the tests and confirm our predictions.

GENERAL CONCLUSION:

The goal of our thesis was to design and come up with ways to install high precision electronic equipment on our Wind Tunnel without compromising the accuracy or the stability of our models which was accomplished successfully.

The 4 electronic sensors consisting of the Force Load Cell, the Airspeed Sensor, the accelerometer and the PIC Microcontrollers all have their proper place within the design with the innovative support pieces ready for assembly and coinciding perfectly with the equipment so as to ensure complete stability while performing the tests.

The numerical results were also very satisfactory to serve as a comparison point in order to validate our work. The data comprised from the ANSYS Fluent analysis of NACA 0012, NACA 0015 and NACA 4412 was very consistent with real-life research data.

This is not where it stops, future enthusiasts can also add and innovate and make use of our designs. The support pieces are specifically designed to uphold any aerodynamic body with complete stability which opens the door for any interested researchers to conduct any kind of tests in the Wind Tunnel using our refined parts.

The production part has confirmed all of our design studies and was 100% our creation with light and cost saving materials that anyone can easily use to conduct their own aerodynamic Wind Tunnel tests.

I- SOLIDWORKS:

The SOLIDWORKS® CAD software is a mechanical design automation application that lets designers quickly sketch out ideas, experiment with features and dimensions, and produce models and detailed drawings.

I-1. Concepts:

Parts are the basic building blocks in the SOLIDWORKS software. Assemblies contain parts or other assemblies, called subassemblies.

A SOLIDWORKS model consists of 3D geometry that defines its edges, faces, and surfaces. The SOLIDWORKS software lets you design models quickly and precisely.

SOLIDWORKS models are:

- Defined by 3D design
- Based on components

I-2. 3D Design:

SOLIDWORKS uses a 3D design approach. As you design a part, from the initial sketch to the final result, you create a 3D model. From this model, you can create 2D drawings or mate components consisting of parts or subassemblies to create 3D assemblies. You can also create 2D drawings of 3D assemblies.

When designing a model using SOLIDWORKS, you can visualize it in three dimensions, the way the model exists once it is manufactured.

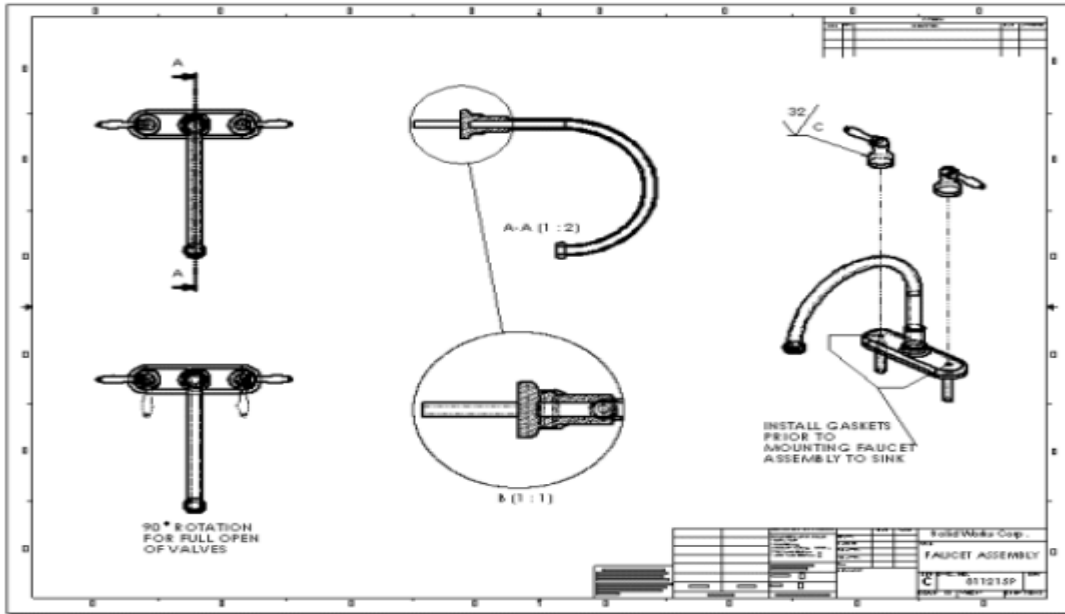


Solidworks 3D part



solidworks 3D assembly

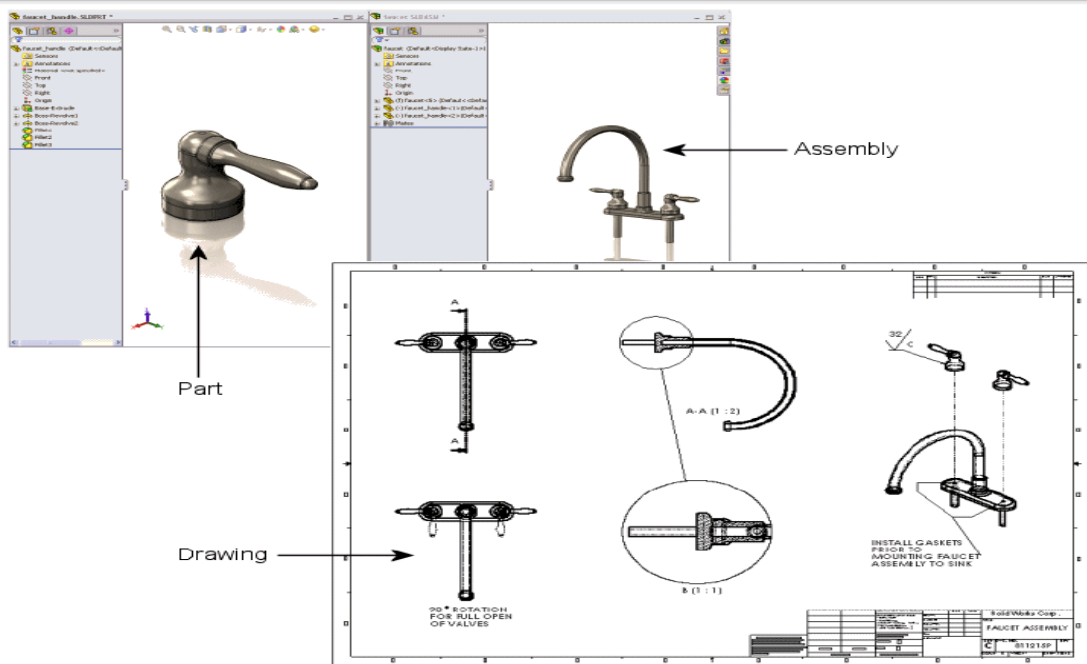
APPENDIX A: Software Used



SOLIDWORKS 2D drawing generated from 3D model

I-3. Component Based:

One of the most powerful features in the SOLIDWORKS application is that any change you make to a part is reflected in all associated drawings or assemblies.¹² SOLIDWORKS Fundamentals



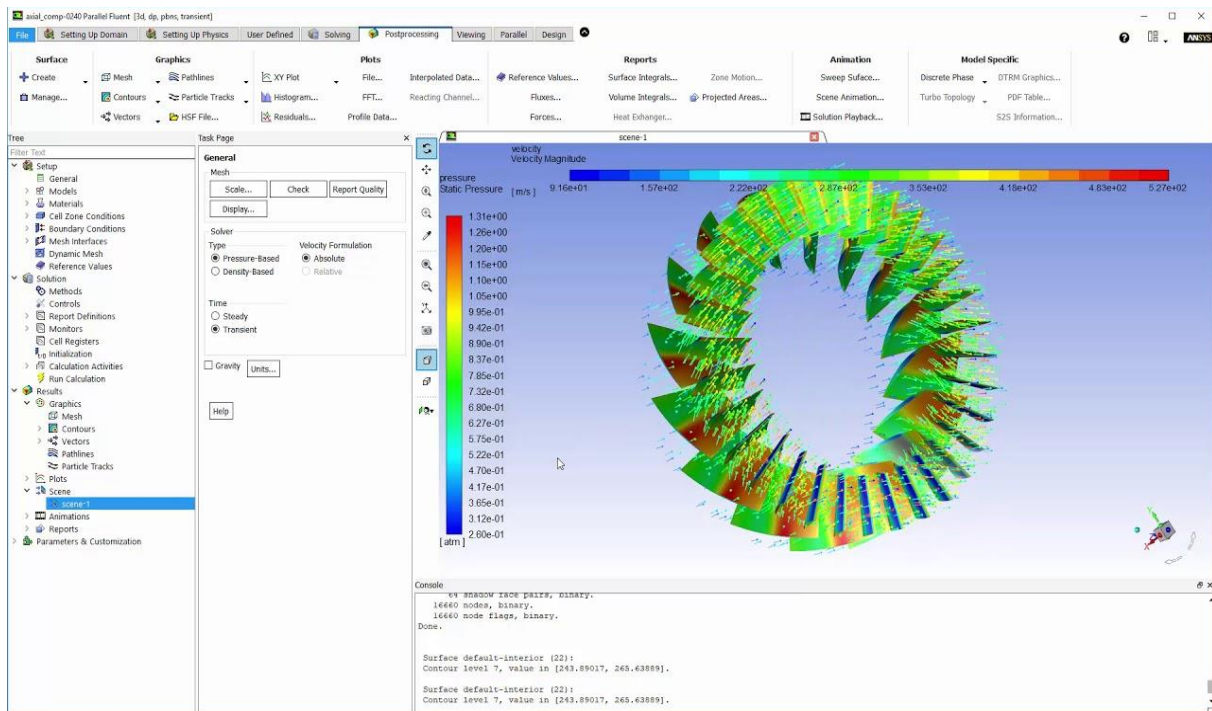


II- Ansys:

Ansys develops and markets engineering simulation software for use across the product life cycle. Ansys Mechanical finite element analysis software is used to simulate computer models of structures, electronics, or machine components for analyzing strength, toughness, elasticity, temperature distribution, electromagnetism, fluid flow, and other attributes. Ansys is used to determine how a product will function with different specifications, without building test products or conducting crash tests. For example, Ansys software may simulate how a bridge will hold up after years of traffic, how to best process salmon in a cannery to reduce waste, or how to design a slide that uses less material without sacrificing safety.

Most Ansys simulations are performed using the Ansys Workbench system, which is one of the company's main products. Typically Ansys users break down larger structures into small components that are each modeled and tested individually. A user may start by defining the dimensions of an object, and then adding weight, pressure, temperature and other physical properties. Finally, the Ansys software simulates and analyzes movement, fatigue, fractures, fluid flow, temperature distribution, electromagnetic efficiency and other effects over time.

Ansys also develops software for data management and backup, academic research and teaching. Ansys software is sold on an annual subscription basis.



ANSYS Fluent computational fluid dynamics 'CFD' simulation.

APPENDIX B: Airfoils Coordinates

X-Coordinate	Y-Coordinate	NACA 0012
1	0.00126	
0.9928	0.00227	
0.97989	0.00405	
0.96352	0.00627	
0.94455	0.00878	
0.9235	0.01151	
0.90075	0.01438	
0.87658	0.01735	
0.85123	0.02038	
0.82489	0.02343	
0.79774	0.02648	
0.76991	0.0295	
0.74154	0.03248	
0.71275	0.03539	
0.68365	0.03821	
0.65434	0.04093	
0.62492	0.04354	
0.59547	0.046	
0.56607	0.04832	
0.5368	0.05047	
0.50774	0.05245	
0.47895	0.05422	
0.4505	0.05578	
0.42246	0.05712	
0.39488	0.05822	
0.36782	0.05906	
0.34135	0.05965	
0.31551	0.05996	
0.29035	0.06	
0.26594	0.05974	
0.24231	0.0592	
0.21951	0.05836	
0.1976	0.05723	
0.17661	0.05581	
0.1566	0.0541	
0.1376	0.05211	
0.11965	0.04983	
0.1028	0.04729	
0.08709	0.0445	
0.07256	0.04145	
0.05924	0.03817	
0.04717	0.03467	
0.03639	0.03096	

APPENDIX B: Airfoils Coordinates

0.02694	0.02705
0.01885	0.02296
0.01215	0.01869
0.00688	0.01425
0.00308	0.00965
0.00078	0.0049
0	0
0.00078	-0.0049
0.00308	-0.00965
0.00688	-0.01425
0.01215	-0.01869
0.01885	-0.02296
0.02694	-0.02705
0.03639	-0.03096
0.04717	-0.03467
0.05924	-0.03817
0.07256	-0.04145
0.08709	-0.0445
0.1028	-0.04729
0.11965	-0.04983
0.1376	-0.05211
0.1566	-0.0541
0.17661	-0.05581
0.1976	-0.05723
0.21951	-0.05836
0.24231	-0.0592
0.26594	-0.05974
0.29035	-0.06
0.31551	-0.05996
0.34135	-0.05965
0.36782	-0.05906
0.39488	-0.05822
0.42246	-0.05712
0.4505	-0.05578
0.47895	-0.05422
0.50774	-0.05245
0.5368	-0.05047
0.56607	-0.04832
0.59547	-0.046
0.62492	-0.04354
0.65434	-0.04093
0.68365	-0.03821
0.71275	-0.03539
0.74154	-0.03248

APPENDIX B: Airfoils Coordinates

0.76991	-0.0295
0.79774	-0.02648
0.82489	-0.02343
0.85123	-0.02038
0.87658	-0.01735
0.90075	-0.01438
0.9235	-0.01151
0.94455	-0.00878
0.96352	-0.00627
0.97989	-0.00405
0.9928	-0.00227
1	0

X-Coordinate	Y-Coordinate	NACA 0015
1	0.00157	
0.9928	0.00283	
0.97989	0.00506	
0.96352	0.00783	
0.94455	0.01098	
0.9235	0.01439	
0.90075	0.01798	
0.87658	0.02169	
0.85123	0.02548	
0.82489	0.02929	
0.79774	0.0331	
0.76991	0.03688	
0.74154	0.0406	
0.71275	0.04423	
0.68365	0.04776	
0.65434	0.05117	
0.62492	0.05442	
0.59547	0.05751	
0.56607	0.0604	
0.5368	0.06309	
0.50774	0.06556	
0.47895	0.06777	
0.4505	0.06973	
0.42246	0.0714	
0.39488	0.07277	
0.36782	0.07383	
0.34135	0.07456	
0.31551	0.07495	
0.29035	0.075	
0.26594	0.07468	

APPENDIX B: Airfoils Coordinates

0.24231	0.074
0.21951	0.07296
0.1976	0.07154
0.17661	0.06977
0.1566	0.06763
0.1376	0.06513
0.11965	0.06229
0.1028	0.05912
0.08709	0.05562
0.07256	0.05182
0.05924	0.04772
0.04717	0.04334
0.03639	0.0387
0.02694	0.03381
0.01885	0.0287
0.01215	0.02336
0.00688	0.01781
0.00308	0.01207
0.00078	0.00613
0	0
0.00078	-0.00613
0.00308	-0.01207
0.00688	-0.01781
0.01215	-0.02336
0.01885	-0.0287
0.02694	-0.03381
0.03639	-0.0387
0.04717	-0.04334
0.05924	-0.04772
0.07256	-0.05182
0.08709	-0.05562
0.1028	-0.05912
0.11965	-0.06229
0.1376	-0.06513
0.1566	-0.06763
0.17661	-0.06977
0.1976	-0.07154
0.21951	-0.07296
0.24231	-0.074
0.26594	-0.07468
0.29035	-0.075
0.31551	-0.07495
0.34135	-0.07456
0.36782	-0.07383

APPENDIX B: Airfoils Coordinates

0.39488	-0.07277
0.42246	-0.0714
0.4505	-0.06973
0.47895	-0.06777
0.50774	-0.06556
0.5368	-0.06309
0.56607	-0.0604
0.59547	-0.05751
0.62492	-0.05442
0.65434	-0.05117
0.68365	-0.04776
0.71275	-0.04423
0.74154	-0.0406
0.76991	-0.03688
0.79774	-0.0331
0.82489	-0.02929
0.85123	-0.02548
0.87658	-0.02169
0.90075	-0.01798
0.9235	-0.01439
0.94455	-0.01098
0.96352	-0.00783
0.97989	-0.00506
0.9928	-0.00283
1	0

X-Coordinate	Y-Coordinate	NACA 4412
1	0.00126	
0.9928	0.00322	
0.97989	0.00668	
0.96352	0.01098	
0.94455	0.01584	
0.9235	0.02106	
0.90075	0.02652	
0.87658	0.03212	
0.85123	0.03776	
0.82489	0.04337	
0.79774	0.0489	
0.76991	0.0543	
0.74154	0.05952	
0.71275	0.06452	
0.68365	0.06927	
0.65434	0.07374	
0.62492	0.07791	

APPENDIX B: Airfoils Coordinates

0.59547	0.08176
0.56607	0.08526
0.5368	0.0884
0.50774	0.09116
0.47895	0.09353
0.4505	0.0955
0.42246	0.09706
0.39488	0.09821
0.36782	0.09881
0.34135	0.09879
0.31551	0.09818
0.29035	0.09699
0.26594	0.09525
0.24231	0.09298
0.21951	0.09022
0.1976	0.08699
0.17661	0.08334
0.1566	0.07929
0.1376	0.07489
0.11965	0.07019
0.1028	0.06521
0.08709	0.06002
0.07256	0.05465
0.05924	0.04914
0.04717	0.04355
0.03639	0.03791
0.02694	0.03226
0.01885	0.02664
0.01215	0.02108
0.00688	0.01561
0.00308	0.01027
0.00078	0.00506
0	0
0.00078	-0.00475
0.00308	-0.00904
0.00688	-0.01288
0.01215	-0.01629
0.01885	-0.01928
0.02694	-0.02185
0.03639	-0.02401
0.04717	-0.02579
0.05924	-0.0272
0.07256	-0.02826
0.08709	-0.02897

APPENDIX B: Airfoils Coordinates

0.1028	-0.02938
0.11965	-0.02948
0.1376	-0.02932
0.1566	-0.02891
0.17661	-0.02829
0.1976	-0.02748
0.21951	-0.02651
0.24231	-0.02542
0.26594	-0.02424
0.29035	-0.023
0.31551	-0.02175
0.34135	-0.02051
0.36782	-0.01932
0.39488	-0.01822
0.42246	-0.01717
0.4505	-0.01607
0.47895	-0.01491
0.50774	-0.01374
0.5368	-0.01255
0.56607	-0.01139
0.59547	-0.01025
0.62492	-0.00916
0.65434	-0.00812
0.68365	-0.00715
0.71275	-0.00626
0.74154	-0.00544
0.76991	-0.00471
0.79774	-0.00406
0.82489	-0.00349
0.85123	-0.003
0.87658	-0.00259
0.90075	-0.00224
0.9235	-0.00196
0.94455	-0.00173
0.96352	-0.00155
0.97989	-0.00141
0.9928	-0.00131
1	0

REFERENCES

- [1] Bruno Chanetz, «A Century of Wind Tunnels since Eiffel,» *Comptes Rendus Mécaniques*, volume 345, Issue 18, pp. 581-594, August 2017.
- [2] Donald D. Baals, Wind Tunnels of NASA, Scientific and Technical Information Branch, NATIONAL AERONAUTICS and SPACE ADMINISTRATION, Washington D.C, 1981, pp. 1-75.
- [3] Wikipedia contributors, «Wind Tunnel,» Wikipedia, The Free Encyclopedia, 17 April 2020. [En ligne]. Available: https://en.wikipedia.org/wiki/Wind_tunnel.
- [4] Nancy Hall, «Wind Tunnel Parts,» 5 May 2015. [on ligne]. Available: <https://www.grc.nasa.gov/www/k-12/airplane/tunpart.html>.
- [5] R. K. Rajput, A Textbook of Engineering Thermodynamics 4th ed, New Delhi: LAXMI PUBLICATIONS (P) LTD, 2010, p. 877.
- [6] C. Dollfus, «Historical notes on aerodynamic research,» Work of the US Gov, 1924.
- [7] Nancy Hall, «Types of Wind Tunnels,» 5 May 2015. [En ligne]. Available: <https://www.grc.nasa.gov/www/k-12/airplane/tuntype.html>.
- [8] G. K. Ananda Krishnan, Aerodynamic performance of low-to-moderate aspect ratio wings at low Reynolds numbers, Illinois: University of Illinois at Urbana-Champaign, 2012.
- [9] Usman, Muhammad & Hanif, Asad & Kim, In-Ho & Jung, Hyung-Jo., Experimental validation of a novel piezoelectric energy harvesting system employing wake galloping phenomenon for a broad wind spectrum, 2018.
- [10] J. D. ANDERSON, Fundamentals of Aerodynamics, Boston: McGraw-Hill, 2001, pp. 16-277.
- [11] Woodbank Communications Ltd, «Aerodynamic Lift and Drag and the Theory of Flight,» Woodbank Communications Ltd, 2005. [En ligne]. Available: https://www.mpoweruk.com/flight_theory.htm. [Accès le 2020].
- [12] J. D. ANDERSON, Introduction to Flight, Boston: McGraw-Hill, 2016.
- [13] M. Kaushik., Theoretical and Experimental Aerodynamics, Singapore: Springer Singapore, 2019.
- [14] Cantwell, «AA200 Course Material,» chez *The NACA Airfoil Series*, Stanford, Stanford University, 2013, pp. 1-5.
- [15] A Flight Learning Production, «Airfoils-Airfoil Types,» 3 2015. [En ligne]. Available: <https://www.danubewings.com/airfoils-airfoil-types/>.
- [16] AirfoilTools, «Airfoil Database Search,» 2020. [En ligne]. Available: <http://www.airfoiltools.com/>.
- [17] Think & Learn Pvt Ltd, «Types of Airfoils,» 2020. [En ligne]. Available: <https://byjus.com/physics/aerofoil/>.

- [18] Yousif I. A. Mashhadany., «Design and Implementation of Electronic Control Trainer with PIC Microcontroller,» *Intelligent Control and Automation* 3, pp. 222-228, 2012.
- [19] R. P. Chaudari. Rathod Raju Ambadas, «PIC Microcontroller Universal Board,» *International Journal of Innovative Technology and exploring Engineering*, vol. 3, n° %17, 2013.
- [20] Microchip Technology Incorporated, «PIC18F4620 and PIC18F4520 datasheets. Enhanced Flash microcontrollers with 10-bit A/D and nano-Watts Technology,» Microchip Technology Inc, U.S.A, 2004.
- [21] AVIA SEMICONDUCTOR, «24-Bit Analog-to-Digital Converter (ADC) for Weigh Scales,» AVIA SEMICONDUCTOR, P. R. China.
- [22] National Instruments, «Getting Started with LabVIEW,» National Instruments, Austin, Texas, USA, 2013.
- [23] REVOLUTION FIBRES LTD, «Composite reinforcement 101,» 2017. [En ligne]. Available: <https://www.xantulayr.com/composite-reinforcement>.
- [24] Mahyar, Fazeli ; Jennifer Paola, Florez ; Renata Antoun, Simao, «Improvement in adhesion of cellulose fibers to the thermoplastic starch matrix by plasma treatment modification,» *Composites Part B: Engineering.*, pp. 207-216, 2019.
- [25] Milos B. Volf, Technical Approach to Glass, New York: Elsevier, 1990.
- [26] Dr Laarej Merad., ETUDE PAR SPECTROSCOPIE RAMAN ET MODELISATION D'UNE RESINE COMPOSITE RTM, Tlemcen: Abou Bakr BELKAID University, 2010, pp. 12-25.

-